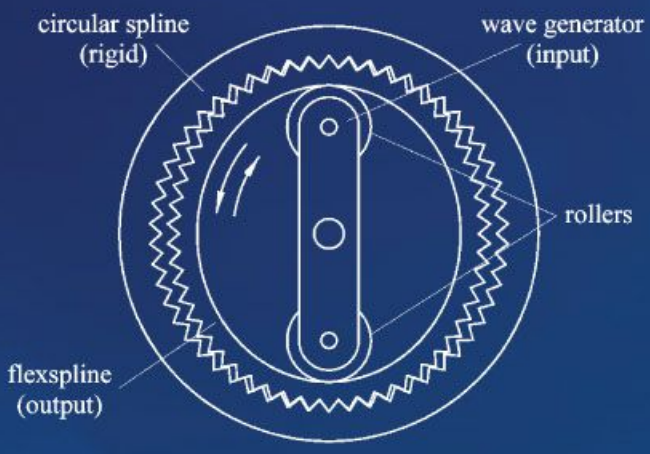

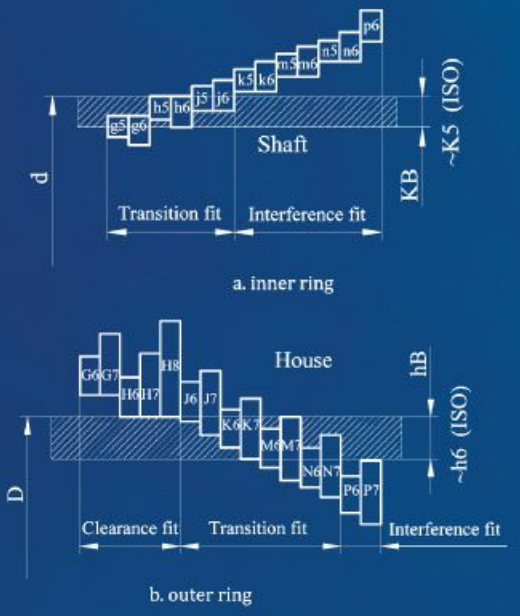

Zsolt Tiba

Drivetrain optimization

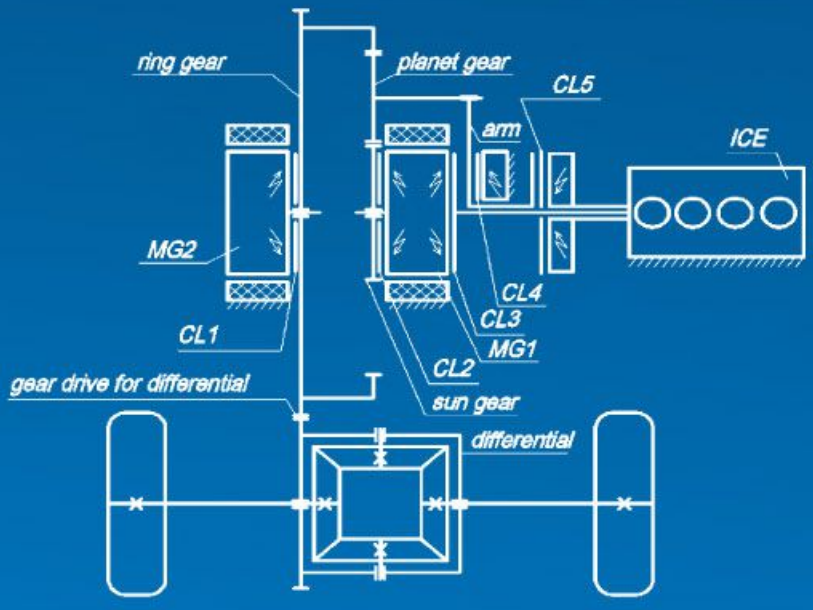

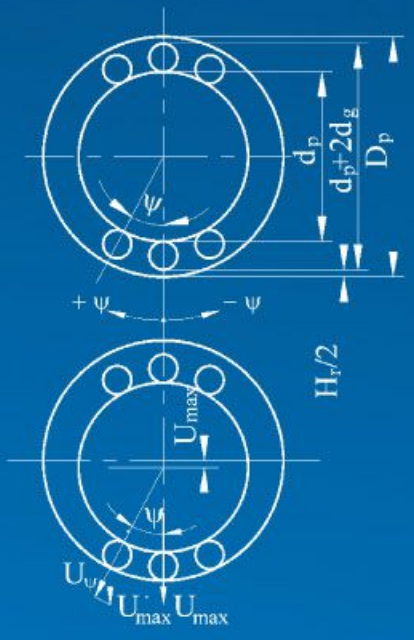

UNIVERSITY OF DEBRECEN
FACULTY OF ENGINEERING

ZSOLT TIBA

Drivetrain optimization

Debrecen University Press
2017

Author:
Zsolt Tiba

Professional Reader:
Imre Kocsis PhD
Gusztáv Áron Szíki PhD

ISBN 978 963 318 621 3

Published by Debrecen University Press
www.dupress.hu
Publisher: Gyöngyi Karácsony
Printed by Debrecen University Press, 2017

CONTENTS

ABBREVIATIONS OF TERMS AND MARKS

a	$[mm]$	centre distance
A	$[m^2]$	area
c	$[mmN^{-1}]$	spring compliance
C_f		surface finish factor
C_r		reliability factor
C_s		size factor
C_t		temperature factor
C	$[N]$	basic dynamic load rating
d, D	$[mm]$	diameter
e	$[mm]$	eccentricity
E	$[Nmm^{-2}]$	modulus of elasticity
E	$[mm]$	belt deflection
f	$[mm]$	displacement
f	$[N]$	load used to set belt tension
F_g	$[N]$	excitation force
g	$[ms^{-2}]$	value of gravity
G	$[Nmm^{-2}]$	modulus of rigidity
$H_{(t)}$	$[N]$	load limit
i		ratio
I	$[cm^4]$	moment of inertia
I_p	$[cm^4]$	polar moment of inertia
J	$[kgm^2]$	mass moment of inertia

$k_{ü}$		operation coefficient
k_i		starting coefficient
k_T		overload coefficient
K	$[cm^3]$	section modulus
K_p	$[cm^3]$	section modulus for torsion
K_f		fatigue stress concentration factor
l	$[mm]$	length
L	$[mm]$	drive span length
L		service life
m	$[kg]$	mass
M	$[Nm]$	moment
N		load circle
n	$[s^{-1}]$	speed of revolution
n		factor of safety
p	$[Nmm^{-2}]$	bearing stress
P	$[kW]$	power
P	$[N]$	equivalent dynamic load rating
R_{eH}	$[Nmm^{-2}]$	yield stress
R_m	$[Nmm^{-2}]$	ultimate tensile strength
R_{Dv}	$[Nmm^{-2}]$	completely reversed endurance limit
$\mathrm{R}'_{\mathrm{Dv}}$	$[Nmm^{-2}]$	completely reversed endurance limit
s	$[Nmm^{-1}]$	spring constant
S		Krülov function
S_a	$[N]$	static shaft load
t	$[s]$	time
T		Krülov function
T	$[N]$	static tension
T_a	$[N]$	load amplitude
T_n	$[N]$	nominal load
$T_{(t)}$	$[N]$	load
U		Krülov function
v	$[ms^{-1}]$	velocity
V	$[m^3]$	volume
V		Krülov function
α	$[radds^{-1}]$	angular frequency of vibration
γ	$[rad(Nm)^{-1}]$	torsion spring compliance
μ		friction coefficient
ρ	$[kgm^{-3}]$	density
σ	$[Nmm^{-2}]$	stress (normal)
τ	$[Nmm^{-2}]$	stress (shear)

σ_{meg}	$[\,Nmm^{-2}\,]$	allowed normal stress
τ_{meg}	$[\,Nmm^{-2}\,]$	allowed shear stress
α	[deg *ree*]	angle of action
φ	[deg *ree*]	angular displacement
ω	$[\,rads^{-1}\,]$	angular frequency
Γ_{i1}	[deg *ree*]	phase angle
Φ_{i1}	[deg *ree*]	angle position
η		efficiency

FIGURES

TABLES

ACKNOWLEDGEMENTS

The book has benefited from the comments, suggestions, and assistance of numerous colleagues. I would like to acknowledge my colleague Zoltán Budai for elaborating the figures and diagrams.

Special thanks to Clemens Nienhaus, former chief engineer of the test and construction division at the Walterscheid Ltd., who provided me the opportunity to conduct researches in the test laboratory in Lohmar, Germany.

1. Tasks and requirements of the drivetrain

Drive trains ensure the mechanical connection between the prime mover and the machinery; however in many cases drivetrains have other requirements to fulfil, as well. These requirements are often contradictory, as their engineering implementations and solutions are contradictory, as well. The main aim when designing the drivetrain is that it operates without any failure until a given service life. As drivetrains are built up of drive elements, the failure of one element causes the failure of the whole drivetrain. Drive elements can operate with different operating features, that affect the whole drivetrain, for instance in the case of a rotating element, where the axis of rotation does not coincide with the centre of mass, or the cardan joint, that transmits the drive with varying angular speed. The above examples show that the drivetrain designed for a given task will not and cannot necessarily operate under uniform, quiet and smooth circumstances. The operational features of the prime mover and the driven machine, which basically define the load-time pattern, the torque pattern and their supplementary loads, must be taken into consideration, as well. The effects that are manifested through the change of the load-time pattern have to be taken into consideration during designing and stressing. We can say that we have to carry out sizing accordingly. It follows from this that a drivetrain is correctly designed, if it can fulfil its service life purposed during stressing. If, however, during designing we neglect to take into consideration any of the factors and a drive that assumes a smooth operation runs uneven after assembly, we will have to face dynamic effects that have not been taken into consideration during the stressing and sizing. Thus, it is unavoidable that the drive train and its elements fail before the end of planned service life. That is why during stressing we have to be aware of the operating features of the drivetrain and the loads that arise during its operation. However, our drivetrain is exposed to continuously acting excitation effects due to non-stationary torque supply and – demand and the operating features of the drive elements. If the frequency of the excitation effects corresponds to or is close to one of the natural frequencies of the drivetrain, resonance or vibration can develop. In this state, the loads that act on the drivetrain exceed the maximum value considered during stressing; hence its service life will decrease significantly. Although, there are machines designed for this operational conditions (vibrators, shaking tables), their stressing was carried out for the load characteristics for a given operational conditions. With that exception, we usually assume when stressing, that no resonance arises during operation. In order to avoid resonance we need to know the natural frequency of the drive train that can be determined during the stressing by dynamic modelling, with calculations. This book describes the steps of the applied dynamic modelling process and introduces the computer simulation software based on this method. It follows from the above that optimizing the drive trains means that the implemented drive train and its elements will operate exactly as planned, its service life will be as prescribed, and the

whole drivetrain will be able to carry out the technological task, it was designed for. In order that a well-designed drivetrain is able to operate appropriately during its prescribed service life, it is required to be assembled and maintained with expertise. Inappropriate assembly may result in such supplementary loads and residual deformations that can damage the drivetrain already during assembly. An inappropriately maintained machine group requires greater and greater power, which results in greater loads on the elements of the drivetrain. Since stressing was not carried out for this load, the service life of the drivetrain will decrease due to the failure of one or more of its elements. A good example for increasing power demand due to wearing is the analogue quartz watch, which requires the change of battery even more frequently due to the continuous wearing of the mechanism, since its electrical current drain increases steadily.

1.1. Service life of the drivetrain, the stressing

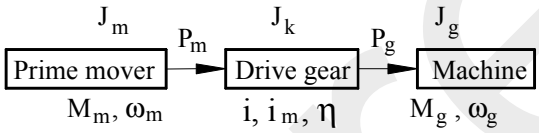

Figure 1.1: Build-up of the drivetrain

The method of designing and stressing of a drivetrain is demonstrated here for the case when the engine, carrying out the given technological process, is chosen from a product catalogue. In this case the main parameters that are required for choosing the prime mover and stressing the drivetrain are available to us from the manufacturer. If we designed the machinery itself, these actual data would be available only by measurements, after the assembly of the machinery.

The most important parameter of the machine is the P_n nominal performance, on which bases the prime mover can be chosen. However, in the previous chapter we have clarified, that the load-time pattern of the drivetrain depends primarily on the operation of the prime mover and the driven machine, as well as the technological process being carried out. A load altering in time causes fatigue loading, so the machine parts have to be stressed for fatigue, for which the load amplitude needs to be determined .From P_n we can calculate only the nominal load, which is the mean value of the load-time pattern. Next, we will see how the load amplitude, required for calculating the stress amplitudes, can be determined in general.

Main causes for the development of load amplitude are the following:

- uneven torque supply and demand (operational features of the prime mover and the driven machine)
- dynamic features of the drivetrain elements
- nature of the carried-out technological process
- frequent starting

The above effects act as excitation effects in a flexible system susceptible to oscillation. The prerequisite of an accurate stressing is to know the load-time pattern as precisely as possible.
Methods for determining the loads:

- Measuring: most accurate, but can only be carried out on an operating machine
- Experience: with data measured on machines with similar parameters
- Load model: by creating a load model based on the nominal performance of the prime mover, and the measured data of machines with similar parameters.
- Calculation: with dynamic modelling

If the drivetrain is not designed for an operation in the resonance range, the load-time pattern can be determined with accurate approximation based on the load model, built up from the measured data on similar drivetrain.

1.1.1. The load model

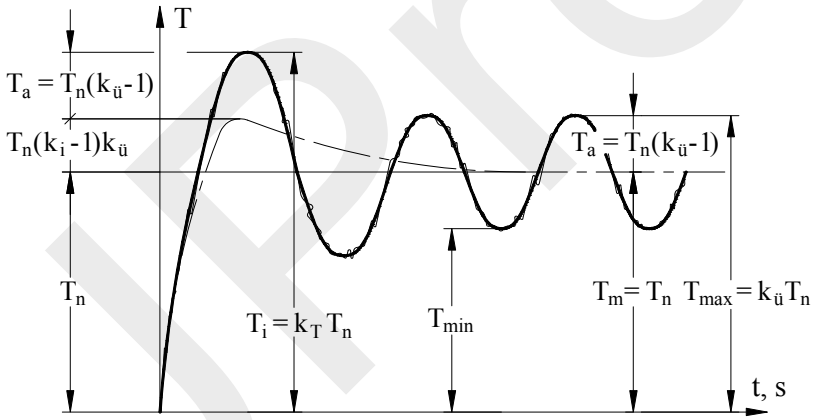

Figure 1.2: The load amplitude and the starting overload
Source: [1]

In order to build up the load model we need $k_{ü}$ operation factor and k_i starting factor aside from the P_n nominal performance. These values depend on the prime mover and the driven machine, so it takes technological process carried out into consideration. Their values have been measured on several different machine groups, and then assembled in engineering directives. We will later see that during the design of different drives (e.g. belt drives) the maximum transmittable performance is derived from the nominal performance and an appropriately chosen factor, which basically corresponds to $k_{ü}$ operation factor. The value of $k_{ü}$ will be detailed in the chapter of the belt drive. The load at starting:

$$T_i = k_T T_n \tag{1.1}$$

where: k_T – overload factor

$$k_T = k_i k_{ü}$$

In non-transient operation the load altering with the time may cause fatigue, this is why we have to check the parts against fatigue. The load amplitude on the basis of the Fig. 1.2:

$$T_a = (k_{ü} - 1) T_n \tag{1.2}$$

The load alternating in time, in the case of a non-transient operation:

$$T_{(t)} = T_n + T_a \sin \omega t \tag{1.3}$$

where: ω – angular frequency of the excitation effects

By choosing the longitudinal dimensions of the machine parts (which later can be modified) and by knowing the loads, the load diagrams can be draw and the medium σ_m and amplitude stresses σ_a can be calculated. The most important requirement during stressing is that the machine part works without failure during its service life. The part is safe to operate if the coefficient of safety is:

$$n = \frac{H_{(t)}}{T_{(t)}} \geq 1 \tag{1.4}$$

where: $H_{(t)}$ load limit

$T_{(t)}$ load

As the load limit (in this case the endurance limit) depends on the material and the load-time pattern, we have to apply a stressing method, considering this relation appropriately (c.f. Goodman and Smith diagram).

If the cycle number of the load alteration of the machine part, for which stressing has to be carried out is planned to be:

- $N = 10^4 - 10^7$ with a prescribed survival probability, we can determine the endurance limit for a given service life applying the Wöhler diagram. For instance, choosing rolling bearings or stressing machine parts of an airplane are carried out this way, as well.
- $N > 10^7$, we have to stress for fatigue. The endurance limit R_{D_a} required for stressing for fatigue, will be determined with 1the Smith diagram.

The coefficient of safety for fatigue is:

$$n_f = \frac{k_1 k_2}{\beta} R_{Da} \frac{1}{\sigma_a} \tag{1.5}$$

where: β fatigue stress concentration factor

k_1 surface finish factor

k_2 size factor

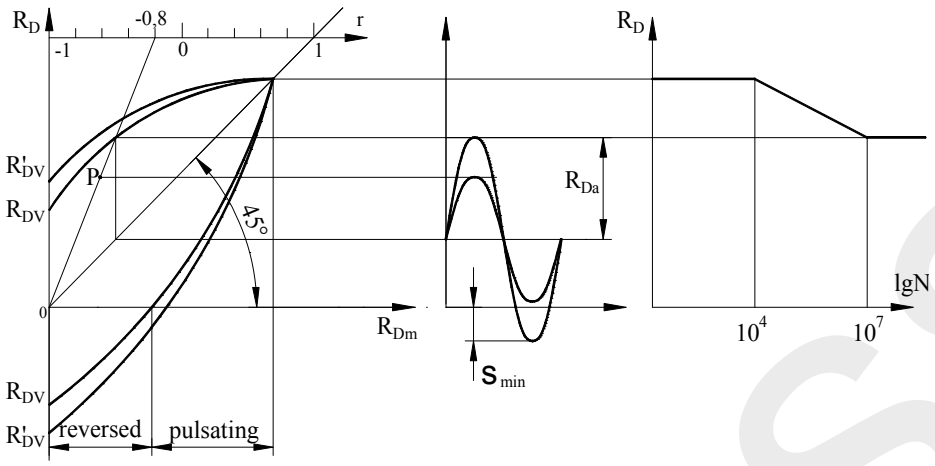

Figure 1.3: Smith diagram

The Smith diagram, determined for given materials through experiments, is valid only for test specimen, that is why the shape of the parts and the type of the stress are taken into consideration by using β, whereas the size and surface finish of the part are taken into consideration by using k_2 size and k_1 surface finish factor. These coefficients are determined experimentally, by using them we will get a safety diagram of decreased surface area, characteristic to the shape and finishing of the given machine part. When determining the coefficient of safety, the main uncertainty is caused by the lack of knowledge regarding the load-time pattern. The coefficient of safety geometrically expresses in which way point P, corresponding to the state of stress arising at a given load, will get out of the safe area.

For determining the fatigue amplitude stress, we usually use the $\frac{\sigma_a}{\sigma_m} = cons.$ stress model see Fig. 3. The Smith diagram represents the mean and amplitude stresses arising in the particular cross section. The factor of safety may be determined by the ratio of the sections specified by applying different stress models. Commonly the $\frac{\sigma_a}{\sigma_m} = cons.$ model is applied.

Its disadvantage is that, although it can be applied simply by graphic representation, it has to be constructed.

1.1.2. Fatigue failure theories

The brittle or ductile character of a material is relevant to the mechanism of the fatigue failure. However the distinction between ductile and brittle material itself is not simple. Brittle and hard materials suffer a brittle fracture with little or no deformation hence the fracture criterions are applied for checking against fatigue. In mild steels highly localized yielding occurs this is why yield criterions are applied for

checking the parts made of these materials. For preliminary design commonly the Goodman criterion may be applied with almost any material, see Fig. 1.4.

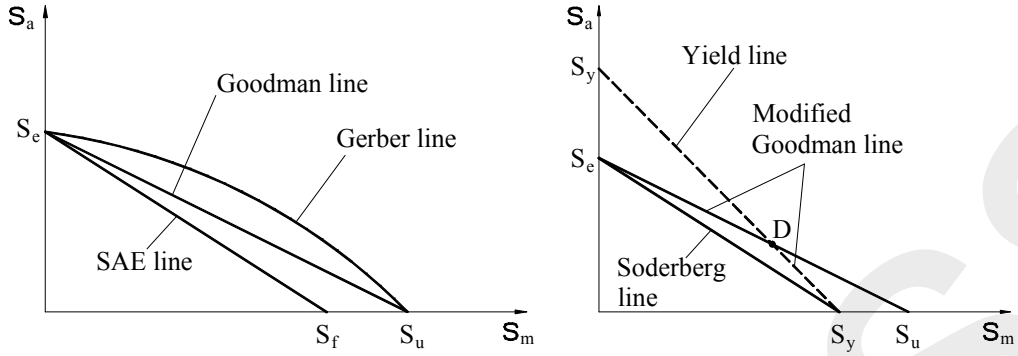

Figure 1.4: Fatigue diagrams
Source: [2]

From the above represented criterions we review the modified Goodman theory, which application results in similar achievement as one gained by the application of the Smith diagram with the assumption of $\frac{\sigma_a}{\sigma_m} = cons.$ model.

1.2. Design for simple fluctuating load

The modified Goodman theory is the combination of the Goodman and the Yield theories, which lines have an intersecting point D.
The intersection point of the lines:

$$D = \frac{R_{Dv}(R_m - R_{eH})}{R_m\left(R_{eH} - R_{Dv}\right)} \tag{1.6}$$

The equation of the Goodman line applied for checking, if ($\frac{\sigma_a}{\sigma_m} \geq d$):

$$\frac{\sigma_a}{R_{Dv}} + \frac{\sigma_m}{R_m} = 1 \tag{1.7}$$

The equation of the Yield line applied for checking, if ($\frac{\sigma_a}{\sigma_m} \leq d$):

$$\frac{\sigma_a}{R_{eH}} + \frac{\sigma_m}{R_{eH}} = 1 \tag{1.8}$$

The endurance limit of the part can be determined from the endurance limit of the material by taking the shape and the surface finishing of the part and any other influencing conditions into account. The factors expressing the influencing conditions are determined experimentally.

$$R'_{Dv} = C_f C_r C_s C_t \left(\frac{1}{K_f}\right) R_{Dv} \tag{1.9}$$

where:
- R_{Dv} completely reversed endurance limit of the test specimen
- R'_{Dv} c completely reversed endurance limit of the a member
- C_f surface finish factor
- C_r reliability factor
- C_s size factor
- C_t temperature factor
- K_f fatigue stress concentration factor

Now we are introducing the application of Goodman theory ($\frac{\sigma_a}{\sigma_m} \geq d$).

For designing purpose let substitute the R_{Dv} / n and R_m / n into the Eq. 1.7:

$$\frac{1}{n} = \frac{\sigma_a}{R'_{Dv}} + \frac{\sigma_m}{R_m} \tag{1.10}$$

$$\frac{R_m}{n} = \sigma_m + \frac{R_m}{R'_{Dv}} \sigma_a \tag{1.11}$$

The factor of safety for simple fluctuating load:

$$n = \frac{R_m}{\sigma_m + \frac{R_m}{R'_{Dv}} \sigma_a} \tag{1.12}$$

1.3. Design for combined fluctuating loads

$$\frac{1}{n} = \frac{\sigma_{ea}}{R'_{Dv}} + \frac{\sigma_{em}}{R_m} \tag{1.13}$$

Applying the maximum distortion energy theory (HMH theory), the equivalent stress can be written in the following form:

$\sigma_{ea} = \left(\sigma_{xa}^2 + 3\tau_{xya}^2\right)^{1/2}$ equivalent amplitude stress

$\sigma_{em} = \left(\sigma_{xm}^2 + 3\tau_{xym}^2\right)^{1/2}$ equivalent mean stress

The factor of safety for combined fluctuating stress:

$$\frac{1}{n} = \frac{1}{R'_{Dv}} \left(\sigma_{xa}^2 + 3\tau_{xya}^2\right)^{1/2} + \frac{1}{R_m} \left(\sigma_{xm}^2 + 3\tau_{xym}^2\right)^{1/2} \tag{1.14}$$

The safety factors are based on the life limit of a ductile material. For brittle material the safety factors must be approximately doubled. Proposed values of the safety factor are as follows:

n = 1.25 to 1.5 for exceptionally reliable materials used under controlled conditions and subjected to loads and stresses can be determined with certainty.

n = 1.5 to 2 for well-known materials under normal operating conditions, subjected to loads and stresses can be determined.

n = 2 to 2.5 for usual materials operated under normal operating conditions, and subjected to loads and stresses can be determined.

n = 2.5 to 4 for materials of unknown strength under usual operating conditions, load and stress can be determined.

n =3 to 4 for well–known materials used under indefinite operating conditions or subjected to indefinite stresses.

2. Loads on rotating shafts and shaft bearings

The rotating shaft bearings are implemented either with sliding or rolling bearings depending upon the operation circumstances and the application field. The sliding bearings are applied commonly either for light load and where the construction should be simply in design or for shaft bearing subjected to extreme heavy operation circumstances and high rpm where rolling bearings could not operate.

Let's survey the sliding bearings featuring different lubrication conditions:

- dry lubrication sliding bearing: it is applied where the lubrication is not permitted or because of the high operation temperature the lubrication is not feasible. A reasonable friction condition is provided by the appropriate choosing of the bearing bushing. Typical application field: food industry, chemical industry, pharmacy, metallurgy and other high temperature workshops.
- mixed lubrication sliding bearings: the peaks of the irregularities of the shaft and bearing surfaces touch each other and the load bearing is shared by the metal contact and the lubrication. The mixed lubrication condition may be sustained by intermittent lubrication. Typical application field: light load, low rpm shaft bearing where the construction is simply in design.
- hydrodynamic lubrication sliding bearings: it may be implemented either with hydrostatic or with hydrodynamic bearings. The oil pressure required for the hydrodynamic lubrication is provided by an oil pump in the case of hydrostatic bearing, whereas in the case of hydrodynamic bearing it is provided by achieving a required rpm. The service life of this bearing is infinite since there is no metal contact hence wearing. Typical application field: high rpm turbine shaft bearing, crankshaft bearing of internal combustion engines.

The production of sliding bearings normally does not require special machines and manufacturing technology. This is why it is a relative cheap bearing. Its repairing and replacement require subsequent machining, thus it is time consuming.

Power transmitting shafts bearings, apart from the turbine shaft bearings operating at high rpm, are implemented with rolling bearings. Its advantages are that, although the service life of the bearing is limited (the selection is based on the S-N curve of the

bearing), it can be replaced simply and the special supporting demands of the bearings may be implemented by the application of appropriate bearing type.

2.1. Designing criterions of shaft bearings

When designing shaft bearings it is a basic rule to support the shaft radially at least at two places, and to retain the shaft axially in both directions. For instance, the crankshaft bearings of the four-cylinder internal combustion engine, which is supported radially by three or five shaft bearings, is retained axially by sliding bearings in both directions, at one of the shaft bearings. If we carry out axial retainment in both direction with only one bearing, then this bearing will be the locating bearing, the rest of them will be non locating (floating or dilatation) bearings. This bearing method is usually used for shafts with greater length to diameter ratio. Either the outer ring of the floating bearing can slide in the seat of the bearing housing, or the inner ring can slide along the seat of the shaft, or the axial displacement can occur inside the bearing, itself. Floating bearings are capable of carrying on only radial reaction forces. If axial retainment is ensured by two separate bearings, we talk about cross locating bearings. It is important to allow an adequate axial clearance between the two bearings, and to adjust it correctly during assembly in order to ensure play for dilatation caused by change in temperature. Usually, the axial load of shafts arises only from external loads, however there are bearing types, for instance taper-roller bearings, where the radial load can accommodate axial reaction forces due to the cone angle of the raceway; these reaction forces are supported by the other bearing built in “O” or “X” arrangement. In case of bearings of special design, these reaction forces arising from external or internal loads have to be calculated according to the instructions of the product catalogue.
There are several technical solutions for the same shaft bearing implemented with different type of bearings. The optimal construction may be designed considering the bearing stiffness, flexibility and the running accuracy requirements. The price of the rolling bearings depends on its type and dimensions. This is why if there is no special technical requirement then the previous aspect should be considered (most often applied rolling bearing is the single row deep grooving ball bearing).

2.1.1. Shaft bearing options

When designing shaft bearings we have to be familiar with the features of the available bearing types, its angular and radial stiffness. Bearings are grouped according to its line of action determining commonly the feasible supporting and retaining tasks.
The line of action is the line in which direction the rolling elements transmit the load from a ring (disc) to the other one. This way the load gets from the shaft to the bearing housing.

The angle of action is the angle between the line of action and the plane perpendicular to the axis of rotation.

Bearings with feasible line of actions:

1. Bearings having the line of action perpendicular to the axis of rotation: $\alpha = 0°$
   Eligible bearings: needle-roller bearing, cylindrical roller-bearing without supporting discs.
2. Bearings having variable angle of action: $\alpha = \alpha_{(F_a)}$

   The actual angle of action is determined by the ratio of the acting radial and axial bearing forces.
   Eligible bearings: deep grooved ball bearings, self aligning ball and roller bearings.
3. Angular contact bearings: $0^0 \leq \alpha \leq 90°$
   The race way lays at a particular angle to the axis of rotation.
   Eligible bearings: angular contact ball bearings, taper roller bearings.
4. Bearings having the line of action parallel to the axis of rotation: $\alpha = 90°$
   Eligible bearings: Single and double row ball thrust bearings.

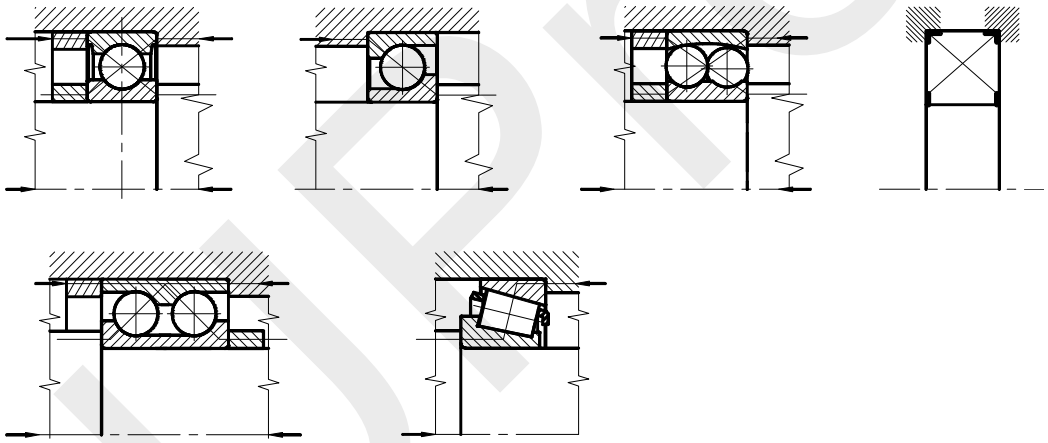

Figure 2.1: Eligible bearings with the lines of action

Bearings in the shaft bearing system have different tasks. The given tasks may be achieved by different bearing types with the appropriate supporting of their rings. When dismantling a shaft bearing assembly, we have to record the place and position of every component like: distance disc, distance piece, position of the bearings for the assembly. If the shaft bearing assembly is reassembled not properly, it causes the premature failure either the bearings or the parts assembled on the shaft, e.g. gear drive. It is expedient to make a rough sketch of the bearing construction revealed at dismantling, and we have to understand the operation of the shaft bearing to be able to carry out the reassembly professionally. Fig. 2.1 shows different bearing types with the appropriate ring retaining requirements for radial and axial loads. The lines

of action represent the transmission of the bearing forces from the shaft to the bearing housing.

2.1.1.1. Radial supporting

The radial supporting works as a non-locating bearing.

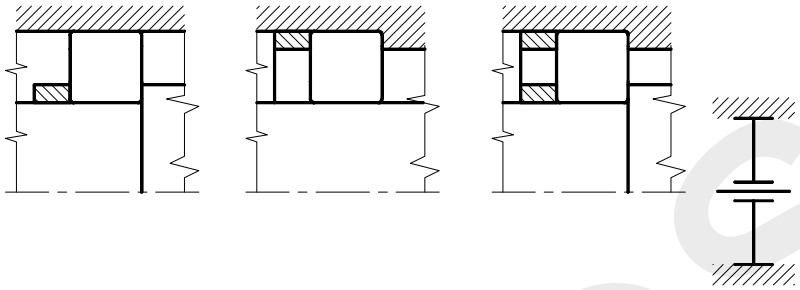

1-2 bearings 3-4 bearings

Figure 2.2: Radial supporting

Some bearings of the shaft bearing assembly must be constructed to take up only radial forces. It can be implemented either by bearings appropriate only for taking up radial forces (e.g. cylindrical roller-bearings) or by variable angle of action bearings with appropriate retaining of the bearing ring in order to take up only radial forces (floating bearings).

Fig. 2.2 shows four bearings with the necessary bearing ring retaining acting as floating bearing.

1. deep groove ball bearing
2. self aligning ball and roller bearings
3. cylindrical roller-bearing without supporting discs
4. needle-roller bearing

2.1.1.2. Radial supporting and both axial direction retaining

The bearing works as a locating bearing.
Locating bearings require the retaining of both bearing rings in both axial directions.
Eligible bearings:

- deep groove ball bearings
- self aligning ball and roller bearings
- double row angular contact ball bearing
- cylindrical roller-bearing without supporting discs

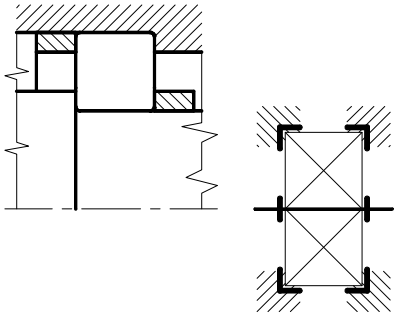

Figure 2.3: Locating bearing

2.1.1.3. Radial supporting and one axial direction retaining

The bearing works as a cross locating bearing.
Eligible bearings with appropriate retaining of bearing rings:

- deep groove ball bearing
- self aligning ball and roller bearings
- single row angular contact ball bearings
- taper roller bearings

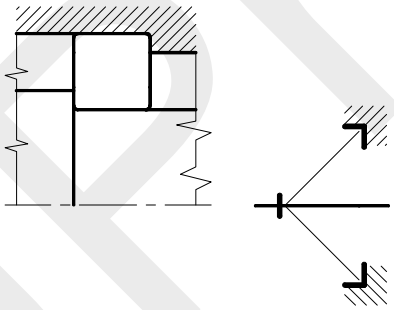

Figure 2.4: Cross locating bearing

2.1.1.4. One axial direction retaining

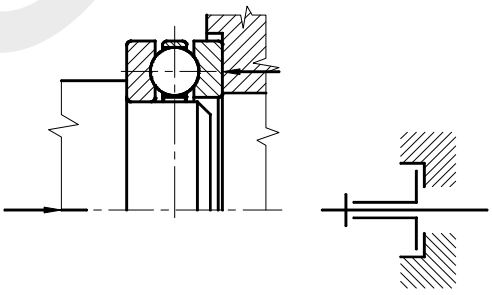

Figure 2.5: Bearing retaining of a single row thrust ball bearing

Pure axial direction retaining can be carried out with thrust ball bearings. When designing the bearing housing the bearing disc can't be supported radially in the housing, this is why the bearing can't transmit radial force to the housing. The other disc has to be fitted on the shaft of course.

2.1.1.5. Both axial directions retaining

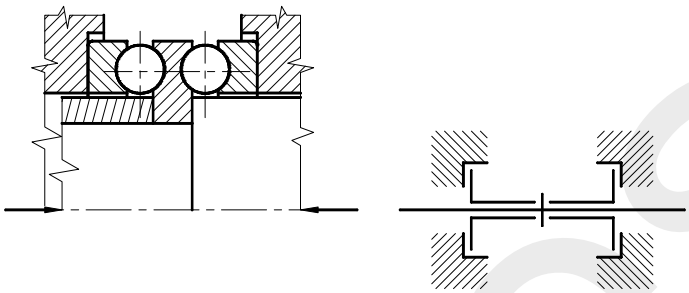

Figure 2.6: Bearing retaining of a double row thrust ball bearing

The central bearing disc has to be fitted and retained on the shaft in both axial directions by a shaft shoulder and e.g. distance piece. The two outer discs mustn't contact neither the bearing housing nor the shaft in radial direction.

2.1.1.6. Large angular stiffness shaft locating bearings

Eligible bearings for large angular stiffness shaft bearings:

- single row angular contact ball bearings in pairs
- taper roller bearings in pairs

The „O" and „X" arrangement designations refer to the position of the line of actions of the bearings, see Fig. 2.7 and Fig. 2.8.. Out of the two arrangements the „O" one has bigger angular stiffness due to the greater retaining distance.

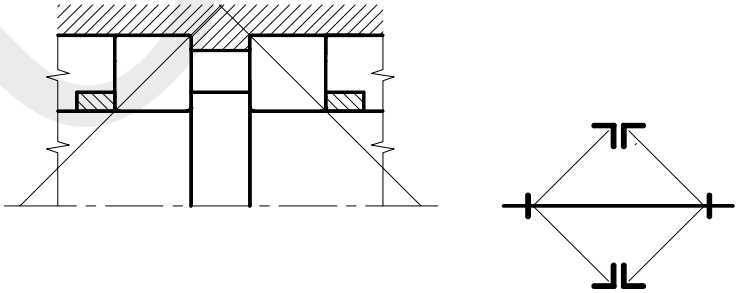

Figure 2.7: O arrangement shaft locating bearing

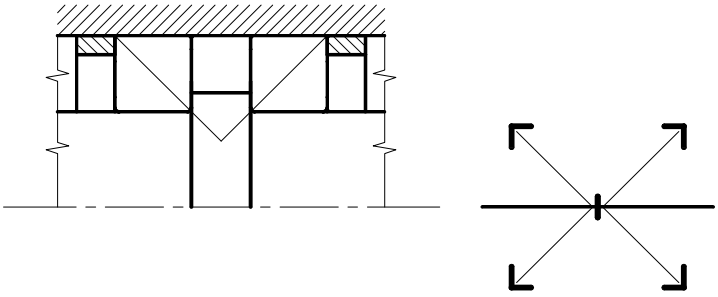

Figure 2.8: X arrangement shaft locating bearing

2.2. Shaft bearing constructions

The bearing of the shaft may be implemented by the appropriate application of the above detailed shaft supporting and retaining bearings. When designing the following rules have to be complied with:

- the shaft must be supported radially at least two places,
- the shaft must be retained axially in both directions implemented either by one bearing or in two different bearing places.

2.2.1. Locating and non-locating bearing arrangements

The locating and non-locating bearing arrangements are applied for shafts, having a great length in proportion to its diameter, which longitudinal dimensional change because of its dilatation is bigger than the working clearance of the bearings that could cause becoming stuck of the shaft. The required dimensional change is provided by the non-locating bearing allowing axial displacement. The locating bearing can be implemented either with one bearing (see Fig. 2.9.a) or with large angular stiffness shaft locating bearings (O or X arrangements, see Fig. 2.9.c and d), or the axial and radial loads can be shared with the separated bearings appropriate only for radial supporting and for both axial directions retaining respectively (see Fig. 2.9.b). The possible solutions are demonstrated by the line of actions of the bearings. The optimal solution from the feasible constructions may be chosen considering the order of magnitude of the bearing forces, the angular stiffness and the running accuracy requirements. The corresponding bearing type may be chosen with respect to the bearing rings retaining requirements.

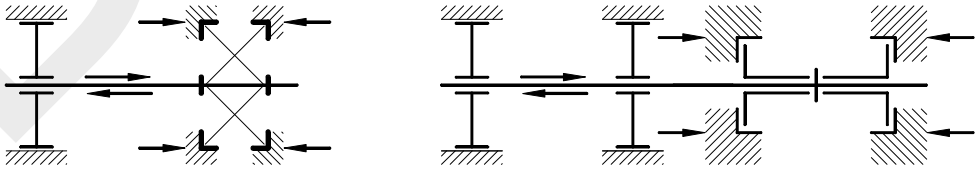

a. b.

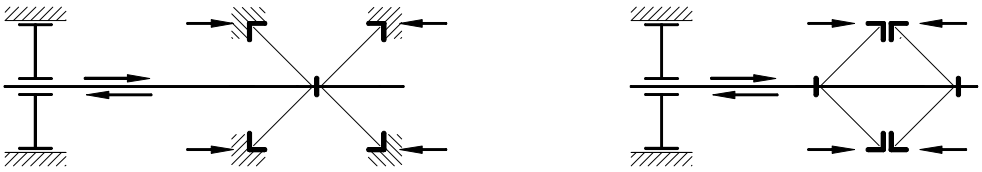

c. d.

Figure 2.9: Locating and non-locating shaft bearing arrangements

2.2.2. Cross located bearing arrangements

These arrangements may be applied for short shaft length having a smaller longitudinal dimensional change due to its dilatation than the axial working bearing clearance. Considering the bearing forces the following arrangements may be applied:

- Cross located, floating bearing arrangements: In the case of moderate axial loads single row deep groove ball bearings or self aligning ball (roller) bearings may be applied. The axial play of the shaft is adjusted by gaping the floating rings with the bearing housing caps.
- Cross located adjusted bearing arrangements: For greater axial load angular contact ball bearings or taper roller bearings may be applied in O or X arrangements. The axial play of the shaft is the adjusted bearing clearance. The bearing clearance is adjusted with feeler gauge when having easy access to the raceway and the rolling elements, or with dial gauge in the case of smaller bearings. When the construction is simply in design the bearing clearance may be adjusted by loosening the shaft nut with a specific degree in the knowledge of the thread pitch.
- Thrust ball bearings application individually for taking up the axial loads.

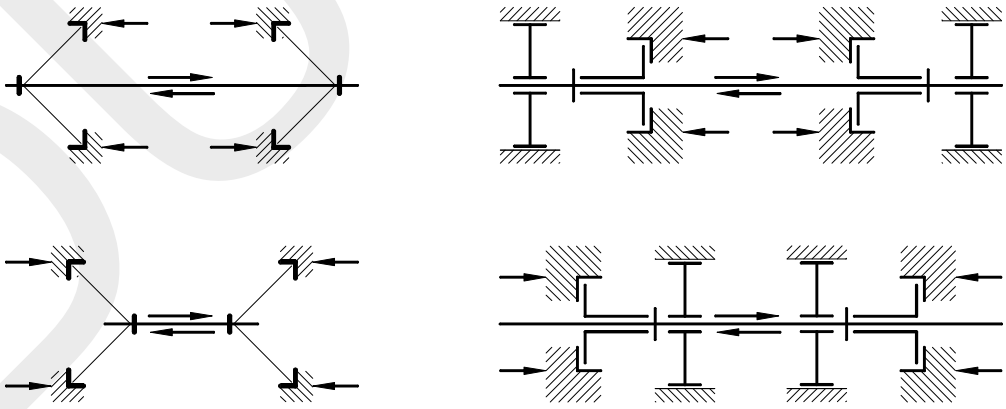

Figure 2.10: Cross located bearing arrangements

2.3. Selection of fit, general guidelines

As you saw, different supporting and retaining requirements may be implemented by different bearing types with the appropriate bearing ring retaining. For example, a deep groove ball bearing can operates as a locating bearing if its both bearing rings are retained in axial direction and as a non-locating bearing if one of its rings is not retained at all in axial direction. However this ring should slide either on the sit of the shaft or in the seat in the housing, which can be ensured by the prescription of the appropriate fit. However the fit influences the working clearance of the bearing having a direct effect on the running accuracy and the service life of the bearing. Due to the fact that the selection of fit is a very complex task, we will go into details in the following chapters.

2.3.1. Tolerance of the diameter of the bearing rings

The tolerances of the bearing rings diameters are set forth in international standards different from the ISO standard, see Fig. 2.11.

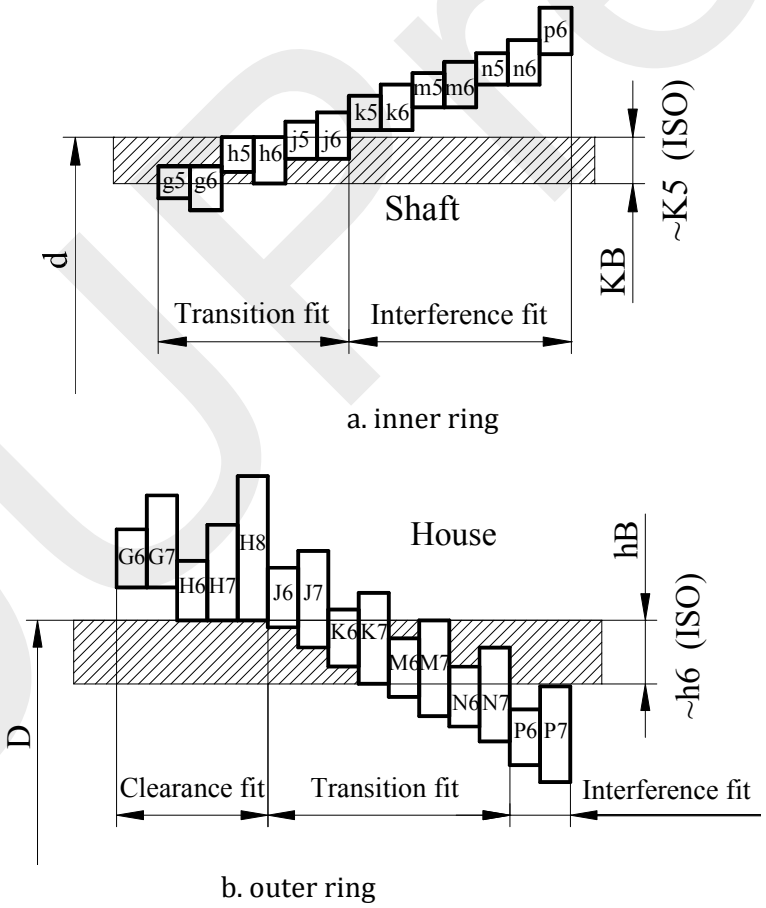

Figure 2.11: Tolerance zone of the bearing rings

However the tolerances of the parts connecting with the bearing rings (the shaft diameter and the hole diameter of the bearing housing) have to be prescribed in the ISO system, since the manufacturing accuracy is based on this system. Fig. 2.11.a. shows the position of the hole tolerance of the inner ring (KB) relating to the nominal size (base line) which corresponds approximately to the K5 hole tolerance in the ISO system, while the Fig. 2.11.b. pertains to the tolerance of the outer ring (hB) which corresponds approximately to the h5-h6 ISO tolerances. The proper fit can be achieved by prescribing the tolerance of the shaft diameter and the bearing housing on the basis of Fig. 2.11.

Aspects of fitting bearing rings

The load carrying ability of a bearing may be fully utilized if its fitted ring is supported fully around its circumference. The support must be firm and bearing rings must be secured to prevent them from turning on or in sit under load. However, when easy mounting and dismounting are desirable or when axial displacement is required, with non locating bearing an interference fit cannot always be used. Aspects for selecting fits:

1. bearing clearance
2. ring wandering
3. axial displacement facility
4. mounting and dismounting facility

2.3.1.1. Bearing clearance

Depending upon the bearing type, different bearing clearances may be defined. It can be defined in radial and in axial directions. The bearing clearance is the measure of the displacement of the rings relative to each other traveling from one terminal position to the other one in radial and axial directions.

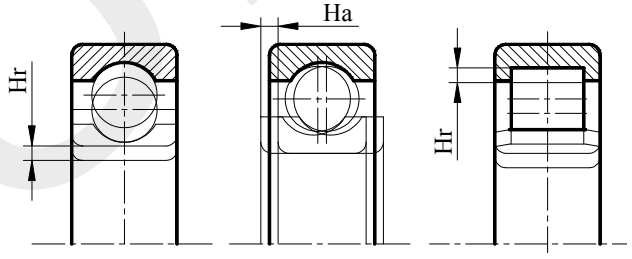

Figure 2.12: Definition of the bearing clearance

In the case of not separable bearings the following clearances may be defined:

- initial clearance
- mounting clearance
- working clearance

The separable bearings feature mounting and working clearances however initial clearance, depending on its type, may be partially defined. For example a cylindrical

roller bearing features only radial initial clearance, but a taper roller bearing features neither radial nor axial one at all.

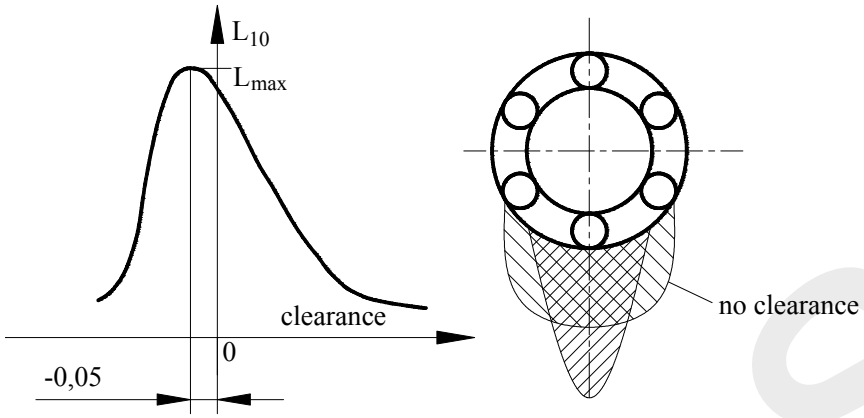

Figure 2.13: Effect of the bearing clearance on the servile life

The initial clearance of the bearing becomes mounting clearance after installation due to the bearing rings fit, which is decreasing further under operating circumstances because of the operation temperature until the working bearing clearance develops. The measure of the working clearance should be 0 or little prestressed in order to achieve the optimal service life.

The optimal service life may be achieved only with application of different initial clearance bearings considering the aspects of bearing fit and operational circumstances. The normal initial clearance bearings are not designated, the others differ from the normal one are designated with letters C_1-C_5 on the end face of the bearing ring, see Fig. 2.14. As an example we are referring to the application of the C_3 initial clearance deep groove ball bearings as the crankshaft bearings of the two stroke internal combustion engines, which are increased clearance bearings required because of the high operation temperature. The bearing clearance decreases always when assembling the bearing rings with interference fit. We have to consider the fact as well, namely the same fit of the rings results in different measure of bearing clearance decreasing and different join pressure between the outer ring and the bearing housing, adequately the bearing housing material and the wall thickness.

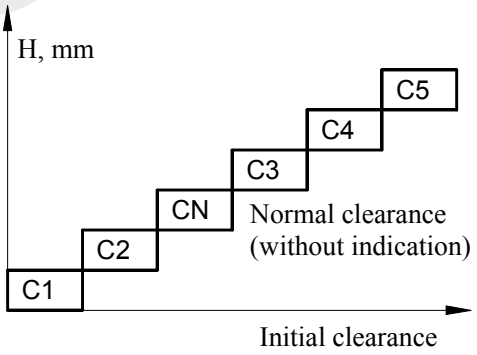

Figure 2.14: Initial clearance of the bearing

The proper operation of the rolling bearing can be ensured by the appropriate fit of the bearing rings (considering the ring wandering, axial displacement facility, mounting and dismounting facility) which should results in approximately 0 working clearance.

2.3.1.2. Ring wandering

In shaft bearings implemented by rolling bearing there can be relative turning only between the bearing rings or discs. Accordingly neither the inner ring on the shaft nor the outer ring in the housing can turn not even if the bearing load enforced it.

The direction of load may be:

- stationary load which may cause:
  - rotating load on the rotating inner ring: all points of the raceway are subjected to load in the course of one revolution., see Fig. 2.15. To prevent bearing ring from turning (creep or wander) interference fit must be used between the inner ring and the shaft seating,
  - stationary load on the stationary outer ring: the load is always directed towards the same position on the raceway. The outer ring doesn't require interference fit.
- direction of load indeterminate: both rings must be fitted with interference fit. If the outer ring must be free to move axially in the housing, somewhat looser fit may be used.

Recommendations for fits considering the magnitude and direction of load are compiled in Tab. 2.1 and Tab. 2.2.

Table 2.1: Fits for solid steel shafts

Rotating inner ring load or direction of load indeterminate	Light loads, the axial displacement of inner ring on shaft necessary	j6
	Normal and heavy loads	k5, k6
	Very heavy loads and shock loads with difficult working conditions	n6
Stationary inner ring load	Easy axial displacement of inner ring on shaft desirable	g6
	Easy axial displacement of inner ring on shaft unnecessary	h6

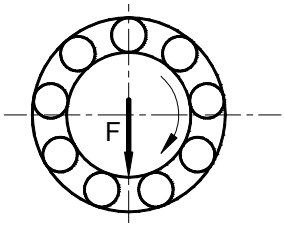

Figure 2.15: Definition of load direction

Table 2.2: Fits for cast iron and steel housings

Rotating outer ring load	Heavy loads on bearings in thin-walled housing	P7	cannot be displaced
	Normal and heavy loads	N7	cannot be displaced
	Light and variable loads	M7	cannot be displaced
Direction of load indeterminate	Heavy shock loads	M7	cannot be displaced
	Normal and heavy loads, axial displacement of outer ring unnecessary	K7	cannot be displaced as a rule
Direction of load indeterminate	Light and normal loads, axial displacement of outer ring desirable	J7	can be displaced
Stationary outer ring load	Light and normal loads with simple working conditions	H8	can be displaced
	Heat conduction through shaft	G7	can be displaced

2.3.1.3. Axial displacement facility

One ring of the non-locating bearing must be fitted appropriately in order to allow axial displacement. This ring can be subjected only to stationary load.

2.3.1.4. Mounting and dismounting facility

When designing a shaft bearing assembly the easy mounting and dismounting requirements of the parts may be considered. When dismounting a gear box or alternator housing by pulling away its two halves the rolling bearings stay either on the shaft or in the housing. If there is no other special requirement for the bearing fitting the intended position of the bearing after dismantling may be provided with the appropriate selection of the rings fit. If the bearing stays in the housing we should design threaded holes in the bearing houses to throw out the outer ring with screws. If the bearing stays on the shaft, a special puller may be used for replacing the rolling bearing.

2.4. Selecting bearing size using the life equations

The selection of rolling bearing is based on the magnitude of the load causing failure. The raceway of the bearing rings or discs are subjected to pulsating load because of revolving of the rolling element on it which may result in the fatigue of the raceway surface.

The selection of the rolling bearings with 90% survival probability is based on the S-N curve of the particular rolling bearing. If the bearing is well maintained and operates at moderate temperature, metal fatigue is the cause of failure alone. Namely the contact stress occurs on the raceways and on the rolling element are higher than the endurance limit of the material.

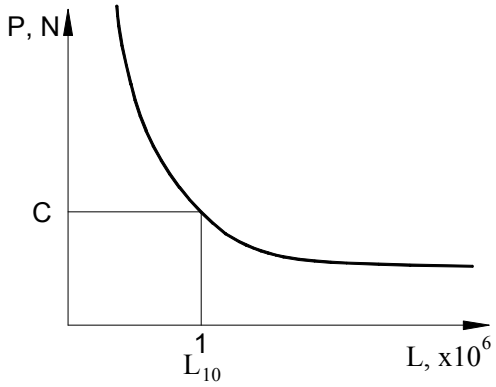

$$L_{10} = \left(\frac{C}{P}\right)^{p}$$

p=3 for ball bearings

p=$\frac{10}{3}$ for roller bearings

Figure 2.16: S-N curve of the rolling bearings

This is why the rolling bearing has limited life. The reason for any other bearing failure may be the not expert mounting, the operation not under the design circumstances which consequents are the overload, the overheating and the unsatisfactory lubrication condition.

The designed service life of the bearing depends on the application field of the machine determining the equivalent dynamic bearing load desired. The S-N curves of the different bearing types with different sizes are identified by two matching points. These are the C basic dynamic load rating and the L_{10}=1, the service life expressed in millions of revolutions. Accordingly, the servile life is 1 million revolution if the C is the equivalent dynamic bearing load.

Desired service life of the bearing depending upon the application field:

L_h [hours]	4.000 – 8.000	intermittent operation
	14.000 – 20.000	8 hours operation a day
	50.000 – 60.000	continuous operation

The service life:

$$L = L_h[h]n\left[\frac{1}{min}\right]60\left[\frac{min}{h}\right]\frac{1}{10^6} \qquad (2.1)$$

The basic dynamic load rating:

$$C = \sqrt[3]{L}P \qquad \text{ball bearings} \qquad (2.2)$$

$$C = \sqrt[\frac{10}{3}]{L}P \qquad \text{roller bearings} \qquad (2.3)$$

where: P [kN] equivalent dynamic bearing load

The method of determining the P equivalent dynamic bearing load for different bearing types based on the bearing forces are detailed in bearing catalogues.

3. Designing drivetrain

Loads on the shafts are transmitted through the bearings onto the bearing housing in the form of reaction forces that can be calculated on the basis of our statics studies. For calculations we need to determine the external loads. In order to build an adequate mechanical model we have to realize all acting forces and loads as adequately as possible. This is the key point during stressing, since we have to be fully familiar with the operation features of the machine group, nobody will specify the loads instead of us, and the consequences of the stressing carried out by wrongly or incompletely assumed loads, will be realized only during test operation. In the following chapters we demonstrate through simple examples, what are the types of loads can occur in the case of different drives and drive components.

3.1. Prime mover output

The fundament for clarifying the power-output of the prime mover is the energy equilibrium. Basically all perpetual motion machines exist only in imagination, none has ever been made, and their theory fails on this equation; that is energy cannot be created or extinguished, but it can change form. Although, in a wider sense, there are no losses in a given system, the expression of mechanical loss, used in engineering terminology, is correct, since it expresses what amount of the available energy cannot be transformed into mechanical energy. Using incorrect engineering terminology can easily lead to misunderstandings, for example if we simply use the expression 'losses' instead of 'mechanical losses'. When determining the power-output transmitted through a drivetrain, we first have to define if the predefined performance of the prime mover is mechanical performance, or if it refers to all forms of energy provided by the prime mover. The mechanical energy provided by the prime mover compared to the utilized amount of energy (fossil, electric, etc.) can be characterized by the mechanical efficiency of the prime mover, which is around 30-35% for gasoline engines, 40-45% for diesel engines and 60-80% for electric motors.

It means, that by burning fuel, a gasoline engine utilizes about 1/3 part as mechanical energy, 1/3 part gets out in the environment in the form of heat with exhaust gases, and the rest 1/3 is radiated to the environment also in the form of heat from the operating engine and through the cooling system. In the case of internal combustion engines and electric motors, usually the value of the mechanical performance is provided in the owner's manual, since this parameter is required for the operation of the engine. In the case of electric motors, it is necessary to provide information on the total electrical performance, because when connecting the electric motor to the

power network we have to know the current drain of the motor. For example, the following information can be found on an LG-brand hoover: nominal performance of the electric motor: 1600W, suction power: 340 W. The available suction power depends on not only the efficiency of the electric motor, but on the efficiency of the whole, electric motor-driven hoover machine. The difference between the two powers is radiated in the form of heat flow into the environment, and heats up in a short period of time, for example, a small closed room.

Regarding the mechanical performance provided by the prime motor, there is one important notion to clarify: the prime motor provides exactly as much mechanical power, as much is taken up by the machinery through the drivetrain. This mechanical performance take-off can only be increased until the point the prime mover can deliver. If we detach e.g. an electric motor from the drivetrain, the momentary electric power of the motor (calculated from its current drain) will cover the heat flow generated from the mechanical losses, the warming-up of the motor inevitable and the air resistance. In other words the electric power of the motor is used in its entirety for heating the environment.

The performance provided by different prime mover depends on their construction and load level. During stressing we have to consider the torque of the motor shaft as the nominal torque, based on which the load model is built. The motor torques pertaining to different motor RPM's are included in the motor characteristic curves, which will be discussed later in the chapter for prime mover characteristic curves.

3.2. Inertia of the translating and rotating elements

The power transmitting elements of the drivetrain can carry out translating and rotating movements at altering velocity and angular speed. Altering velocity results in dynamic effects because of accelerating-decelerating masses and mass moments of inertia of parts, that have to be taken into account with supplementary force ($F_d = ma$) and supplementary torque

($M_d = J\varepsilon$). It follows, that if we bring a drivetrain with great RPM and great mass moment of inertia to a stop in a short period of time, the supplementary torque ($M_d = J\varepsilon$) may exceed the transmittable torque on the given section of the drivetrain, resulting in fracture. A quick starting of the drivetrain can result in a similar situation, in which case we can decrease the supplementary loads by installing e.g. a centrifugal clutch.

3.3. Dynamic force arising from external actions

Depending on the technological process carried out by the machinery, the effects of collision of moving masses have to be taken into account. The collision may result in different forces depending on the elasticity of the impact point. Let us assume a

simple example, where we examine the impact of an element with mass 'm', and the mechanical stress of the given machine part has to be determined. The dynamic force can be determined by the following equation: $F_d = ma$. The main difficulty here is to determine the deceleration of the impacting mass. Although there are already high-speed cameras, with which we can even track a bullet shot from a gun, thus determining its deceleration, these are not necessarily available to us at any time. We can also use a decelerometer, which is usually applied in measuring techniques. It is built in the impacting mass and directly measures deceleration. Of course the decelerometeris only a part of the measuring system, in order to get usable data, we need to have the whole measuring system: data acquisition, amplifier, evaluating software. If the measuring system is not available, then we can proceed from the spring model of the given machine part. The machine part's spring diagram may be determined by static measuring, by measuring the load and deformation (deflection). Afterwards, measuring the deformation (deflection) at impact, F_d dynamic force may be determined on the basis of the predefined spring diagram.

3.3.1. Radially load-relieved drivetrains

Let's study the operation of the pillar drilling machine drilling a workpiece vertically. We can assume that the cutting edges of the drilling tool are symmetrical. The cutting forces equalize each other radially, so no radial load will act either on the drilling tool or the shaft of the electric motor. The shaft's load derives from the torque provided by the electric motor, so we have to carry out stressing for pure torque. Ideally, the shaft bearings are loaded only by the own weight radially, in case of vertical position not even by that.

3.3.2. Load pattern of the rotating shaft

Elements of the drivetrain are subjected to altering loads due to uneven torque supply and demand. The load-time pattern may be modelled by defining the $k_{ü}$ and k_T coefficients. As the load amplitude is superimposing to the mean value calculated from the nominal performance, the load is fluctuating. However, in the case of rotating shafts, cross-sections rotate, so the mean stress is zero and the stress amplitude $\sigma_a = k_{ü}\sigma_n$, hence the stress is reversed.

3.3.3. Loads arising from belt drives

Belt drives are frictional connection drives. Performance transmitting is carried out by peripheral force acting on a given disc diameter. However, the peripheral force provides not only torque, but at the same time results in radial loads, as well. Radial loads may be taken into account with the pretention load of the shaft necessary for

tensioning the belt. This has to be considered when drawing the load diagrams of the shaft, as well. When designing the belt drive we start out with the nominal performance, from which the transmittable performance can be calculated after defining the $k_{ü}$ operation coefficient. The belt profile and the number belts depend on the transmittable performance.

Table 3.1: c_2 operation coefficient of the belt drive

Driven machine	**Prime mover**	
	mono-phase electric motor with starting torque, tri-phase totally enclosed electric motor (normal starting torque) direct-current motor, internal combustion motor and turbine $n > 600\frac{1}{\min}$	mono-phase electric motor with starting torque, tri-phase totally enclosed electric motor (normal starting torque) direct-current motor, internal combustion motor and turbine $n \le 600\frac{1}{\min}$
	c_2	c_2
Light operation Centrifugal pumps, compressors, fans	**1.1**	**1.3**
Medium operation Sheet cutter, press machines, vibrators, machine tools,	**1.1**	**1.4**
Heavy operation Piston compressor, press machines, excavators, forging machine,	**1.2**	**1.6**
Extreme operation grinder, stone-breakers, manglers, woodworking mach.	**1.3**	**1.8**

In this chapter we use the notation system of "Optibelt", often applied for designing.

$$P_B = Pc_2 \tag{3.1}$$

where: P [kW] nominal performance

P_B [kW] design performance

c_2 operation coefficient

The value of c_2 operation coefficient depends on different for prime movers and driven machines, see Tab. 3.1 (this operation coefficient is used for building the load model). In the case of a belt drive containing 2 pulleys, driver and driven shafts are subjected to loads, arising from belt force, of the same value but acting in opposite directions.

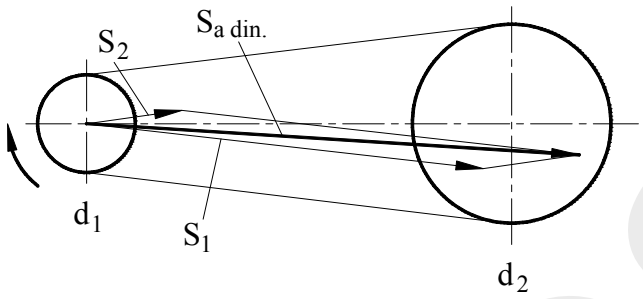

Figure 3.1: Belt side tensions and dynamic shaft force

In order to determine the exact value and direction of $S_{a\,dyn}$ shaft force, we have to determine S_1 tight and S_2 slack belt forces as vectors.

$$S_1 \approx \frac{1,02 P_B}{c_1 v} \tag{3.2}$$

$$S_2 \approx \frac{(1,02 - c_1) P_B}{c_1 v} \tag{3.3}$$

$$S_{a\,dyn} \approx \sqrt{S_1^2 + S_2^2 - 2 S_1 S_1 \cos\beta} \tag{3.4}$$

where: c_1 coefficient depending on the contact angle

β contact angle of the small pulley

v belt velocity

For simplified calculations the shaft force is assumed to be on the mutual centre-line and is calculated with the following equation:

$$F_{a\,dyn} = \frac{K - c_1}{c_1} \frac{c_2 P}{v} \tag{3.5}$$

where: K coefficient

$K = 3.0$ for classical V-belts

$K = 2.04$ for narrow V-belts

The calculated value of $F_{a\ dyn}$ equals approx. $F_{a\ dyn} = (2.3 \ \ldots \ 2.5) F_{per}$, where F_{per} is the peripheral force of the belt drive. The stressing of the shaft carried out by $F_{a\ dyn}$ belt force is adequate only if the belt is not over-tensioned. The belt tension is

appropriate if there is a given amount of deflection resulting from a prescribed pushing force acting in the middle of the belt. The following checking procedure is applicable for belt sections: SPZ, SPA, SPB, SPC, A/13, B/17, C/22, 25 and D/32.

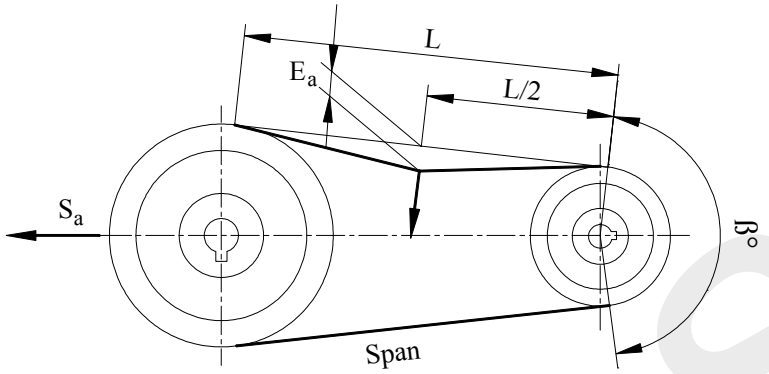

Figure 3.2: Belt tensioning

E = deflection of the belt on a 100 mm span (mm)
E_a = deflection of the belt on a given span (mm)
f = load applied for belt tensioning (N)
L = belt span (mm)
S_a = minimum static shaft load (N)
T = minimum static tension force per belt (N)

The static belt tension force can be determined with the following equation:

$$T_0 = \frac{F_a\, dyn}{2z} + kv^2 \tag{3.6}$$

$$T \approx \frac{1}{2}\frac{(K - c_1)}{c_1}\frac{P_B}{zv} + kv^2 \tag{3.7}$$

where: k [kg/m] belt weight per running meter
z number of belts

E, deflection of the belt on a 100 mm span can be determined from the following belt tension/belt deflection graph, see Fig. 3.3. E_a is the deflection of the belt on a given span:

$$E_a \approx \frac{EL}{100} \quad \text{[mm]} \tag{3.8}$$

$$L = a_{nom} \sin\frac{\beta}{2} \tag{3.9}$$

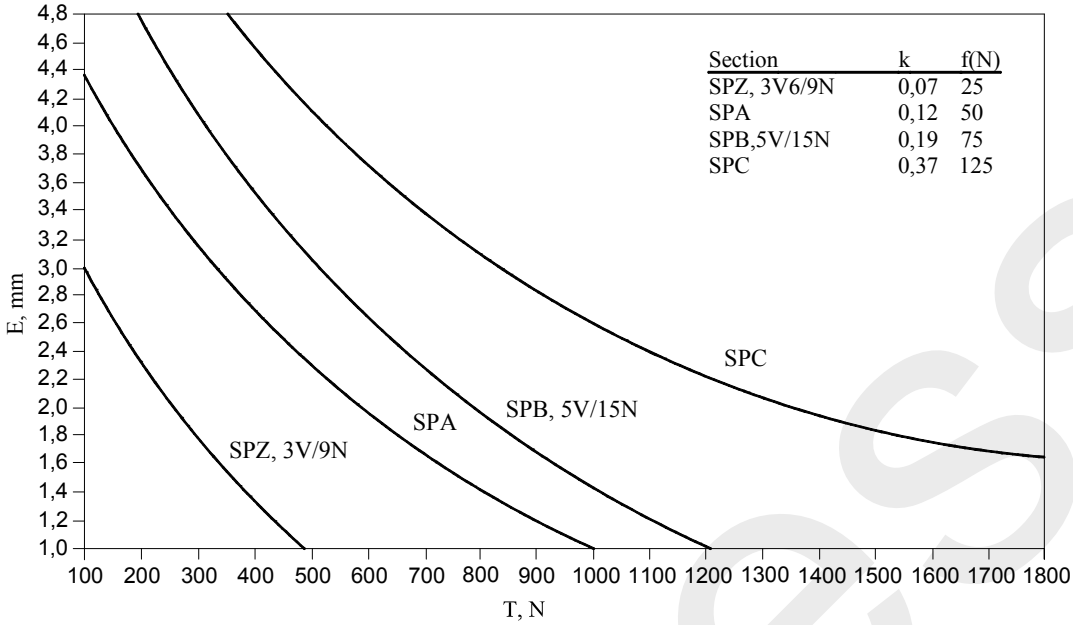

Figure 3.3: Magnitude of the belt deflection
Source: [5]

In order to adjust the belt tension to an adequate value, we have to modify the shaft distance, until we measure the prescribed E_a belt deflection for the given "f" load applied for the belt tensioning.

3.3.4. Loads resulting from chain drives

In contrast with belt drives, the transmittable performance and peripheral force does not depend on the tensioning in the case of chain drives. It follows, that chain drives are operable without tensioning, and very often they are used without it. Chain tensioning is usually used in order to avoid chain swinging, to position the driving and driven shafts (cam shaft of internal combustion engines), or to avoid tooth skipping on chain drives with low depth of teeth. It follows from the above, that the nominal shaft load resulting from the chain drive (of course also taking into account the own weight) is calculated from the peripheral force arising in the tight chain strand, which is determined from the torque to be transmitted. After moving the vector of the peripheral force parallel with itself to the centre-point of the sprocket, we resolve it to its components, corresponding to the planes, determined for calculating the reaction forces of the shaft.

When using roller chains we have to take into consideration the polygon effect, which, as we will see it, is determined from the tooth number of the smaller sprocket, see Fig. 3.4.

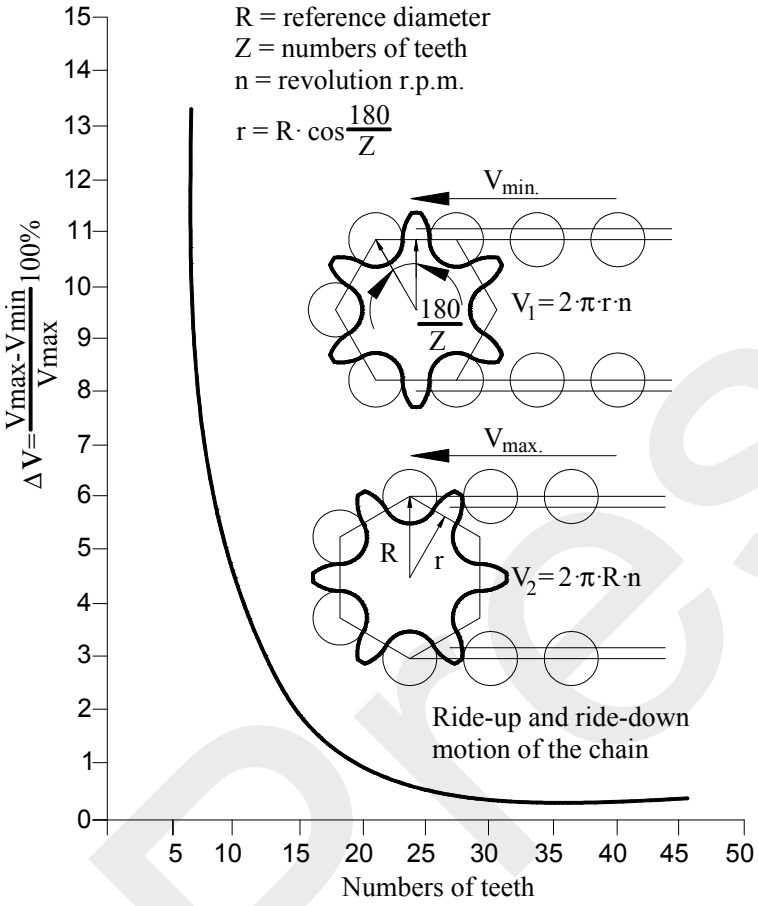

Figure 3.4: Polygon effect
Source: [6]

Its tooth number has to be selected considerately, since in order to ensure a given gear ratio, the tooth number of the larger sprocket only allows a small degree of chain wear, so the chain has to be changed often. The chain wear is characterized by the elongation of the chain, expressed in per cent. As a matter of fact, the chain does not strain itself, only its length changes, due to the fact that every second chain-link pitch will be greater, even if not necessarily equally. Wearing occurs between the bush of the inner link and the chain pin of the outer link, whereas chain pitch will remain the same between the bushes of the inner and the outer links. Due to the wearing the cross section area of the pins decrease till the fatigue fracture occurs because of the altering load (tight and slack belt sides). Based on experiences, below 1.5% of elongation of the chain no fatigue fracture of the chain pins are supposed. Commonly the allowed chain elongation may be 3% in case the consequence of the chain break is only a simply machine fault.
The Fig. 3.4 shows the effect of the tooth number of smaller sprocket on the polygon effect. To avoid its detrimental effect, the recommended tooth number of the sprocket:

9-10 teeth: to be avoided. Suitable for moving linkages, where smooth operation is not a requirement. Chain speed should be lower than 1 m/s.

10-12 teeth: chain speed up to 2 m/s. Suitable for light chain loads, where smooth operation is not a requirement.

13-14 teeth: chain speed up to 3 m/s. Suitable for light chain loads, where smooth operation is not a requirement.

15-17 teeth: chain speed up to 6 m/s. Suitable for light chain loads, where smooth operation is not a requirement.

18-21 teeth: chain speed up to 10 m/s. It provides a smooth operation.

22-25 teeth: chain speed up to 15 m/s. It provides a smooth operation.

26-40 teeth: chain speed up to 30 m/s. Suitable for driving sprocket with heavy loads and great speed. Polygon-effect is negligible. Meets the strictest requirements for vibration and noise.

45-120 teeth: most suitable tooth number for driven sprockets. Meets the strictest requirements for vibration and noise. Due to the reduced take-up capacity of the teeth, the allowed chain elongation resulting from chain wear will decrease, as well, for example, see Fig. 3.5:

Z = 70 2.8%
Z = 80 2.3%
Z = 90 2.0%
Z = 100 1.7%
Z = 120 1.2%

125-200 teeth: to be avoided. It does not improve operation conditions considerably compared to tooth number 45-120, but the allowed chain elongation resulting from chain wear will greatly decrease.

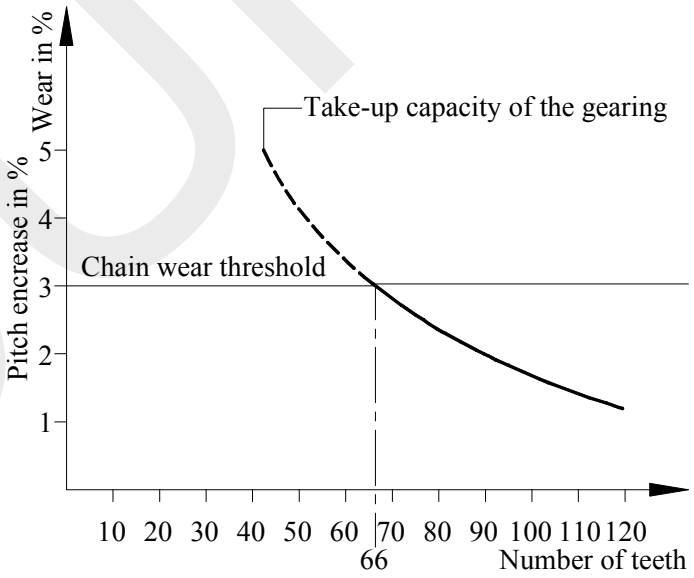

Figure 3.5: Take-up capacity of the gearing
Source: [7]

Designing a chain drive is based on the nominal performance, from which, with the use of $k_{ü}$ operation coefficient, we can determine the transmittable performance. From this the chain pitch can be determined. In this chapter we apply the notation system of "Fenner Roller Chain Technical Manual", often applied for designing.

$$P_B = YP$$

where:	P	[kW]	nominal performance
	P_B	[kW]	design performance
	Y		operation coefficient

The way of defining Y operation coefficient (used for building the load model) for prime mover and driven machines is similar to those seen in the case of belt drives, providing that we complied with the recommendations for choosing the number of teeth.

3.3.5. Loads arising in gear-drives

With gear drives power is transmitted from one shaft to another. The torque, to be transmitted at a given RPM is provided by the tangential component of the tooth force, arising in the contact point of the tooth profiles. In practice, tooth force is calculated from the peripheral force by considering the shape and dimensions of the tooth; the peripheral force is determined from the transmitted torque. Depending on the type of the gear-drive, tooth force can be resolved to tangential (previously used for calculating tooth force), radial and axial components in the contact point. In straight-toothed cylindrical gear drives no axial force arises, whereas in helical gear-drives it does. The radial component's line of action goes through the rotational axis of the gear. So, this component does not affect any torque or bending moment on the shaft. The vector of the tangential force component can be moved parallel with itself to the centre-line of the gear, with consideration to the torque provided by the tangential force. The vector of the axial component, which results in the axial loading of the shaft and has to be supported by bearings, can be moved to the centre-point of the gear by considering the bending effect of the axial force on the shaft with a concentrated bending moment: $M_{hj} = F_{ax} r$ where "r" equals with the distance between the work point of the tooth load and the centre-line.
After moving the force components and concentrated moments to the centre-line intersection point, they can be resolved to $x - z$ and $y - z$ components, from which the required reaction forces can be determined.

3.3.6. Load arising on angle compensating couplings

Angle compensating couplings can be grouped not only by their types, but also by their operation features. From this viewpoint, it can be in three categories: non-

homokinetic, quasi homokinetic, or homokinetic. We will deal with the non-homokinetic angle compensating couplings in detail, within this group with cardan-drives. We will give only some examples for the other two categories. The most common example for homokinetic angle compensating couplings is the constant velocity joint, developed from the Zappa joint, which has already become the most often applied one for shaft axle joint (prop shaft) of independent suspension vehicles. Homokinetic operation means that the angular speed of the two shafts connected by the joint are identical, independently of the angle of the two shafts. This is achieved by the fact, that the six balls in the bearing cage always align in one plain, the bisector of the angle of the outer boot and the inner hub; this ensured by the geometry of the ball races. Since there is no angular speed fluctuation between the driving and the driven shafts, there is no supplementary load during operation. The build-up of the inner part of the prop shaft, connecting to the differential gear, can be of different types. We can utilize a 6-ball homokinetic coupling, which has to enable axial compensation, so the ball races have a helical shape. For vehicles with lower power, the prop shaft connects to the differential with a bipod or a tripod joint. These two joint are however not homokinetic, so this method is not applied higher performance vehicles.

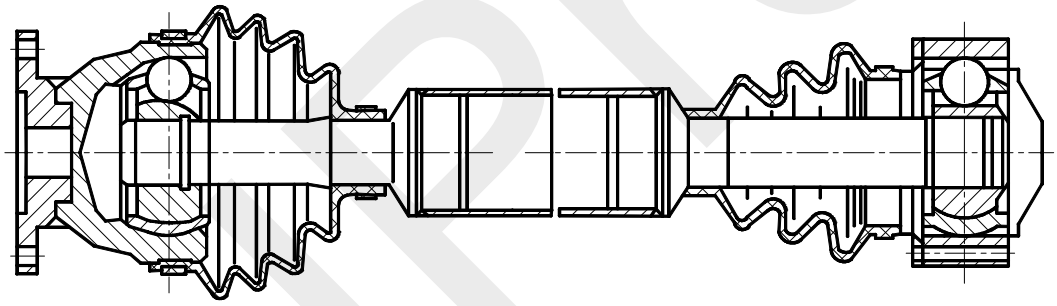

Figure 3.6: Prop shaft with homokinetic joints
Source: [10]

An example for the quasi-homokinetic joint is the joint containing a double cardan-joint. This type was used in the two-stroke Wartburg and Barkas brand mark (east German) vehicles.

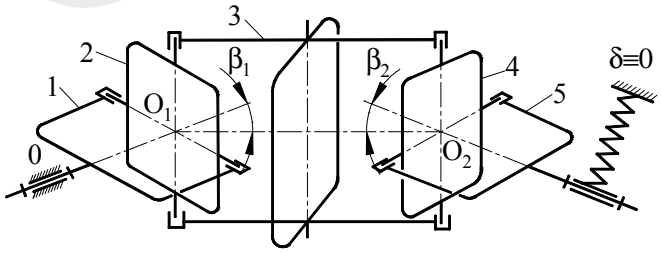

Figure 3.7: Double cardan joint without centralization
Source: [9]

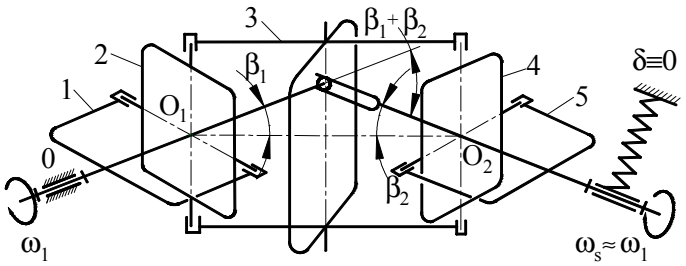

Figure 3.8: Double cardan joint with centralizer ball
Source: [9]

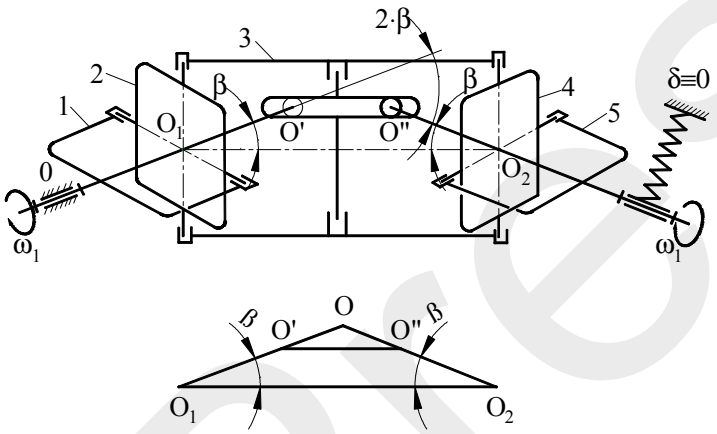

Figure 3.9: Double cardan joint with centralizer disc
Source: [9]

This is characterized by being homokinetic at exactly two angle positions, when the angle of deflection is 0°, and at an angle position, which was designed to be equal with the angle position resulting from an average load and at a straight course of drive. When operating under the right circumstances, the two cardan-joints can compensate each other's faults. This right circumstance for the double cardan-joint is provided by the centralizer ball, which ensures these two angle positions. In order to transmit power from a low RPM tractor to an agricultural machinery, usually two centralizer balls and one centralizer disk are used, resulting in a homokinetic drive, although it can only be used at low RPM, due to the great centrifugal force of the centralizer disk (see Fig. 3.9). Cardan-joints are widely used for transmitting power, in spite of transmitting it with alternating RPMs. The reason for this is that under the right circumstances the two joints can compensate the fluctuation of one another's angular speeds, resulting in an equal angular speed of the driving and driven shafts. The most common example for this are cardan-joints of front-engined, rear wheel driven vehicles and trucks, where the cardan-joints have a plane lay-out and contains two joint. As we will see, even though this drive operates without fluctuation, considerable supplementary loads arise resulting in vibration, and has to be considered as excitation effect during dynamic calculations. Later, we will examine,

what are the conditions to assemble a homokinetic spatial cardan-drive with any number of joints; and how to calculate the above-mentioned supplementary loads.

3.3.6.1. Operation features of cardan joint, cardan drive

Cardan drive without fluctuation of the angular velocity of the driven shaft may be implemented by applying appropriate drive arrangement.
In this chapter we determine the precondition of homokinetic spatial cardan drive and the supplementary loads arising. Fig. 3.10 shows the deviations of angular displacements of the shafts coupled by a cardan joint in the function of angular displacement of the drive shaft.

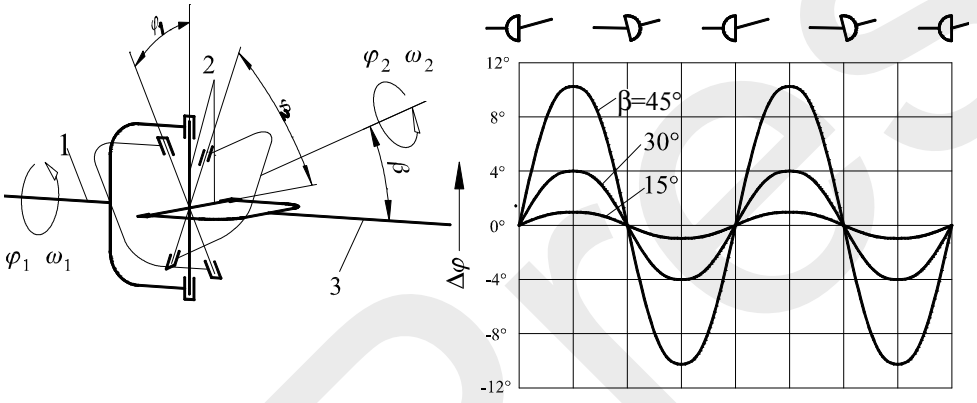

Figure 3.10: Operation features of cardan joint

For the analysis and the dynamic modelling of cardan-drive, we need to know the angular velocity and angular acceleration of the driven shafts. For simplification purposes we assume, that the driver shaft of the first joint has a constant angular velocity: $\omega_{11} = const$. The relation between the angular displacement of the driving and driven shafts, coupled by the cardan drive, is the following:

$$tg\varphi_{11} = \frac{1}{\cos\beta_1} tg\varphi_{12} \tag{3.11}$$

$$\varphi_{12} = arctg\left(\frac{1}{\cos\beta_1} tg\varphi_{11}\right),$$

where β_1: deflection angle of the joint

$$\varphi_{12} = arctg\left(\lambda_1 tg\varphi_{11}\right), \text{ where } \lambda_1 = \frac{1}{\cos\beta_1} \tag{3.12}$$

The difference between the angular displacements of the shafts:

$$\psi = \varphi_{12} - \varphi_{11} = \left(\lambda_1 tg\varphi_{11}\right) - \varphi_{11} = \Psi\left(\varphi_{11}; \lambda_1\right) \tag{3.13}$$

By the fourier expansion into series of ψ and by introducing σ_1 we get the following:

$$\psi = \varphi_{12} - \varphi_{11} = \sigma_1 \sin 2\varphi_{11} + \frac{1}{2}\sigma_1^2 \sin 4\varphi_{11} + \frac{1}{3}\sigma_1^3 \sin 6\varphi_{11} + \ldots + \frac{1}{n}\sigma_1^n \sin 2n\varphi_{11}$$

(3.14)

$$\text{where: } \sigma_1 = \frac{\lambda_1 - 1}{\lambda_1 + 1}$$

As a simplification of Eq. 3.14, the difference between the angular displacements:

$$\Psi = \varphi_{12} - \varphi_{11} \cong \sigma_1 \sin 2\varphi_{11} \quad (3.15)$$

$$\text{where: } \sigma_1 = \frac{\beta_1^2}{4}$$

The above approximation method provides adequate accuracy for $\beta = 30^o$ maximum angle of deflection. The angular speed and angular acceleration of the driven shaft can be determined by derivation. Assuming that $\omega_{11} = const$, the motion characteristics of the driven shaft are:

$$\varphi_{12} = \sigma_1 \sin 2\varphi_{11} + \varphi_{11} \quad (3.16)$$

$$\omega_{(t)} = \omega_{11}(1 + 2\sigma_1 \cos 2\varphi_{11}) \quad (3.17)$$

$$\varepsilon_{(t)} = -4\sigma_1 \omega_{11}^2 \sin 2\varphi_{11} \quad (3.18)$$

3.3.6.2. Homokinetic cardan drive

As we have seen, a "Z"-shaped, plane-layout two-joint drive used in vehicles, is a special method to transmit power between two parallel shafts with altering height. It is a common task to transmit power between two fixed-position shafts, in a broken line (for instance in the case of agricultural harvesters), where the drive has a spatial lay-out. In order to solve a spatial task, we need to formulate the general premises of the homokinetic drive, from which we can already derive the two-joint, plane lay-out drive as well.

In order to formulate the premises we define the following concept:

- Reference plane of a joint: plane defined by two shafts, connected by the joint, in the case of presence of a deflection angle.
- Normal position of the drive: the angular position of the drive, where the driver fork of the first joint lies in its reference plane.
- Γ_{i1} :phase angle of the joint member "i"; angle between the driver fork of the joint member "i" and its reference plane, if the driver fork of the first joint lies in its reference plane (by definition it is the normal position of the cardan shafts coupled in series).
- Φ_{i1} : angle position of the joint member "i"; angle between the driver fork of the joint member "i" and its reference plane, in a given displacement position of the drive.

Possible drive layouts:

a. One-joint cardan-drive

$$\varphi_{12} = arctg\left(\frac{1}{\cos\beta_1} tg\varphi_{11}\right) = arctg\left[\lambda_1 tg\varphi_{11}\right],$$

$$\text{where } \lambda_1 = \frac{1}{\cos\beta_1} \tag{3.19}$$

The above equation shows, that the premise of $\varphi_{12} = \varphi_{11}$ can be true only in the trivial case when deflection angle equals zero ($\beta_1 = 0^o$), that is a homokinetic drive cannot be built with only one cardan joint.

b. Drives with several cardan-joints when all phase angles are 0°

$$\Gamma_{i1} = 0^o,\ i = 1 \ldots n$$

$$\varphi_{n2} = arctg\left[\lambda tg\varphi_{11}\right],$$

$$\text{where: } \lambda = \frac{1}{\cos\beta_1}\frac{1}{\cos\beta_2}\ldots\frac{1}{\cos\beta_n} \tag{3.20}$$

From λ equation we can see, that the drive can operates without angular speed fluctuation ($\lambda = 1$) only in the trivial case, when $\beta_1 = \beta_2 = \ldots\beta_n = 0^o$. We can see that homokinetic drive can not be built with joints of identical phase angles.

c. Drives with several cardan-joints, where the phase angles of all cardan-joints are either $\Gamma_{i1} = 0^o$, or 90^o, but at least one differs from the others.

$$\varphi_{n2} = arctg\left[\lambda' tg\varphi_{11}\right],$$

$$\text{where: } \lambda' = \left(\cos\beta_1\right)^{-1}\left(\cos\beta_2\right)^{\pm 1}\ldots\left(\cos\beta_n\right)^{\pm 1} \tag{3.21}$$

The above equation shows, that if the phase angle of at least one joint is different from the others, there exist a drive arrangement built with the adequate angle disposition, for which $\lambda' = 1$, and a homokinetic drive is realizable.

d. Drives with several cardan-joint, phase angle of at least one cardan-joint does not equal 0°or 90°. The premise $\lambda' = 1$ can not be fulfilled, so a homokinetic drive is not realizable.

It follows from the above, that the conditions for a homokinetic drive are the following:

- The phase angle of the joints can only be 0° or 90°, but at least one of them has to be different from the others
- The angle deflection of the joints (β_i) has to be chosen, so that $\lambda' = 1$

In the case of a drive containing "n" number of joint, we can assemble altogether $2^{n-1} - 1$ number of different drive variations, independently from the fact, that the shafts lie in one plane or they have a general, spatial lay-out. The Fig. 3.11 shows all the variations of a four-joint, planar lay-out drive.

The number of drive variations are $2^{n-1}-1=7$. The algebraic sign of β_i angles are determined relatively to β_1.

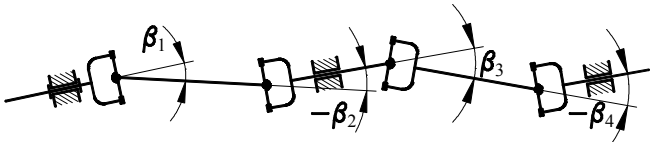

$$\cos\beta_1=\cos\beta_2\cos\beta_3\cos\beta_4$$

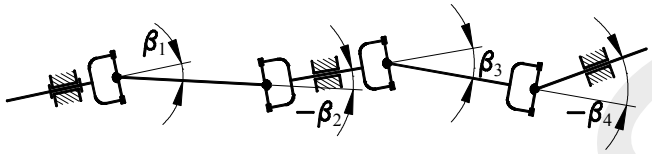

$$\cos\beta_2=\cos\beta_1\cos\beta_3\cos\beta_4$$

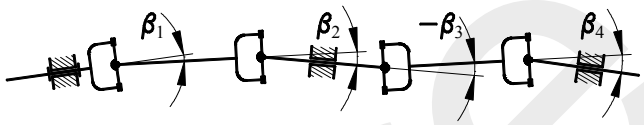

$$\cos\beta_3=\cos\beta_1\cos\beta_2\cos\beta_4$$

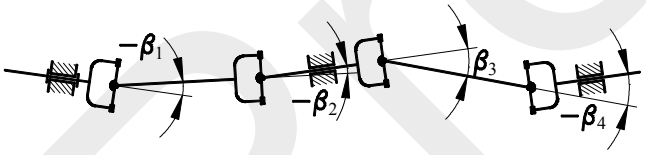

$$\cos\beta_4=\cos\beta_1\cos\beta_1\cos\beta_3$$

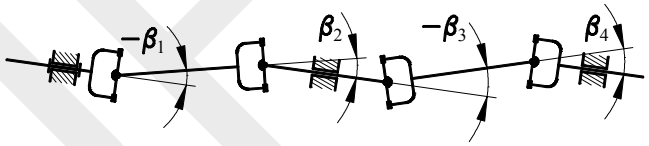

$$\cos\beta_1\cos\beta_2=\cos\beta_3\cos\beta_4$$

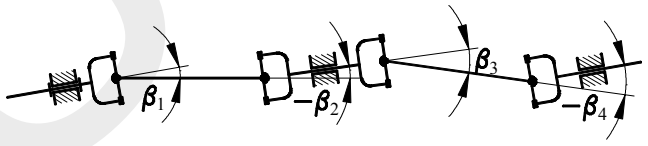

$$\cos\beta_1\cos\beta_3=\cos\beta_2\cos\beta_4$$

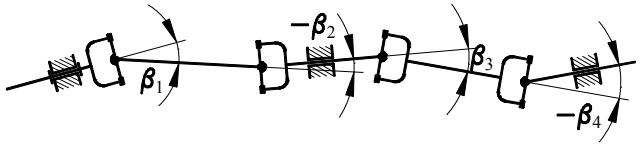

$$\cos\beta_1\cos\beta_4=\cos\beta_2\cos\beta_3$$

Figure 3.11: Eligible homokinetic cardan drive arrangements
Source: [11]

Let us examine a two-joint plane-layout cardan-drive in "Z" and "W" layout. The number of assembly variation is: $2^{n-1} - 1 = 2^{3-1} - 1 = 1$, that is it can be assembled in only one way. In general it means that if the driving fork of the first joint lies in its reference plane, then the driver fork of the second joint has to be perpendicular to its reference plane. In a planar case it means, that the joint-forks on the middle cardan-shaft are in the same angle position. This shaft is often made in a telescopic construction with splined shaft joint in order to ensure axial displacement. When applying splined shaft joint, the cardan-drive can be assembled in several positions (Lada's cardan-shaft), that is why we have to pay attention the identical position of the joint-forks during assembly.

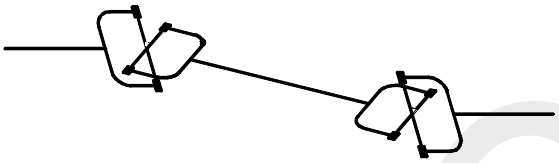

Figure 3.12: Z layout cardan drive

The premise $\lambda' = \frac{1}{\cos\beta_1}\cos\beta_2 = 1$ will be fulfilled only if $\beta_1 = \beta_2$ or $\beta_1 = -\beta_2$, which can be ensured by "Z" or "W" shaped lay-out.

3.3.6.3. Supplementary loads of cardan joint

Since cardan drives can only transmit and not modify power, disregarding the mechanical losses (friction between the journal cross and the joint-fork in the needle-roller bearing), the following equation of equilibrium can be used:

$$M_{11}\omega_{11} = M_{12}\omega_{12} \tag{3.22}$$

$$M_{12} = M_{11}\frac{\omega_{11}}{\omega_{12}} \tag{3.23}$$

It can be seen, that M_{12} torque changes in the function of the angular displacement. Rotating with fluctuating angular velocity can cause serious damage, due to the supplementary loads of the inertial rotating masses:

$M_d = J\varepsilon$, where J is the mass moment inertia of the drive section rotating with fluctuating angular velocity.

In case we assemble a drive with two joints in "Z" or "W" plane lay-out (Fig. 3.13), the situation is more advantageous, because even thought there is supplementary moment:

$M_d = J_{cardan\ shaft}\varepsilon$, here $J_{cardan\ shaft}$ is the mass moment of inertia only of the shaft between the two joints.

The value of this mass moment of inertia determines how smoothly the adequately assembled drive will operate or if it is going to undergo vibration during operation,

(of course there is no fluctuation in the angular speed even in the case of applying only one joint if the deflection angle equals zero). The causes for vibration are the supplementary forces arising on the joint-forks.

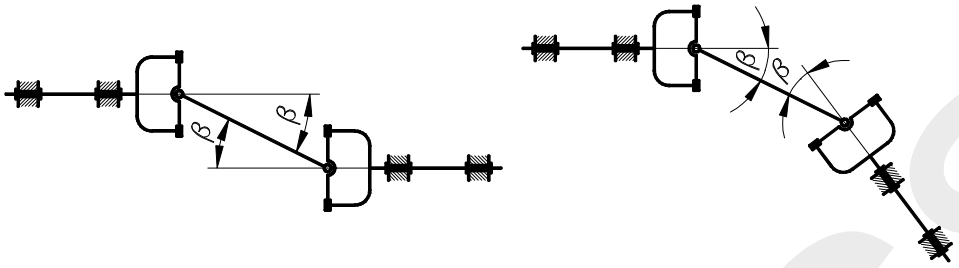

Figure 3.13: Cardan drive in Z and W arrangements

The most accurate way to determine the efficiency of the cardan drive is by measuring. The heat flow resulting from the friction of the needle-rolling bearing is measured under laboratory circumstances, which afterwards will be compared to the input power. The following equation gives a good approximate value for the efficiency of the cardan-drive for $\beta = 15^o$ maximum deflection angle [12]:

$$\eta = 100(1 - 0.003\beta) \ [\%] \tag{3.24}$$

Let's examine the drive in Fig. 3.14, which transmits only torque from the prime mover to the machine (radially load-relieved drive). In a lay-out without deflection angle ($\beta = 0^o$), the shafts are loaded only be torque, so no reaction force arises on the shaft bearings.

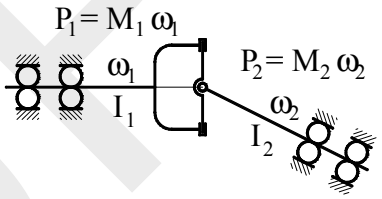

Figure 3.14: Application of a cardan joint

In a cardan drive assembled with deflection angle, supplementary loads arise on the joint-forks altering in the function of angular displacement, see Fig. 3.15.

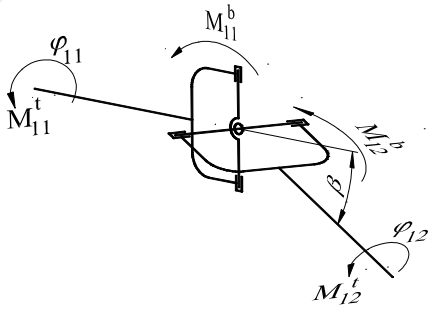

Figure 3.15: Force diagram of the cardan-joint

$$\frac{M_{11}^{h}}{M_{11}^{t}} = tg\,\beta \sin \varphi_{11} \tag{3.25}$$

$$\frac{M_{12}^{h}}{M_{11}^{t}} = tg\,\beta \cos \varphi_{11} \sqrt{1 - \sin^2 \beta \cos^2 \varphi_{11}} \tag{3.26}$$

$$\frac{M_{12}^{t}}{M_{11}^{t}} = \frac{1 - \sin^2 \beta \cos^2 \varphi_{11}}{\cos \beta} \tag{3.27}$$

where: M_{11}^{t}: driving torque of the joint

M_{12}^{t}: torque of the shaft driven by the joint

M_{11}^{h}: supplementary bending moment loading the driving joint-fork

M_{12}^{h}: supplementary bending moment loading the driven joint-fork

We can see from the above equation, that in lay-out without deflection angle ($\beta = 0^{o}$), no supplementary moment arises on the joint-forks hence the torques of the two shafts connected by the joint are equal.

In general case, in possession of supplementary loads, the reaction forces at the bearings can be calculated and the stressing of the shaft (the load of the shaft is completely reversed) can be carried out for fatigue. Cardan-joints, chosen from product catalogues, are stressed for the loads detailed above. A well-designed and well-operating cardan drive must not be rebuilt with increased joint angle without careful checking calculations because of the increasing supplementary loads acting on the drivetrain parts.

3.3.6.4. Excitation effects of the out-of-balance rotating elements

Shafts and other parts of a drivetrain are not rigid bodies but elastic and suffer elastic deformation under loads. During the dynamic analysing we have to take into consideration the effects of the elastic deformation, the inaccuracy of the manufacturing and the operation allowances.

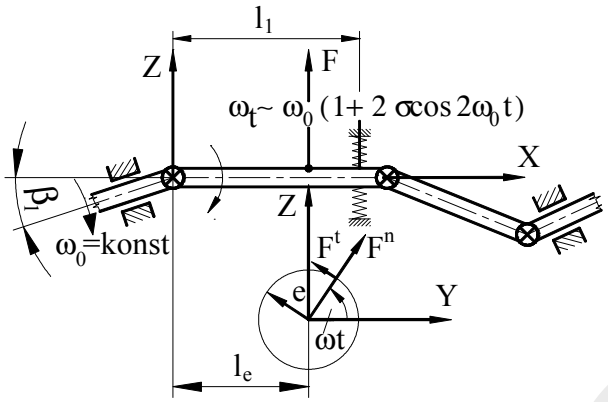

Figure 3.16: Effects of the out-of-balance of rotating elements

Let's examine the dynamic effects of an interstage shaft (as an out-of-balance shaft) of a common cardan-drive, which rotates with a $\omega_{(t)}$ periodically fluctuating angular velocity.

The arising excitation force:

$F = F_c + F_t$ where: F_c centrifugal force

F_t force arising from the mass moment of inertia

The centrifugal force and the force arising from the mass moment of inertia of rotating elements have no designated directions, but if we wish to define not only their absolute value, but also their effects acting in a given direction, we can characterize them with their frequency. We carry out the calculation in the vertical direction, and we determine the components of the arising forces accordingly.

$$F_z = F_c \sin \omega_{(t)} t + F_t \cos \omega_{(t)} t \tag{3.28}$$

where: $F_c = \Delta m \left(e + y\right) \omega_{(t)}^2$ (3.29)

$$F_t = \Delta m \left(e + y\right) \varepsilon_{(t)}$$

where Δm : the out-of-balance mass,

$$F_z = \Delta m \left(e + y\right) \omega_{(t)}^2 \sin \omega_{(t)} t + \Delta m \left(e + y\right) \varepsilon_{(t)} \cos \omega_{(t)} t \tag{3.30}$$

with the submission of:

$$\omega_{(t)} = \omega_0 \left(1 + 2\sigma_1 \cos 2(\omega_0 t)\right) \tag{3.31}$$

$$\varepsilon_{(t)} = -4\sigma_1 {\omega_0}^2 \sin 2\left(\omega_o t\right) \tag{3.32}$$

$$F_z = A\cos(\omega_0 t) + B\cos 2(\omega_0 t) + C\cos 3(\omega_0 t) \tag{3.33}$$

where A, B and C are constants

From the above equation we can see that the frequencies exciting the drivetrain are: ω_0, $2\omega_0$, $3\omega_0$. It is important to mention, that long rotating shafts deflecting due to their own weight behave the same way, as out-of-balance shafts, so we have to

choose the shaft profile and its dimensions, so that the deflection stays within the permitted limit.

3.4. Designing shaft

In the following we survey the steps of shaft designing.
Preliminary design of the shaft:

1. Building up the load model, starting from the nominal performance and assessing the operation factor.
2. Ascertaining the loads acting on the shaft, considering its functions (belt drive, chain drive, gear drive, supplementary loads, etc.)
3. Assessing the longitudinal dimensions of the shaft, considering its functions.
4. Drawing the load diagrams of the shaft and calculating the reaction force at the bearings.
5. Determining the critical cross sections and calculating the resultant value of the bending moments and the torque in the critical cross sections (the torque is known since the load diagrams are determined on the basis of it).
6. Material selection. The shaft diameter may be calculated from the material properties and from the allowed stresses.
7. Constructing the shaft (supporting and non supporting shoulders, end and neck journals, key and splined joints).
8. Checking the stress calculations with the actual dimensions of the shaft. If it is necessary, modifying the dimensions and reconstructing the shaft. The checking process has to go on with recalculations till the dimensions of the shaft are fixed.

Checking the shaft for:

1. Fatigue
2. Plastic deformation
3. Allowed elastic deflection
4. Critical speed

Without derivation we give some, often applied formulas for calculating the shaft diameter in the case of static load (preliminary design) and altering load (checking for fatigue).

Combined static load:

$$d_{min} = \sqrt[3]{\frac{\sqrt{M_h^2 + \frac{3}{4} M_{cs}^2}}{0,1\sigma_{meg}}} \tag{3.34}$$

where: $\sigma_{meg} = \frac{R_{eH}}{n}$, $n = 2.5 - 3$

Fluctuating and shock load:
Applying the maximum energy of distortion theory with modified Goodman fatigue criteria:

$$\frac{R_{eH}}{n}=\frac{32}{\pi d^3}\left[K_{sb}\left(M_{h_m}+\frac{R_{eH}}{R'_{Dv}}M_{h_a}\right)^2+\frac{3}{4}K_{st}\left(M_{cs_m}+\frac{R_{eH}}{R'_{Dv}}M_{cs_a}\right)^2\right]^{\frac{1}{2}} \tag{3.35}$$

where: K_{sb} and K_{st} shock factor for bending and torsion

K_{sb} and K_{st} for steady load: 1

minor shock: 1.5

heavy shock: 2.0

With the K_{sb} and K_{st} factors the dynamic loads are considered, over the $k_{ü}$ operation factor applied in the load diagram.

In the case of rotating shaft ($M_{h_m}=0$), the shaft diameter:

$$d^3=\frac{32n}{\pi R_{eH}}\left[K_{sb}\left(\frac{R_{eH}}{R'_{Dv}}M_{h_a}\right)^2+\frac{3}{4}K_{st}\left(M_{cs_m}+\frac{R_{eH}}{R'_{Dv}}M_{cs_a}\right)^2\right]^{\frac{1}{2}} \tag{3.36}$$

4. Determining the stiffness of rolling bearings

The bearings of rotating shafts, except from turbine shafts rotating at a high RPM, are usually implemented by rolling-contact bearings. Depending on the function of the shaft and its construction, we can apply several constructional methods to design the bearing place. If we have to implement shaft bearings with prescribed distances from each other (gear-drive), we have to design a mutual bearing housing.

If there are no such requirements, in general there are three options:

- Designing a mutual bearing housing, where the coaxiality of the bearing housing is ensured by the applied manufacturing process.
- Designing individual bearing housings or choosing them from product catalogues. We can only use self-aligning bearings, since the coaxiality of the bearing housings can only be adjusted during assembly with some sort of position tolerance.
- Designing and implementing individual, rubber block suspended bearing housing (suspending the cardan shafts from the frame or the chassis).

The radial and angular stiffness of the bearings affects the vibration conditions of the drivetrain, and as we will see later, it will also affect the natural frequencies. It is important to note, that in practice, under bearing stiffness we usually mean angular stiffness; whereas during dynamic calculations the radial stiffness of the bearing is authoritative.

The radial stiffness of the bearing assembly depends on the stiffness of partly the rolling-contact bearing, partly bearing housing, as well as the suspension, since these elements can be modelled by series connected springs. It follows, if we implement the shaft bearing in a high-stiffness bearing housing, then the stiffness of the rolling-contact bearings will be decisive, but if we implement it in a high elasticity rubber block, we have to take into consideration only the stiffness of the rubber block.
The bearings of the cardan shafts, similarly to other shafts with a greater length-to-diameter ratio, are designed with self-aligning or deep-groove ball-bearings. The reason behind this is that the bearings of shafts, whose flexibility results from their geometric dimensions, have to ensure the angular deflection of the shafts arising from elastic deformation. Later, we will determine the radial spring stiffness for these two bearing-types. The elasticity of the rolling-contact bearings can be determined with the Sjövall stiffness model (based on Hertz theory).
When determining the contact stresses and deformations, the following simplifications were made:

- the material of the contacting bodies is perfectly elastic, follows Hook's law,
- the material of the contacting bodies is homogeneous and isotropic,
- the contacting areas are small relating to the sizes of the bodies,
- the load is perpendicular to the mutual contact surface,
- there is no friction arising between the bodies during deformation.

4.1. Deformation in single deep-grooved ball-bearings

The loads of the ball-bearings are transmitted from one raceway to the other by the rolling elements, while in the contact of the raceway and the rolling elements Hertz stress arises. The elastic deformation of the bearing results from the sum of the deformation of the outer ring – rolling element, and that of the inner ring – rolling element [15]:

$$\delta = \delta_{out} + \delta_{in} \tag{4.1}$$

The general equation describing the connection between the load and the deformation is:

$$Q = K_n \delta^n \tag{4.2}$$

where: $n = 3 / 2$ for bearings with point-contact

$$K_n = \left[\frac{1}{\left(\frac{1}{K_{in}}\right)^{\frac{1}{n}} + \left(\frac{1}{K_{out}}\right)^{\frac{1}{n}}} \right]^n \tag{4.3}$$

where: K_{in} and K_{out} are contact coefficients for the inner

and the outer ring, which equals (in the case of a point-like contact):

$$K_{in} = 2.14 \;\; 10^4 \frac{1}{\sqrt{\sum \rho_{in} \delta_{in}^3}} \;\; \text{daN/mm}^{1,5} \tag{4.4}$$

$$K_{out} = 2.14 \;\; 10^4 \frac{1}{\sqrt{\sum \rho_{out} \delta_{out}^3}} \;\; \text{daN/mm}^{1,5} \tag{4.5}$$

where: $\sum \rho_{in}$ and $\sum \rho_{out}$ are the sum of the principal curvatures on the inner and outer rings

$$\sum \rho_{in} = \frac{1}{d_g}\left[4 + \frac{2\gamma}{1-\gamma} - \frac{1}{f_b}\right] \qquad \sum \rho_{out} = \frac{1}{d_g}\left[4 - \frac{2\gamma}{1-\gamma} - \frac{1}{f_k}\right]$$

where: $\gamma = \frac{d_g \cos\alpha}{d_m}$ medium diameter coefficient of the bearing

α angle of action of the bearing,

d_g diameter of the rolling element,

d_m medium diameter of the bearing

$$f_{out} = \frac{r_{out}}{d_g}, \; f_{in} = \frac{r_{in}}{d_g}$$

f_{out} and f_{in} are the ball raceway-rolling element osculation defined between the inner raceway and the rolling elements, as well as between the outer raceway and the rolling elements (Fig. 4.1). The radial displacement of the inner raceway of a stiffly supported, radially loaded bearing adds up of half of the radial clearance and the maximum elastic deformation.

$$u = \delta_{max} + \frac{H_r}{2} \tag{4.6}$$

where: δ_{max} a maximum deformation

H_r radial clearance of the bearing

u displacement in radial direction

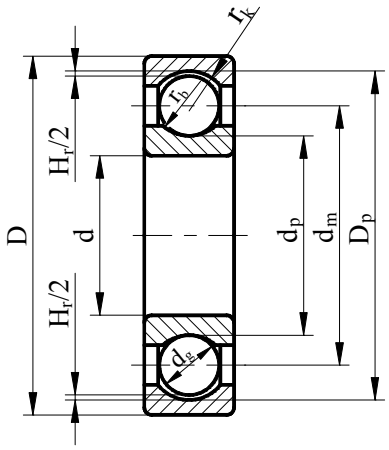

Figure 4.1: Geometric dimensions of rolling-contact bearings

For a given rolling element under an optional ψ angle, the elastic deformation (fig. 4.2):

$$\delta_{\psi} = u\cos\psi - \frac{H_r}{2} \tag{4.7}$$

By introducing ε load-distribution coefficient:

$$\varepsilon = \frac{1}{2}\left(1 - \frac{H_r}{2u}\right), \text{ from which} \tag{4.8}$$

$$\delta_{\psi} = \delta_{max}\left[1 - \frac{1}{2\varepsilon}(1-\cos\psi)\right] \tag{4.9}$$

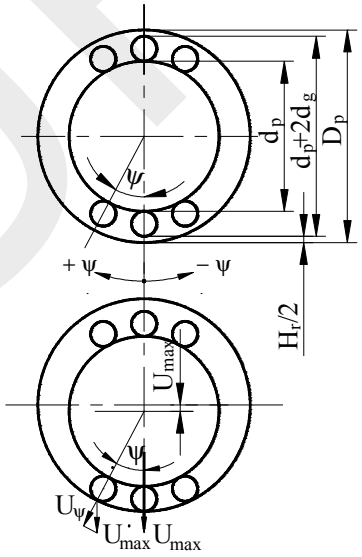

Figure 4.2: Components of the radial displacement of the inner ring

The ε load-distribution coefficient characterizes the dimension of the load-zone, its value depending on the load and the size of the radial clearance. If $\varepsilon < 1$, we can characterize the load-zone with ψ_e half contact angle (fig. 4.3).

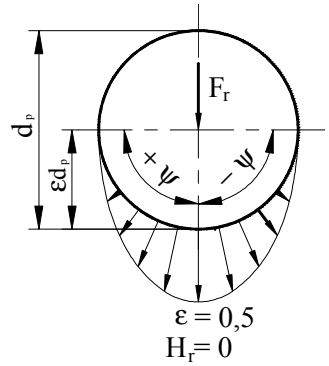

Figure 4.3: Load-zone of the bearing

The value of ψ_e from $\delta_\psi = 0$:

$$\psi_e = \arccos(1 - 2\varepsilon) \tag{4.10}$$

Load of the rolling element in a given angle position:

$$Q_\psi = Q_{max}\left[1 - \frac{1}{2\varepsilon}(1 - \cos\psi)\right]^n \tag{4.11}$$

where: Q_{max} a maximum load of the roll-element

The condition for the static balance of the bearing is that the sum of the vertical components of the rolling-element loads equals the external radial load.

$$F_r = \sum_{\psi=1}^{\psi=\pm\psi_e} Q_\psi \cos\psi \text{ ,thus } F_r = Q_{max} \sum_{\psi=1}^{\psi=\pm\psi_e}\left[1 - \frac{1}{2\varepsilon}(1 - \cos\psi)\right]^n \cos\psi \tag{4.12}$$

Instead of concentrated loads on the rolling elements, Sjövall proposed a constantly varying load in the load-zone, from which:

$$F_r = ZQ_{max}J_r \tag{4.13}$$

where: Z number of rolling elements in a row

J_r radial Sjöval integral, whose value is:

$$J_r = \frac{1}{2\Pi}\int_{-\psi_e}^{+\psi_e}\left[1 - \frac{1}{2\varepsilon}(1 - \cos\psi)\right]^n \cos\psi d\psi \tag{4.14}$$

It follows, that the maximum rolling-element load equals:

$$Q_{max} = K_n\left(u - \frac{H_r}{2}\right)^n \tag{4.15}$$

The values of the radial Sjövall integral, in the function of the ε load-distribution coefficient, are summed up in a table of [15], also included by the computer software.

The relationship between the radial load and the load-distribution coefficient is described by the following equation:

$$F_r = ZK_n \left(H_r \frac{\varepsilon}{1-2\varepsilon} \right)^n J_r \tag{4.16}$$

The correlating, J_r and ε value pairs, included in the above equation, is determined by interpolation. After determining the values of J_r and ε, the radial displacement of the inner raceway of the bearing, measured from the geometric axis of the bearing, can be determined, as well.

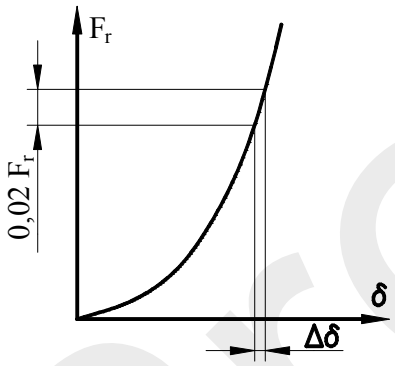

Figure 4.4: Spring characteristic of the bearing

The course of the calculations:

1. Determining the correlating $\varepsilon - J_r$ value pairs
2. Determining the radial displacement of the inner raceway

$$u = \frac{H_r}{2(1-2\varepsilon)} \qquad \varepsilon \neq 0.5 \tag{4.17}$$

$$u = \frac{F_r}{ZK_n J_r} \qquad \varepsilon = 0.5 \tag{4.18}$$

3. Determining the elastic deformation of the bearing from „u”

$$\delta = u - \frac{H_r}{2} \tag{4.19}$$

4. Determining the stiffness of the bearing

$$s = \frac{dF_r}{d\delta} \cong \frac{\Delta F_r}{\Delta\delta} \tag{4.20}$$

By repeating the calculations of δ with load values increased, as well as decreased by 2%, we can determine the radial stiffness of the bearing for a given load (Fig. 4.4).

In order to apply the Sjövall bearing stiffness model, we have to know the contact coefficients of the different bearings for the given bearing type and sizes. The data required for these, such as geometrical shapes and sizes of the bearing rings, are

available only to the manufacturers of the bearings, but these information are not publicly available.

4.2. Approximate calculations of the elastic deformation

In engineering practice, we often use such approximate calculations (based on measured data), whose accurate calculations would either be too complicated (there is no calculation model for it), or it has so many uncertainties, that it is not so reliable than one concluding from measurements. We will demonstrate this method for determining the radial elastic deformation of bearings. The relationship between the elastic deformation of bearings and the load is determined by measurements, on which a mathematical function is placed, whose input data are the main geometrical dimensions and other parameters of the bearing. For the calculations a formula is created, which adequately follows the function relationship acquired from the measurements for any bearing size in the case of a given bearing type. So these formulas cannot be deduced, and the included physical variables have to be substituted in the prescribed units (these constructed formulas are often called empirical formulas).

4.2.1. Single-row ball-bearings

The elastic deformation of the bearing [15]:

$$\delta = \frac{0.002}{\cos\alpha}\sqrt[3]{\frac{Q_{res}^2}{d_g}} \tag{4.21}$$

$$Q_{res} = Q_r + Q_{ax} \tag{4.22}$$

$$Q_r = 5\frac{F_r}{Z\cos\alpha} \quad Q_{ax} = 5\frac{F_{ax}}{Z\sin\alpha} \tag{4.23), (4.24}$$

where: F_r and F_a the radial and axial loads of the bearing

α actual angle of action

$\alpha = 0°$ for deep-groove ball-bearing in the case of purely radial loads

$\alpha = 20\ldots25°$ for deep-groove ball-bearings if axial load arises, as well

$\alpha = 0°$ for angular contact-bearings

Z number of rolling elements in a row

d_g rolling element diameter

4.2.2. Double-row ring-bearings in case of purely radial loads

Elastic deformation of the bearing [15]:

$$\delta_r = \frac{0.0032}{\cos\alpha}\sqrt[3]{\frac{Q^2}{d_g}} \tag{4.25}$$

The load of the rolling element:

$$Q = \frac{5F_r}{iZ\cos\alpha} \tag{4.26}$$

The nominal angle of action of the self-aligning rolling-bearing can be determined from the geometrical sizes:

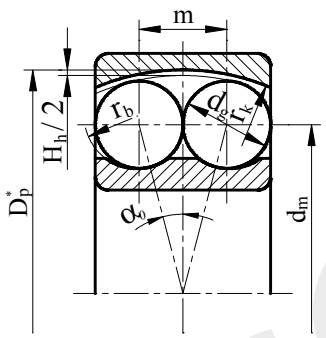

Figure 4.5: Dimensions of the self-aligning rolling-bearing

$$\alpha_0 = \arcsin\left(\frac{m}{2r_k - d_g - H_h/2}\right) \tag{4.27}$$

Determining the bearing stiffness with approximate calculations can be carried out by the following: by repeating the calculations of δ with load values increased, as well as decreased by 2%, we can determine the radial stiffness of the bearing for a given load.

$$s = \frac{dF_r}{d\delta} \cong \frac{\Delta F_r}{\Delta\delta} \tag{4.28}$$

4.2.3. Calculations of the stiffness of the bearing

The maximum rolling element load and the radial elastic deformation of the inner ring of the deep-groove ball-bearing type 6208 can be determined with the approximate calculations.

$F_r = 400\,\text{daN},\ F_{ax} = 0\,,\ \alpha = 0°$

$d_g = 11.906\ \text{mm}$

$Z = 9$

$$Q_{össz} = Q_r = 5\frac{F_r}{Z\cos\alpha} = 5\frac{400}{9} = 222.222\,daN$$

$$\delta = \frac{0.002}{\cos\alpha}\sqrt[3]{\frac{Q_{össz}{}^2}{d_g}} = \frac{0.002}{\cos 0°}\sqrt[3]{\frac{222.222^2}{11.906}} = 0.03213\,mm$$

For loads increased by 2%:

$$Q_{össz} = 226.666\,daN$$

$$\delta = 0.03256\,mm$$

For loads decreased by 2%:

$$Q_{össz} = 217.777\,daN$$

$$\delta = 0.03170\,mm$$

Spring stiffness of the bearing for the given load:

$$s = \frac{\Delta F_r}{\Delta\delta} = \frac{16}{0.00086} = 18604\frac{daN}{mm} \approx 186\frac{kN}{mm}$$

5. Excitation frequencies generated by the bearings

The finite number of the rolling elements of the drivetrain's bearings, the dimension tolerances, the bearing clearance and the different support methods of the bearings all result in numerous excitation frequencies. The influential effect of the bearing clearances can be explained by the fact that the vibration amplitudes and speeds increase, resulting in increasing bearing loads. It results in an increasing spring stiffness of the bearing, which already has a direct influence on the natural frequencies.

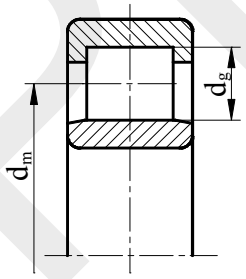

Figure 5.1: Single-row cylindrical roller-bearing

The rotating bearing elements exert excitation effects on the drivetrain. Assuming, that the rolling elements are geometrically perfect, the angular velocity and the excitation frequency of the bearing elements are:

$$\omega_g = \frac{\frac{d_m}{d_g} - \frac{d_g}{d_m \cos^2\alpha_0}}{2}\omega \qquad \omega_g = \frac{1 - \frac{d_g}{d_m \cos\beta}}{2}\omega \qquad \text{(5.1), (5.2)}$$

$$\omega_{inrace} = (\omega - \omega_k)\,z \qquad \omega_{outrace} = \omega_k\,z \qquad \text{(5.3), (5.4)}$$

where: ω angular velocity of the shaft

ω_g angular velocity of the rolling elements

ω_k angular velocity of the bearing cage

ω_{inrace} milling frequency of the inner raceway

$\omega_{outrace}$ milling frequency of the outer raceway

z number of the rolling elements

α_o angle of action of the bearing

The above equations are correct if the outer ring is stationary. So the ω_{inrace} excitation frequency is different from ω operation frequency, that is not only the natural frequencies α_i of the drivetrain are dangerous and to be avoided, but also the ω operation frequencies belonging to frequencies $\alpha_i = \omega_{inrace}$, $\alpha_i = \omega_{outrace}$.

The lubricants of roller-bearings have spring and damping tasks too, hence it influences the natural frequencies. It follows that the appropriate lubrication conditions of the bearings are important not only because of its service life, but also because of its effects on the vibrating system.

6. Assembly of the drivetrain

In engineering practice, we do not have to design every element of the drivetrain in all cases, as there are designers and manufacturers specialized in he given field. A good example for this is the design and manufacture of internal combustion engine or electric motors. The situation is similar for machineries and transmissions (gears, pumps, fans, grinders…), although designing a single purpose machine is already an everyday task for engineers. In the following, we work from the principle that for the required power of the machinery, there is a motor available with the adequate power. The drivetrain is chosen and built afterwards for the above motor and machinery, by designing or choosing the transmission and other drivetrain parts necessary for the matching. Drivetrain optimization deals with choosing the proper drivetrain elements and assembling them, so that their service life and operating conditions comply with the design goals. In general, it is ensured by operating the drivetrain with the right efficiency and without vibrations.

The build-up of a common drivetrain is shown in Fig. 6.1, with its main components:

prime mover: provides mechanical power with good efficiency for a given form of motion, which can be translational (v) or rotational (n, ω) motion

machinery: has a power requirement while carrying out a technological process with the correspondent form of motion.

transmission: brings the motor and the machinery to an identical speed and form of motion (if they are different).

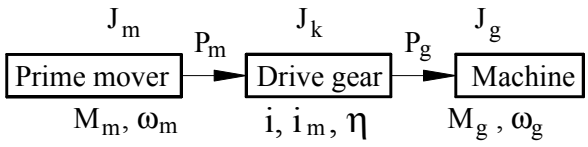

Figure 6.1: Schematic diagram of the drivetrain

When choosing and matching the motor and the machinery we have to know their mechanical parameters, as well as their static characteristic curve. In the next chapter, we will list and analyse the characteristic curves of some generally used motor and machinery types.

6.1. Characteristic curve of prime movers

The characteristic curve of motors is determined by motor bench tests, during which the torque provided by the motor is measured and represented in the function of the motor RPM (M-n characteristic curve). The Performance-RPM (P-n) characteristic curve is obtained from calculation by using the equation $P = M\,\omega$.

6.1.1. Characteristic curves of direct-current electric motors

6.1.1.1. Direct-current side-current motor

They are characterized by being RPM maintaining, and used where a constant RPM is required. The motor's characteristic of being speed maintaining results from the fact, that in case the load of the motor increases, its RPM decreases, for which a greater torque will be available. This ΔM excess torque will accelerate the drive-train up to the operation RPM.

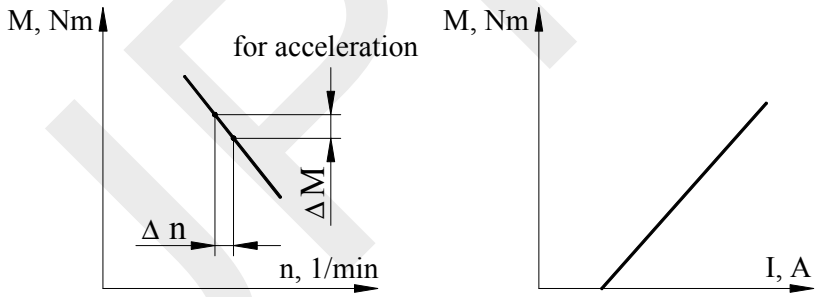

Figure 6.2: Characteristic of the direct-current side-current motor
Source: [16]

6.1.1.2. Direct-current main current motor

It is characterized by being power keeping and during starting there is a risk for runaway, see Fig.6.3 . It is used for situations, when the motor is required to start under load (cranes, trolley buses, trams etc).

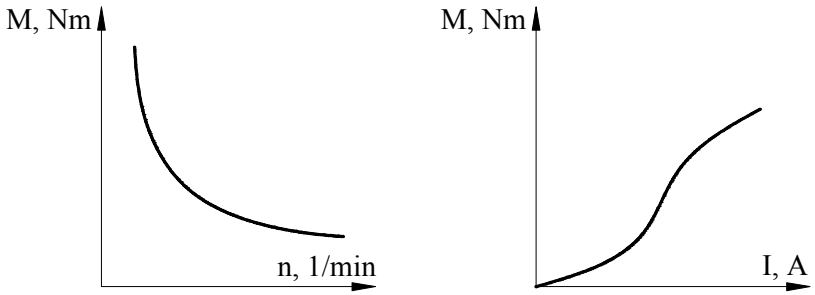

Figure 6.3: Characteristic of the direct-current main current motor
Source: [16]

6.1.1.3. Direct-current mixed circuit motor

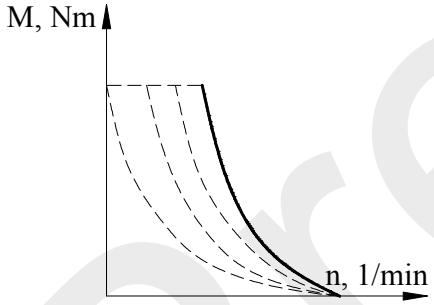

Figure 6.4: Characteristic of the direct-current mixed circuit motor
Source: [16]

6.1.1.4. Short-circuited asynchronous motor

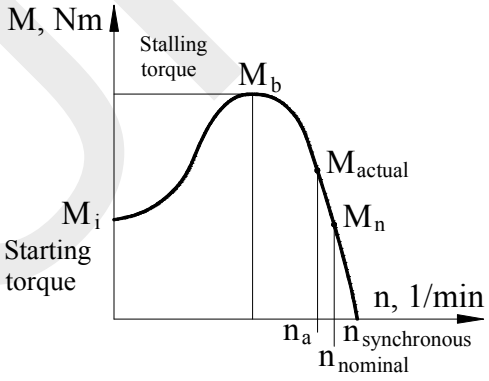

Figure 6.5: Characteristic of the short-circuited asynchronous motor
Source: [16]

The motor cannot operate at synchronous RPM, since in this case there is no flux-line intersection between the rotating magnetic field and the coils of the rotor.
The matching synchronous and asynchronous RPMs [1/min]:

3000 – 2880; 1500 – 1440; 1000 – 960; 750 - 720

Depending on the manufacturer of the motors, the usual ratio of the characteristic torque and RPM values are the following:

$$\frac{M_i}{M_n} = 1.2 - 1.8\,;\quad \frac{M_b}{M_n} = 1.75 - 2.5\,;\quad \frac{n_n}{n_{sz}} = 0.94 - 0.96$$

where:

M_n	nominal torque
M_i	starting torque
M_b	stalling torque
n_n	nominal RPM
n_{sz}	synchronous RPM

The matching M_n - n_n point graphically determines the designing point of the motor $P_n = P_{mm}$, practically the nominal performance of the motor is: $P_n = M_n 2\pi n_n$

The main task when designing a drivetrain is that the motor operates at the nominal torque (at the nominal RPM) efficiently within its service life. As we have mentioned, the motor is capable of delivering as much torque and power, as we can take off of it. This is, of course, limited by the mechanical parameters of the motor, see the characteristic curve. We can see, that theoretically the motor is capable of operating on a torque level even 2.5 times its nominal torque value, also, we can take off multiple times of the nominal performance, although in this case the actual service life will only be a fraction of the nominal service life. The torque-current drain curve of electric motors allow us to determine the load of and the power delivered by the motor, simply by measuring its current drain value. The torque and power delivered by the electric motor can also be determined by the M-n curve, if we can measure the operating RPM of the electric motor with appropriate accuracy. Considering, that a straight line can be matched on the characteristic curve at the nominal torque, the following ratios can be deduced from similar triangles:

$$\frac{M_{ü}}{n_{sz} - n_{ü}} = \frac{M_n}{n_{sz} - n_n}\text{, from which follows:}$$

$$M_{ü} = M_n \frac{n_{sz} - n_{ü}}{n_{sz} - n_n} \tag{6.1}$$

For dynamic calculations we have to be aware of the mass moment of inertia of the rotor, however in the product catalogues we usually can find only the moment of gyration (GD^2) , from which the mass moment of inertia:

$$J_m = \frac{GD^2}{4}\left[kgm^2\right] \tag{6.2}$$

6.1.1.5. Characteristic curve of internal combustion engines

By definition, the nominal torque of the engine is the value pertaining to the nominal (and at the same time the maximum) power, which is delivered at the nominal (an at the same time maximum) RPM, see Fig. 6.6. The difference between the characteristic curves of the gasoline and diesel engines (without supercharger) is determined by the shape of the characteristic curve.

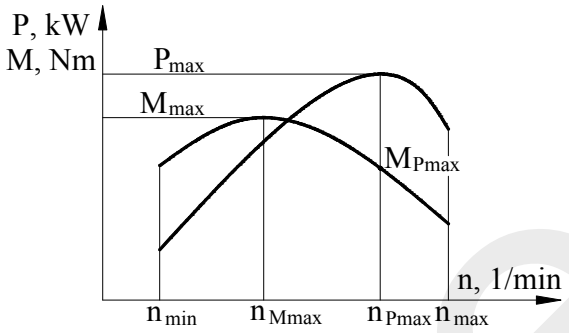

Figure 6.6: Characteristic of ICE

Gasoline engine: $\frac{M_{max}}{M_n} = 1.2 - 1.4$

Diesel engine: $\frac{M_{max}}{M_n} = 1.05 - 1.15$

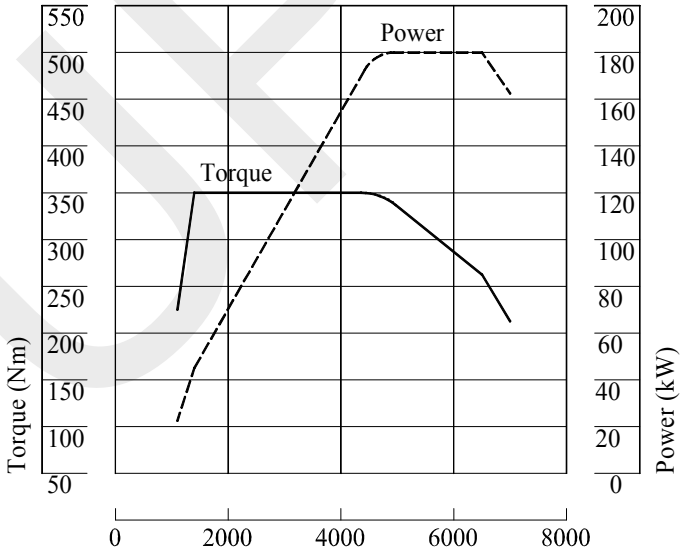

Figure 6.7: Characteristic of the supercharged engine
Source: [17]

The characteristic curves of today's sophisticated ICE change and alter according to the momentary operating conditions, partly with the assistance of altering valve-control, partly with computer control. One way to enhance the engine power in the

case of unchanged stroke volume is the suitable modifying the r/l ratio of the crank mechanism. It results in shorter stroke and increasing engine rpm. Although the torque of the engine is decreasing however the rpm range of it is widening more, this way the engine power is increasing. Since the idle RPM's are approximately the same, the smaller torque in the low RPM range results in lower engine power.

Two cars, assembled with 1400 and 1600 cm^3 stoke volume engines having approximately the same power, would be identical in terms of vehicle dynamic if the vehicle with smaller stroke volume engine would operate with transmission having more gears in order to provide higher engine RPM for more speed ranges of the car. In general, these inexpensive cars aren't assembled with transmission having high number of gears because of its expense. The car with bigger stoke volume engine can utilize bigger torque in a narrower rpm range which provides a convenient drive in the city traffic.
The other way to enhance the engine power is the application of superchargers, either compressors or turbo charger. The torque curve reaches the maximum value at about 1500-1600 rpm and it stays horizontal until the regulated RPM provided with the ECU of the engine controlling the supercharging pressure, see Fig. 6.7.

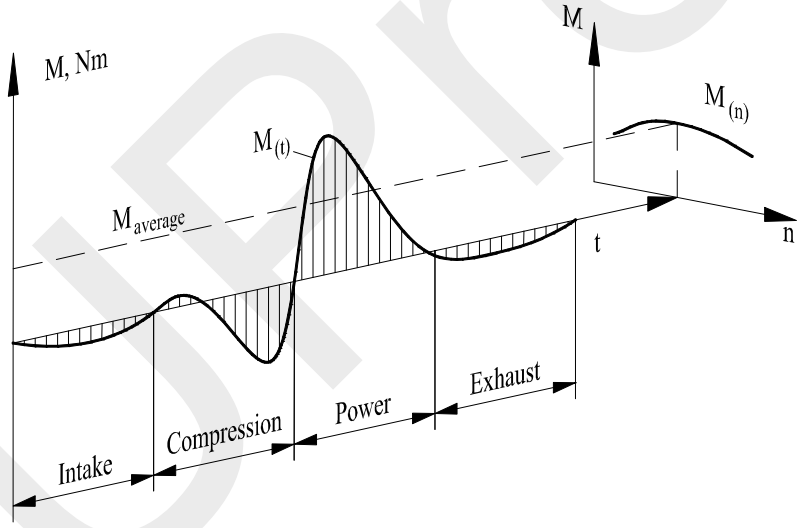

Figure 6.8: Torque curve of a four stroke ICE
Source: [16]

The Diesel cars are popular because of its engine characteristic. However it is well known that nowadays almost all of the diesel cars are assembled with supercharger. Consequently the vehicle dynamic is provided not by the Diesel technology but by the supercharging.
The four stoke internal combustion engines provides power only in every fourth stroke, while it crankshaft turns two, see Fig. 6.8.

It follows from this that even the multicylinder engines run uneven, which fact must be considered by applying a suitable operation coefficient when designing the drivetrain.
We see examples for this when designing a belt or chain drive by the application of the c_2 and Y operation coefficients.

6.2. Machineries

The characteristic of machineries based on their technological process carried out may be whatever. Here we introduce only three typical one of them which forms depend either on the deformation work or on the resistance of medium overcame by the machinery.

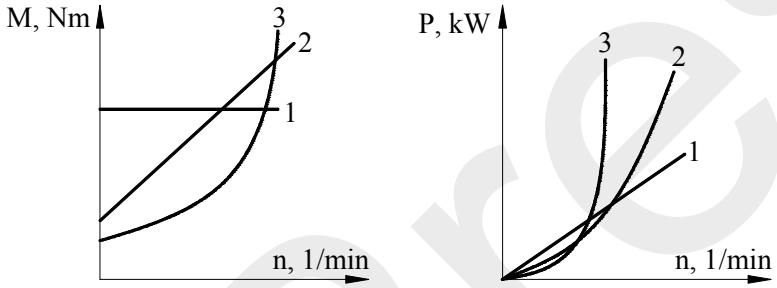

Figure 6.9: Typical machinery characteristics

Characteristic curves of prime movers represented in the same diagram.

1. $M = cons$ independent from the rpm — $P = f_{(n)}$ hoisting engines, conveyors, piston pumps
2. $M = f_{(n)}$ Linear (deformation work is done) — $P = f_{(n^2)}$ press machines
3. $M = f_{(n^2)}$ progressive (resistance of medium is overcame) — $P = f_{(n^3)}$ fan blowers, centrifugal pumps

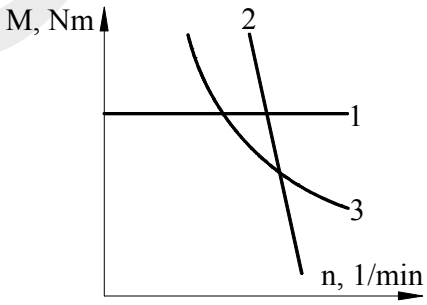

Figure 6.10: Typical prime mover characteristic curves

1.	Moment maintaining	piston steam-engine, load operated clockwork mechanism
2.	Rpm maintaining	direct-current side current motor asynchronous motor
3.	Power keeping	direct-current, main current motor

6.3. Transmission machineries

The task of transmission machineries is to connect the prime mover to the machine mechanically with respect to their rpm and torque requirements. A prime mover and a machine having the same power rating may not be connected by all means directly. In general they work at different speed and the torque deliver and demand of them is unlike as well. Accordingly the task of the transmission machinery is modifying the speed and the torque of the prime mover to meet the requirements of the machine if they have the same state of motion, and transforming the form of motion if they were different to connect them together. This task is performed automatically by the frictional and positive connection drives hence they only transmit the power. A good example for altering the form of motion is the mechanism applied in the hair clipper, which connect the electric motor shaft having a rotational motion with the knife section having a circular arc movement.

6.3.1. Choosing transmission machinery

A drivetrain may fulfil the service life requirement if the prime mover and the machinery are working at their (P_m) design point since at this point the efficiency is good providing the desired service life. The ($P_{ü}$) service point of the drivetrain is the intersection point of the characteristic curves. The service point is appropriate if it is on the stable section of the prime mover characteristic curve and coincides or nearly coincides with the design point of the prime mover and the machinery (P_{mm} and P_{gm}).

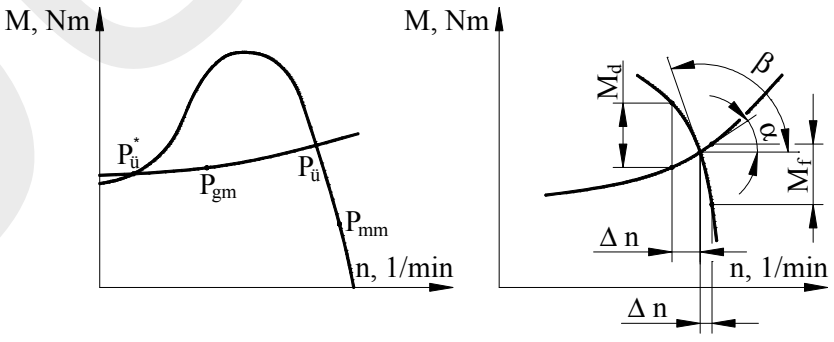

Figure 6.11: The service point, the condition of stability
Source: [16]

In Fig. 6.11 there are two intersection points from which the $P_{üi}^{*}$ is instable service point. It may be realized when studying the following disorder step by step:

- the load of the drivetrain is decreasing resulting in higher prime mover speed,
- the prime mover torque belonging to the increased rpm is higher than one at the service point,
- the increasing torque will accelerate the drivetrain till reaching either the maximum rpm of the prime mover or the another $P_{üi}$ service point which is stable.

The $P_{üi}$ service point is on the stable section of the characteristic curve, so the criterion of stability is that for the angular position of the tangent lines of the prime mover's and the machine's characteristic curve at the service point the following criterion must be fulfilled: $\beta > 90°$, ill. $\alpha < 90°$.

6.3.2. Cases of choosing transmission machinery

Transmission machinery has to be applied every case if the state of motion of the prime mover and the machinery is different. In addition to this, now we survey the cases may occur when set-up drivetrain.

1. The characteristic curves of the prime mover and the machinery have $P_{üi}$ intersection point which coincides or closely coincides with the P_m design points. There is sufficient torque at disposal for starting and there is no restriction regarding the acceleration of the drivetrain. For transmission machinery any clutch or coupling may be applied which do not modify the characteristic curves.

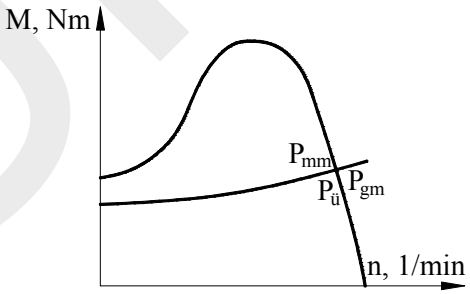

Figure 6.12: The service point coincides with the design points

   The choosing of the coupling based on the coaxiality requirements and the rigidity features of the coupled shafts.

2. The design points of the prime mover and the machinery are far-away from each other moreover the characteristic curves may not have any intersection points (service point).

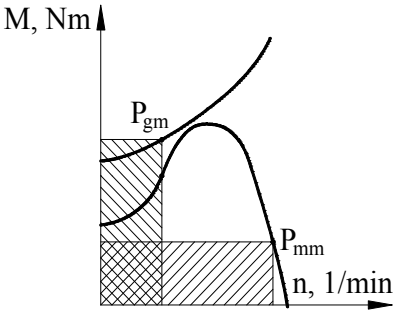

Figure 6.13: Characteristics without service point

If the areas of the hatched rectangles belonging to the matching M-n values are equal, it means that the prime mover and the machine have the same performance, accordingly as transmission machinery any friction or positive connection drive (belt drive, chain drive, gear drive, ect.) may be applied bringing the speeds to the same value. For choosing couplings to insert the transmission machinery, the same aspects should be considered than in the previous point.

3. The service point coincides with the design points but the torque provided by the prime mover is not sufficient or not enough for accelerating the drivetrain with a required value.

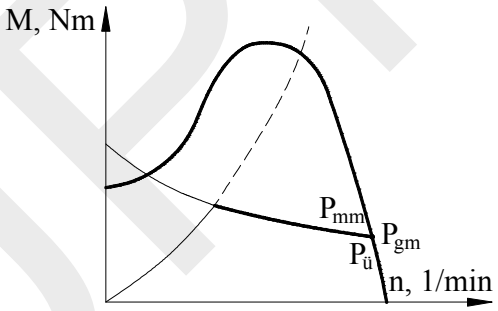

Figure 6.14: Characteristic curves with insufficient starting torque

For transmission machinery rotary speed governed coupling may be applied, which transmits the torque to the machinery gradually in the clutching phase while the speed and the torque of the prime mover are increasing. The most common rotary speed governed couplings are the following:

- centrifugal coupling
- hydrodynamic coupling
- induction clutch
- magnetic clutch

The fundamental difference in their operation is that the slip occurs either only during clutching (e.g. centrifugal coupling) or during operation (e.g. hydrodynamic coupling) that can not work without slip. Couplings belonging

to latter one cut the torque peaks this is why they work as torque limiter too affecting the torsional oscillations.

4. Any combination of the three cases discussed previously.

The special transmission machinery of drivetrains is often attempt to be replaced (not by experts) by cheaper one simple in design (replacing rotary speed governed or flexible coupling with coupling sleeve). Its consequence is that although the replacing coupling would not fail but other parts of the drivetrain go wrong because of the arising supplementary loads. The stressing was namely carried out not for the arising supplementary loads.

6.3.3. Kinematic ratio and efficiency of transmission machinery

Transmission machinery operates with mechanical loss. The energy not transformed to mechanical work (this energy is transformed into heat energy) manifest itself in different ways in frictional connection and positive connection drives.

6.3.3.1. Frictional connection drive (e.g.: belt drive)

The efficiency of the transmission machinery is the ratio of the power delivered by the prime mover and the power utilized by the transmission machinery.

$$\eta = \frac{P_g}{P_m} = \frac{M_g \omega_g}{M_m \omega_m} \tag{6.3}$$

$$P_v = P_m - P_g = P_m (1 - \eta) \tag{6.4}$$

loss, manifested in heat flow

Let's introduce the kinematic and the torque ratio after that let's express the efficiency:

$$i_\omega = \frac{n_m}{n_g} \quad \text{kinematic ratio} \tag{6.5}$$

$$i_M = \frac{M_g}{M_m} \quad \text{torque ratio} \tag{6.6}$$

$$\eta = \frac{i_M}{i_\omega} \quad \text{efficiency} \tag{6.7}$$

The torque ratio is constant in normal (non-transient) operation. The prime mover delivers so much power that is taken up by the frictional connection drive plus the heat flux. Accordingly the kinematic ratio depends on the efficiency, however the efficiency depends on the load, eventually the kinematic ratio is dependent on the load.

In loss-free case: $\eta = 1$ and $n_g = n_{g_0}$, from which:

$$\eta = 1 = i_M \frac{n_{g_0}}{n_m} \Rightarrow i_M = \frac{n_m}{n_{g_o}}$$

In loss case, assuming that torque ratio is steady:

$$\eta = i_M \frac{n_g}{n_m} = \frac{n_m}{n_{g_0}} \frac{n_g}{n_m} = \frac{n_g}{n_{g_0}} \Rightarrow n_g = n_{g_0} \eta$$

Introducing Δn_g, the slip may be expressed as the specific value of the RPM's decreasing:

$$\Delta n_g = n_{g_0} - n_g = n_{g_0} (1 - \eta) \tag{6.8}$$

$$s = \frac{\Delta \mathrm{n}_g}{n_{g_0}} = \frac{n_{g_0} - n_g}{n_{g_0}} = (1 - \eta) \tag{6.9}$$

6.3.3.2. Positive connection drives (e.g.: gear drive)

The ratio of the RPMs, thus the kinematic ratio is constant due to the positive connection. The mechanical loss manifesting itself in heat flux causes the torque decreasing on the transmission machinery, thus the torque ratio is dependent on the efficiency.

In loss-free case: $\eta = 1$ and $M_g = M_{g_0}$

In loss case: $M_g = \eta M_{g_0}$ (6.10)

$$\Delta M_g = M_{g_0} - M_g = M_{g_o} (1 - \eta) \tag{6.11}$$

The transmission machineries may be in terms of kinematic ratio:

$i > 1 \Rightarrow n_m > n_g$ reductor; $i < 1 \Rightarrow n_m < n_g$ multiplier

In the following we introduce and analyse some special transmission machineries.

6.3.3.3. CVT and ECVT

The designation CVT and ECVT are common term and refer to the operation principle of the transmission, namely it changes the kinetic ratio continuously. Designation ECVT refers to the way of controlling its ratio by means of variable RPM of an electric motor. In this chapter we compare the operation principles of the mechanical and the electronic control implemented by a three degree of freedom system gear. The control of ratio may need power provided by the prime mover. The measure of removed power and its utilization possibility in the drive influences the operation of the vehicle or any other devices

CVT implemented with V belt drive

Main parts: CVT and a centrifugal coupling, see Fig. 6.15.

The application field of the actual drive: drivetrain of two or four stroke scooter. The drivetrain consists of two centrifugal couplings. The operation principle of CVT is based on the belt drive having constant centre distance and continuously variable ratio. The two pulleys have splitted construction having an adjustable distance between the pulley disc halves. The V-belt runs on the datum diameters of the pulleys determined by the distance between the pulley disc halves and transmit the peripheral force. The precondition of the operation is the appropriate synchronizing of the axial displacement of the disc halves. The axial displacement of the driver disc half is provided by the flyweights, which proportional to the rotational speed exert centrifugal force enforcing the displaceable disc half toward the fixed disc half modifying the datum diameter of the pulley. Since the centre distance and the belt datum length will not change, the momentary position of the movable disc half of the driven pulley has to be in accordance with the datum diameter of the driver disc. This may be implemented simply with a half disc enforced by a cylindrical spring in axial direction.

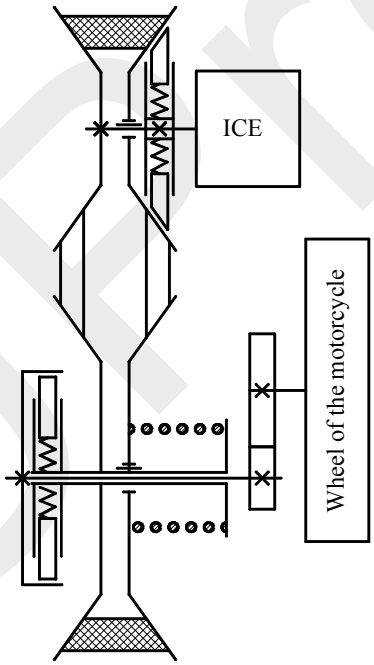

Figure 6.15: CVT with a centrifugal coupling

The lower the stiffness of the spring the lesser the pretension force of the belt drive change when the drive ratio varies. The CVT transmits the power to the driven wheel through another centrifugal coupling. The flying shoes of the centrifugal coupling rotating at the RPM of the driven pulley of the CVT are forced to the inner surface of a drum which is assembled on the output shaft by a splined joint. This output shaft drives the rear wheel of the scooter through a geared transmission.

The control of this type of CVT operating with 2-3% slip, removes negligible power from the prime mover represented by the kinetic energy of the flyweights. In engine brake mode this energy is dissipated into the environment in the form of heat energy. When increasing the RPM again, the kinetic energy of the flyweights is provided by the prime mover.

ECVT based on 3 degree of freedom system gears

The operation principle of ECVT is based on the freedom system of different type of gear drives e.g. planetary gear and harmonic drive. If one of the shafts of a 3 degree of freedom gear is the output (driven) shaft, the other two shafts left are input (driver) shafts. By modifying the speed of one of the input shafts the speed of the output shaft hence the ratio of the transmission may be controlled continuously. Following three ECVT-s are introduced and analysed.

ECVT implemented with harmonic drive.

Fig. 6.16 shows the active steering-gear of AUDI, providing variable ratio between the steering wheel and the wheels.

The circular spline has internal teeth that mesh with external teeth on the flexspline. The flexspline has fewer teeth and consequently a smaller effective diameter than the circular spline. The wave generator is a link with two rollers that rotates within the flexspline, causing it to mesh with the circular spline progressively at diametrically opposite points. The ratio of the drive [2]:

$$i = \frac{z_{circular\ \ spline}}{z_{circular\ \ spline} - z_{flex.\ \ spline}} \tag{6.12}$$

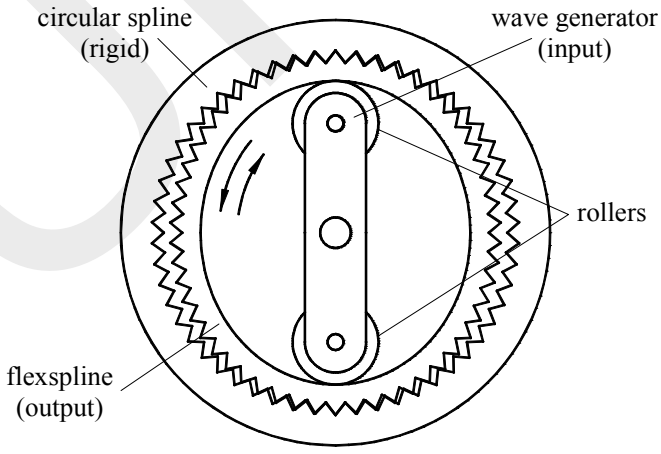

Figure 6.16: AUDI steering unit with harmonic drive
Source: [23]

The circular spline, driving the pinion of the rack and pinion gear, is the output of the harmonic drive. The other two elements serve as input of the harmonic drive. The

flexspline is driven by the steering wheel, while the wave generator is driven by an electric motor having variable RPM in clockwise and counter-clockwise.

ECVT implemented with P(PP)P type planetary gear

Fig. 6.17 shows the active steering-gear of BMW, providing variable ratio between the steering wheel and the wheels.

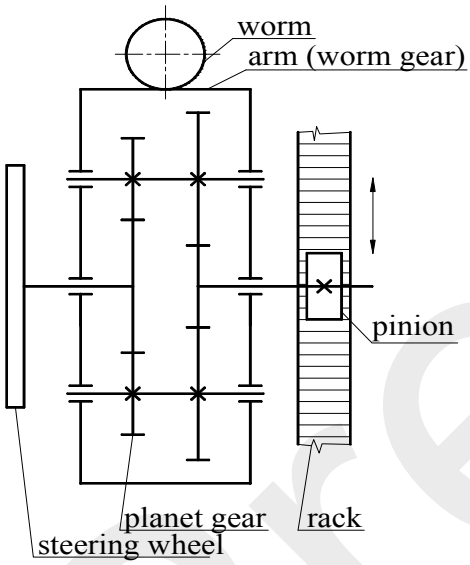

Figure 6.17: BMW steering gear unit with planetary gear
Source: [24]

One of the sun gears, driving the pinion of the rack and pinion gear, is the output of the planetary gear. The other two elements serve as input. The another sun gear is driven by the steering wheel, while the arm of the planetary gears is driven by an electric motor having variable RPM in clockwise and counter-clockwise. The RPM equation of the P(PP)P type planetary gear:

$$n_1 - \frac{r_2}{r_1} + \frac{r_3}{r_2'} n_3 = \left(1 - \frac{r_2}{r_1} + \frac{r_3}{r_2'}\right) n_k \tag{6.13}$$

The control of ECVT implemented with harmonic drive and P(PP)P type planetary gear removes power from the prime mover however the power of the steering unit contains the power of both of the input shafts, hence it is utilised in the drive.

ECVT implemented with P(P)N type planetary gear applied in Toyota Auris HSD 1.8 hybrid car

The Fig. 6.18 shows the simplified scheme of Toyota Auris HSD 1.8 drivetrain in which the ECVT transmits the whole power of the ICE to the driven wheels. In this chapter we determine the power demand of the ECVT control in proportion to the ICE power.

The transmission contains a three degree of freedom system P(P)N type planetary gear which active elements connect to MG1, MG2 and ICE. In the Toyota Full Hybrid

system the momentary kinematic ratio of the ECVT is adjusted by controlling the sun gear's RPM with the MG1 generator.

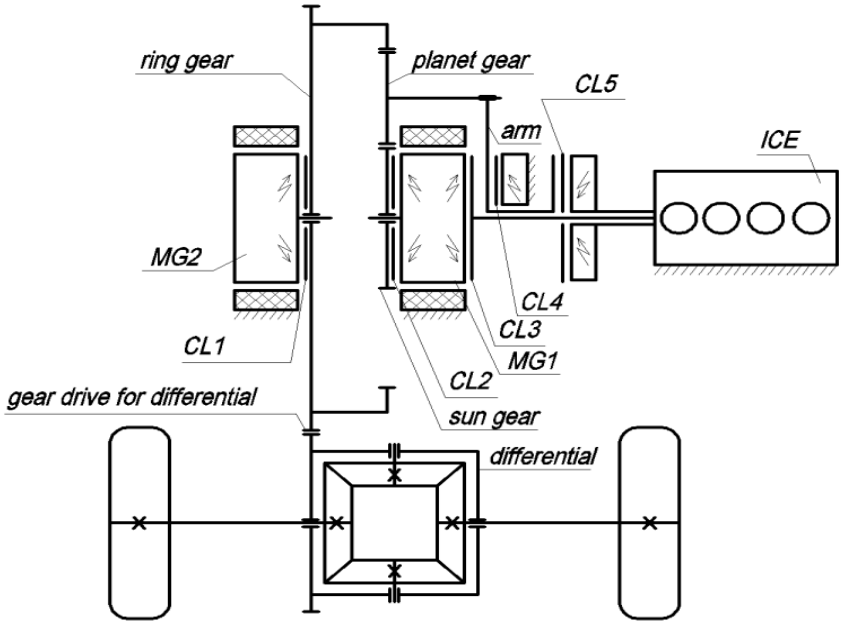

Figure 6.18: Simplified scheme of the Auris HSD drivetrain

The units of the system [25]

HV (high voltage) battery

Liquid-cooled, 201V nominal voltage NI-Mh battery has 6.5 Ah nominal capacity. It is charged via the inverter by the MG1 and MG2 electric motors in generator mode and it supplies the MG1 and MG2 electric motors. The battery can store approximately 1.9 kJ energy provides 2-3 km mobility with pure electrical drive at a low speed. The battery storage capacity is sufficient only for some regenerative braking and it is really not appropriate for assisting the ICE long by supplying the MG2.

Data of the drivetrain:

ICE

Nominal power: 73 kW (99 LE), 5200 1/min;
Nominal torque: 142 Nm, 4400 1/min
Maximal RPM: 5800 1/min
Displacement: 1798 cm3 (Atkinson-Miller) suction petrol engine

RPM equation of the transmission:

$$n_1 + \frac{r_3}{r_1} n_3 = \left(1 + \frac{r_3}{r_1}\right) n_k \qquad (6.14)$$

Electric motors/generators data:

MG1

RPM range: 0-11000 1/min

MG2

Power: 60 kW; maximal torque: 207 Nm; RPM range: 0-5000 1/min

Vehicle

Maximum power: 100 kW (136 LE) (according to the owner's manual)

Max. speed: 180 km/h

Analysing the data of overall power and maximal speed, there is a contradiction between them since the car with 136 LE power should have the max. speed above 210 km/h. To the given 180 km/h max. speed approximately 75-80 LE power corresponds. It is in conformity with the owner's feedback namely the maximum 136 LE power is only for a few minutes at disposal and after that the performance of the ICE drops expendable for drive. We will discover that MG1 generator is responsible for the low performance since it takes off power from the ICE in order to control the ratio.

Operation of the ECVT

A P(P)N type planetary gear has three active elements: ring gear, sun gear and arm. All of the clutches applied are electromagnetic operated and controlled by the ECU (electronic control unit). The ICE is connected to the arm via a single disc friction clutch fixing one degree of freedom. In addition to, the arm connects to the frame via a multi disc clutch as well. The MG2 connects to the ring gear via a multi disc clutch thus to the driven wheels as well fixing one degree of freedom. It follows from this that if the ICE drives the planetary gear in this set-up, only the sun gear representing the only degree of freedom allowed would revolve, forasmuch as that its resistance is substantially less than one represented by the car drive. This is why the kinematic ratio of the ECVT can be modified by the control of the MG1's RPM connecting to sun gear via a multi disc clutch. Apart from reversing, the MG1 operates as a generator to brake the sun gear. In reverse gear the MG1 operates as an electric motor and rotates in the opposite direction. In addition to the basic task of the MG1, it is connected to the ICE via a multi discs clutch in order to start the ICE.

According to the measure of the gas potentiometer and the travelling resistances, the ECU determines the RPM of the ICE and the MG1 required, by this means the momentary kinematic ratio of ECVT.

Fig. 6.19 represents the operation stages of hybrid vehicles. The power requirement of the car is small when creeping in traffic jam or standing at signal lamp; it can be provided by the electric motor as well. In this case the use of the ICE at low RPM, performance and efficiency can be avoided. A common hybrid car with a pure electric drive may run the car at a speed of about 10-30 km/h for approximately 2-5 km distance. In case of higher power demand or discharged battery, the ICE starts and drives the car as well as charges the battery if required. When accelerating the car very hard, the MG2 electric motor helps ICE drive the car provided that enough battery capacity is at disposal. In brake mode the ICE shuts down and the kinetic energy of the vehicle would not transform into friction heat in the mechanical brakes but stored in the battery by driving the MG2 generator. All of these technical solutions result in decreasing fuel consumption; e.g. the combined fuel consumption

of a common Toyota Auris 1.33 is approximately 5.9 l/100 km, and its emission is about 128 g of CO_2/100 km; whereas the urban fuel consumption of Toyota Auris HSD 1.8 (hybrid car) is about 3.8 l/100 km and its emission is about 88 g of CO_2/100 km. Although this data is only informative however it can be seen, that in special traffic circumstances significant fuel consumption decrease can be achieved.

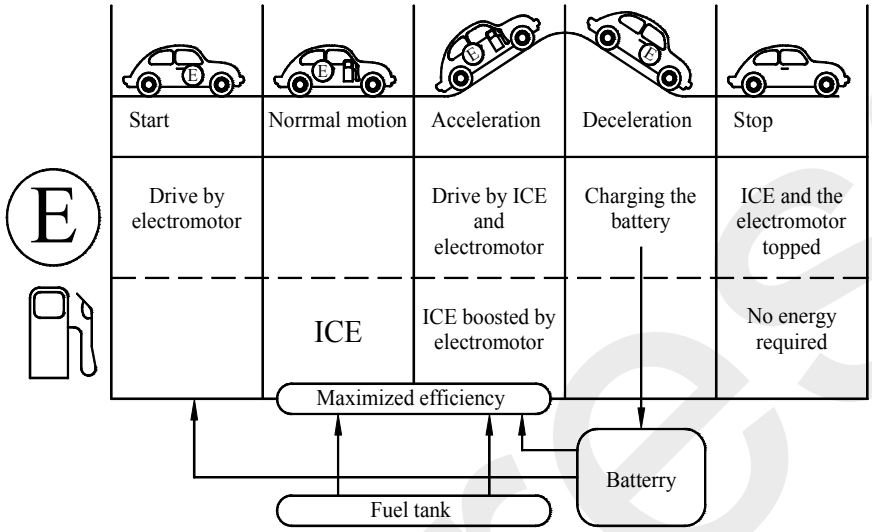

Figure 6.19: Operation stages of hybrid vehicles

Take-off (the ICE is out of order)

In pure electric mode MG2 drives the ring gear via the CL1 (all the other clutches are disengaged).

Acceleration

At intensive speed-up the ICE and the MG2 drive together. For this the ICE must be started effected by the MG1 via the CL3. After that CL3 disengages, CL2 and CL5 engage, by this means the ICE drives the arm and the kinematic ratio results from the MG1's RPM in generator mode (taking off power from the ICE).

The measuring results show that the MG2 utilize the energy stored in the battery very fast, accordingly at intensive speed-up it can assist the ICE only for a few seconds. The ECU controls the ECVT so that the ICE operates at high RPM and efficiency.

Steady operation

The car runs at an approximately steady speed driven by the ICE. The CL1 and CL3 are disengaged; the CL2 and CL5 are engaged. The task of MG1 is to control the e-CVT hence it operates in generator mode taking off power from the ICE. To avoid the battery overcharging, the MG2 is supplied by the battery accordingly the MG2 drives occasionally the ring gear via the engaged CL1.

Braking, downhill

The ICE stops, CL5 disengages and simultaneously CL4 engages. Clutches of MG1 and MG2 (CL1 and CL2) are engaged hence the wheels of the car drive back the MG1 and MG2 generators utilizing the kinetic energy of the moving vehicle.

Charging during drive

In case of run-down battery, one part of the ICE's power is provided for driving the MG2. Apart from CL3 and CL4 all of the clutches are engaged. When the battery is charged-up, the clutch of MG2 (CL1) disengages accordingly the power of ICE is devoted only for driving the car.

Measuring

Measuring were conducted with the Toyota Motor Corporation Techstream application [26] can be connected to the ECU provides ON-LINE diagnostics for data acquisition and evaluation.

Fig. 6.20 shows measuring records of measurement carried out in NORMAL mode with average charged HV battery.

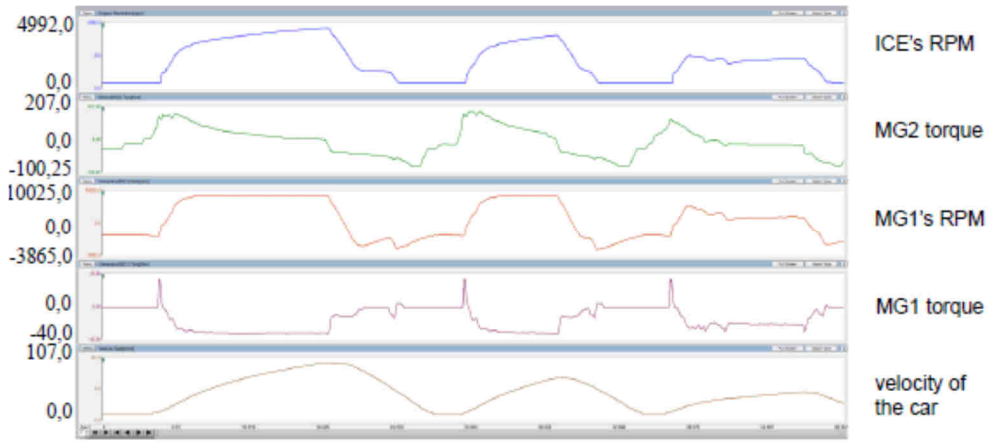

Figure 6.20: "drive performance" on the road
Source: [27]

The records show one minute measuring interval of (from top to down) ICE's RPM, MG2 torque, MG1's RPM, MG1 torque and the velocity of the car in the function of time [27]. It can be seen, that during the measurement we stopped two times, the maximum speed was 107 km/h and the acceleration achieved pertained to 80% gas potentiometer. The fourth diagram from the top represents the MG1 torque. It shows that the MG1 is always in generator mode however there are protuberant peak values when the MG1 connects to the inverter.

The fifth diagram shows that car speed does not proportionally increase with the ICE's RPM, because the necessary tractive force can be provided by increasing RPM of MG1in order to adjust appropriate kinematic ratio. This way MG1 takes off more and more power from the ICE. It is very important to analyse the MG2 torque. At the beginning of speeding up, MG2 assist in driving the car, later on its torque drops to zero. The assists take approximately 5 s. After throttling-down, the MG2 switches into generator mode and the ICE stops.

Facts and figures of measurement:

- Significant part of the ICE power is devoted for driving the MG1 (approx. 40 kW from 73 kW), which is compensated for a limited time with the MG2 power (approx. 60 kW).

- MG2 can assist the ICE for approximately 5 s, since the battery runs down.
- Inference: in case of hard speeding up (continuous, sequential overtaking) the drive dynamic of the car is worse as if it was driven only by the ICE. In braking mode the recuperation effects, however the kinetic energy recovered is not sufficient for charging the HV battery.

Fig. 6.21 shows measuring record of maximal acceleration in NORMAL mode with a slightly run-down HV battery. The test took 90 seconds the car was speed-up to 183 km/h on test stand. This data is only informative since the resistances generated by the test stand can not be considered authoritative. The diagrams show from the top to the bottom the velocity of the car, torque of MG2 and MG1.

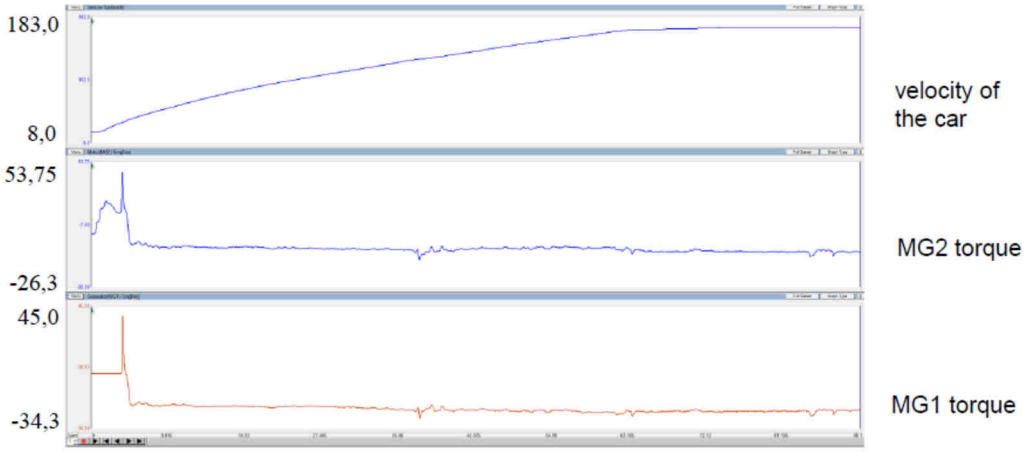

Figure 6.21: Test stand measuring "drive performance"
Source: [27]

Facts and figures of measuring:

- MG1 torque has a transient peak value, which can not be good for power electronics.
- MG2 operates only 5 sec long as electric motor, after that in generator mode it takes off 3-7 Nm torque from the ICE.
- MG1 operates all the time as generator taking off 15-20 Nm torque from the ICE. It is approximately the half of the previous measuring result, which shows that the resistances on the test stand are not real.
- In spite of the driver intention to achieve maximum acceleration, from the 73 kW nominal ICE power only 56 kW is at disposal because of the power demand (17 kW) of the ECVT operation.
- The battery can not be charged during the 90 sec of test operation.

According to the owner manual the power of the ICE is 73 kW. It appeared from the measuring that one part of the ICE power (17/73 = 23 %) is not used for powering the car. It means that actual available total power of the system (ICE and electric motor) is only 56 kW instead of the given 100 kW. Similar to the previous test, MG2 was able to assist the ICE only for 5 sec.

Measurements conducted in ECO and POWER modes were similar to the previous one in NORMAL mode, therefore do not set them forth.

Conclusions
The electronic control of the ECVT removes a lot of energy from the prime mover. Although this energy used for charging the battery is utilized by driving the car with MG2, however the mechanical energy was transformed four times (electrical energy - electric charge – electrical energy – mechanical energy) causing power loss because of the efficiency of energy transformations. Eventually 73 kW max. power ICE can provide only 56kW power in the most disadvantageous operation circumstances for driving the car. The electronic control requires 23% of the power to be transmitted.

6.3.3.4. Sliding gear transmission with engaging dogs

The transmission represented in Fig. 6.22 is a six-speed not synchronized transmission of today's motorbikes. Although it is not synchronized, it is applied widespread in motorbikes up to 200 HP, because of its small dimension, hence small mass and short switching time. Its dimension is only about a quarter of a synchronized transmission applied in a passenger cars. The disadvantage of this transmission is that it requires a big routine for a fast smooth switching or else its engaging dogs are subjected dynamic load because of clashing.

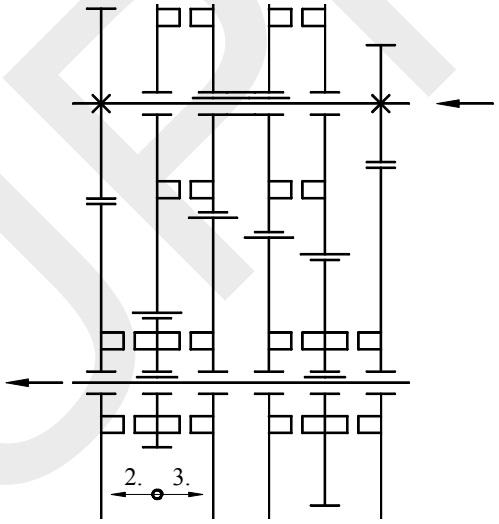

Figure 6.22: Sliding gear transmission with engaging dogs

Before developing the DCT (Dual-clutch transmission), sport cars were assembled with not synchronized coupler jaw transmission requiring instruction regarding its handling. To avoid clashing, during gearing up two times must be clutched. Although this action required routine, driver had to feel the appropriate RPM at which the shafts and gears to be engaged got the same rotational speed to gear up without clash. In Sliding gear transmission with engaging dogs, all the gears are meshed

simultaneously however only one gear set transmits power at the same time (such as in synchronized and coupler jaw transmissions). The other pairs of gears have always one gear spinning freely. When the transmission is in neutral, none of the sliding gears are engaged with adjacent gears, so the output shaft doesn't turn with any force. Of course it is forced to spin a little because of the friction of gears spinning on it.
The slider (coupler) gear meshes a gear too implementing a gear ratio as well. When putting into gear, the appropriate slider gear having dogs on its side faces moves toward the gear to be coupled and its protruding dogs engage slots on adjacent gear. This way the slider gear joins the other gear to the shaft. Because of the sliding operation method, the gears can be only straight gears. In the case of motorbike transmission there is no way to clutch twice during gear changing since in the sequential transmissions the neutral position is between only the first and second gear, and the small dimension gears have small mass moment of inertia, therefore their RPM drop immediately owing to the high resistance of medium of the oil-bath. This is why the gear changing must be performed so fast that the RPM of the gears drop only to the required value.

6.3.3.5. Hydrodynamic coupling

Main parts: impeller (pump) driven by the prime mover, turbine (it does not contain stator, therefore it is not a torque converter), and rotary housing, see Fig. 6.23.

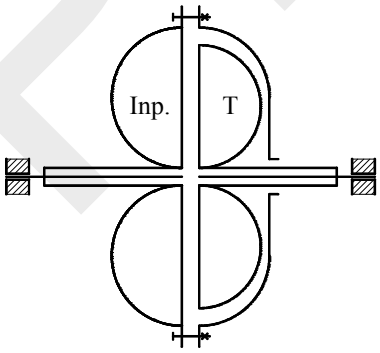

Figure 6.23: Hydrodynamic coupling

The rotary housing containing the impeller and the turbine is filled approximately up to 2/3 level with oil having prescribed viscosity. The oil streams on the rotating impeller blades in radial direction, than getting into the turbine and exerts impulse on the turbine blades resulting in torque. Impulse on the blades can develop if there is a rotary speed difference between the impeller and the turbine, which may be expressed by the slip. The consequence of the 3-4% operation slip is that this loss in terms of mechanical work dissipates into the surroundings as heat energy. The measure of this heat energy is so big, that cars assembled with torque converter must be equipped with oil cooler and considerable consumption excess are realized.

Moment equation of the coupling

$$M_1 = M_2 + M_s \tag{6.15}$$

where: M_1 torque of the impeller

M_2 torque of the turbine

M_s torque of oil friction

According to the equation, the impeller delivers always so big torque which is taken up by the drivetrain through the turbine plus the torque of the oil friction: $M_1 \approx M_2$.

The efficiency-slip-kinematic ratio relation of the coupling:

$$\eta = \frac{P_t}{P_{sz}} = \frac{M_2\omega_2}{M_1\omega_1} = \frac{n_2}{n_1} = i_{21} = 1 - s \tag{6.16}$$

$$s = \frac{n_1 - n_2}{n_1} = 1 - \frac{n_2}{n_1} = 1 - i_{21} \tag{6.17}$$

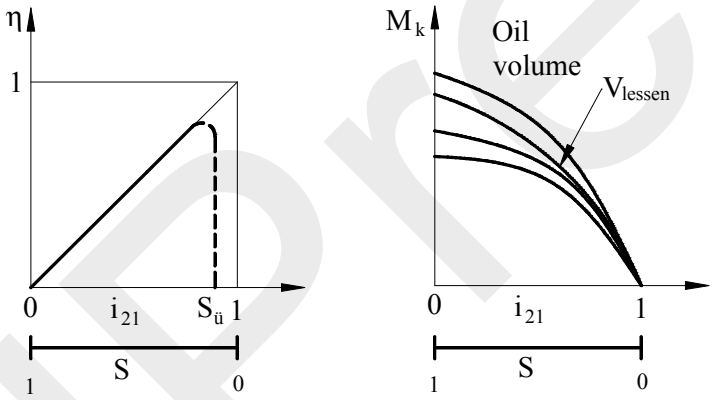

Figure 6.24: Characteristic curve of the hydrodynamic coupling
Source: [16]

The torque and the power transmitted with the coupling may be determined by empirical formula based on laboratory measuring. Therefore every parameter must be substituted in the prescribed unit.

$$M_k = k_M n_1^2 D^5 \quad \text{[Nm]} \tag{6.18}$$

$$P_k = k_P n_1^3 D^5 \quad \text{[W]} \tag{6.19}$$

where: D [m] average diameter of the annulus

k_M, k_P torque and power coefficient

Figure 6.25 represents the M_k torque versus n_1, n_2.

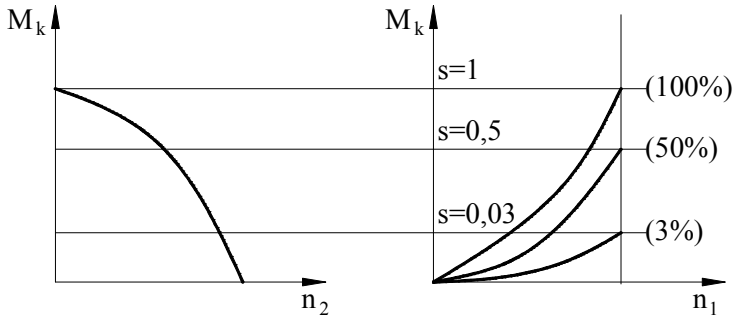

Figure 6.25: Torque of the hydrodynamic coupling
Source: [16]

Figure 6.26 represents the operation point of drivetrain assembled with hydrodynamic coupling.

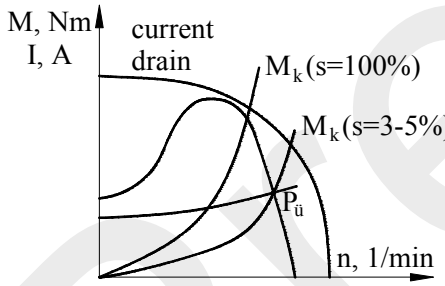

Figure 6.26: Drivetrain characteristic with hydrodynamic coupling
Source: [16]

Aspects of choosing the hydrodynamic coupling:

- the coupling has to be capable transmit higher torque than the maximum torque may be delivered by the prime mover,
- the characteristic cure pertaining to the s=100% must intersect the characteristic curve of the prime mover at right from the stalling torque.

6.4. Linkages

One of the tasks of transmission machineries is to bring the motion of the prime mover and the machinery to the same form, and to provide the required motions in the machine to carry out the given technological process. Generally it is implemented with linkage which points under load move on a specified track and they may be in poise due to an adequate force system. Although in this chapter we can not detail how to derive the displacement, velocity and acceleration functions discussed in the course of Mechanism, we will analyse two linkages in terms of mobility. As it known, the number of freedom of system equal with the number of scalar quantities necessary to specify its position:

in the case of mass point	in plane 2 (x, y)	in spatial 3 (x, y, z),
in the case of solid	in plane 3 (x, y, φ_z)	in spatial 6 ($x, y, z, \varphi_x, \varphi_y, \varphi_z$)

Linkages can connect to the ground with different constraints (external constraint), which depending upon the number of the constraining forces allows displacement for the linkage in a specified direction. The applied constraints and the construction of the joints specify the motion of the linkage whether it is planar or spatial. The mechanisms we will analyse moves in planar therefore we study this case in details. If the freedom of the linkage is "s" and the number of freedoms fixed by constrains (external and inner) "n_k" the mechanism can be:

- statically determinate: $s = n_k$ (it is in rest due to the external forces)
- statically indeterminate: $n_k > s$ (it is in rest but it is redundant)
- unstable $s > n_k$ (it moves under load in a specified direction)

For determining the degree of freedom of an unstable mechanism we have to know the number of freedom restrained by the different external and inner constraints (unknown components of force and moments), therefore we analyse the common types of constrains. Rods of a linkage provide 3 equations (E) per rod in planar case, hence the number of freedom of a linkage is: the number of rods x 3, minus the number of freedom restrained by external and internal constraints (I).

Inner constraints

External constraints		**Freedom(s) restrained**	
		planar	spatial
roller		1 (n)	1 (n)
guide rod		2 (x, M_k)	5 ($x, y, M_{h_x}, M_{h_y}, M_{h_z}$)
ball joint		2 (x, y)	3 (x, y, z)
hinge joint		2 (x, y)	3 (x, y, M_h)
fixation		3 (x, y, M_h)	6 ($x, y, z, M_{h_x}, M_{h_y}, M_{h_z}$)
rodded support		1 (n)	1 (n)

Joint connecting rods together, may be either ball or hinge joint provides 2 equations (unknowns) in planar case. If more than two rods connect to the same joint, then the number of joints = number of rods – 1.Let's analyse the three and five jointed statically determinate mechanism on the Fig. 6.27.

Three jointed mechanism

$E = 2x3 = 6$

$I = 2 + 2 + 2 = 6$,

$s = 0$

Five jointed mechanism

$E = 3x3 = 9$

$I = 2 + 2 + 2 + 2 + 1 = 9$

$s = 0$

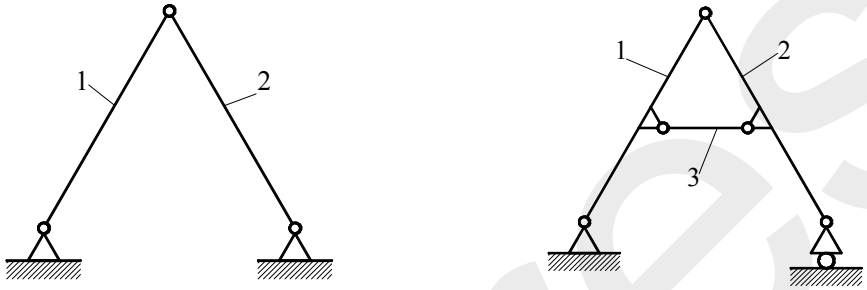

Figure 6.27: Three and five jointed mechanism

Vehicle suspension

Let's study the constraints of a vehicle suspension.

- control arm: connect to the body through the control arm bushing (hinge joint), hence the connecting point restrains 2 freedoms ($I = 2$) in planar case.
- lower and upper ball joints: join the control arm to the steering knuckle (ball joint) which restrain 2 freedom ($I = 2$) in planar case and make possible the turn of the steering knuckle of a steered wheel around the centre line determined by the lower and upper ball joints.
- outer tie rod end: connect the steering gear with the steering arm of the steering knuckle (ball joint).
- upper strut mount bearing: connect the McPherson strut to the tower through rubber bed (ball joint), which makes possible the turning of the steered wheel. It restrains 2 freedoms in planar case ($I = 2$).
- McPherson strut (guide rod): It fixes 2 freedoms in planar case ($I = 2$).

Double-wishbone suspension system

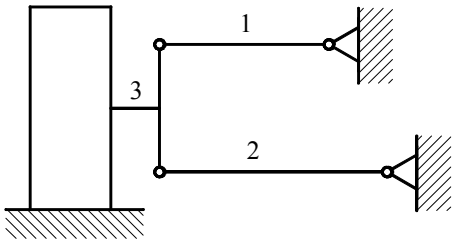

$$E = 3x3 = 9$$
$$I = 2 + 2 + 2 + 2 = 8$$
$$s = 1$$

Figure 6.28: Double-wishbone suspension

The control arm connects to the steering knuckle:

- in the case of not steered wheel through control arm bushing (hinge joint)
- in the case of steered wheel through ball joint (ball joint), which may be replaced in some constructions by kingpin and control arm bushing (hinge joint).

McPherson strut suspension

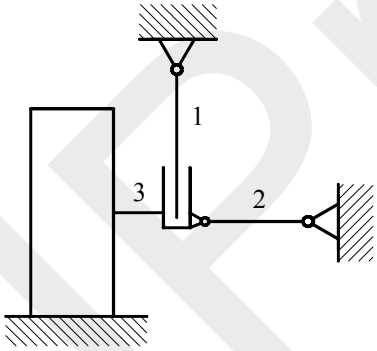

$$E = 3x3 = 9$$
$$I = 2 + 2 + 2 + 2 = 8$$
$$s = 1$$

Figure 6.29: McPherson strut suspension

The connection of the control arm and the steering knuckle is implemented by lower ball joint (ball joint).

The analysed suspensions are accordingly one degree of freedom system, of which stable states are ensured by the reaction forces (tire - road, suspension spring-car body).

7. Dynamic modelling

Depending upon the designer purpose a drivetrain operates either in RPM range doesn't contain the natural frequencies of it, or on the contrary, close to one of the natural frequencies. Any situation occurs we have to know the natural frequencies of the drivetrain which either must be avoided or the drivetrain has to be tuned by modifying its mechanical parameters in order to one of the natural frequencies

coincides with the excitation frequency. The dynamic modelling is based on the equation of motion of the drivetrain which may be written applying the equation of energy equilibrium.

The equation of motion of the drivetrain

The drivetrain built up with parts performs oscillating motions in different directions. They may be torsional, bending and longitudinal oscillation. We will not discuss the longitudinal oscillation since longitudinal resonance is not experienced commonly. For describing the torsional oscillations we apply the spring model while for the bending oscillation the continuum model is applied.

The equation of motion based on the spring model

The parts of the drivetrain subjected to external load deform in a less or larger measure (it increases the energy level of the system). In the form of elastic deformation potential energy is stored in the parts which depending upon the material and construction damping can be got back as a kinetic energy when springing out.

The springing out of a deformed part happens not in a cycle but in several one because of its mass moment of inertia the springing in and springing out take until the stored energy is dissipated from the oscillating system. The means of dissipation are the material and construction damping and the air resistance. Consequently without damping and air resistance the system would oscillate with its natural frequency and constant amplitude infinite. Because of the damping the amplitude of the oscillation is decreasing till the stored energy is transformed into heat energy and into kinetic energy of the surrounding air molecules.

If the oscillation system is subjected to external force having the excitation frequency coinciding with natural frequency, it will oscillate greater and greater amplitude resulting in higher and higher potential energy in the form of deformation work of parts until the arising stress is higher than the ultimate stress of the material which causes the break of the most stressed part. For writing the energy equation of the drivetrain it may be modelled with springs and translation and rotational masses having mass moment of inertia. The spatial position of the "n" degree of freedom mechanical system can be given by "n" pieces of parameters which are independent from each other and dependent only with the time. These parameters are the k_1 generalized coordinates. The generalized coordinates are not identical necessarily with the geometrical coordinates of the system determining the position of its mass points. However the geometrical coordinates can not
depend on the time derivative of the generalized coordinates:

$$x_i = x_i\left(q_1, q_2, \ldots q_n\right) \tag{7.1}$$

The kinetic energy of the system

If the masses of the system perform movement and rotational motion, and the axis x, y, z going through the centre of masses are principal axis of inertia, then the kinetic energy of the i[th] element is:

$$E_i = \frac{1}{2} m_i \left(\dot{x}_i^2 + \dot{y}_i^2 + \dot{z}_i^2 \right) + \frac{1}{2} \left(Q_{i1} \dot{\varphi}_{ix}^2 + Q_{i2} \dot{\varphi}_{iy}^2 + Q_{i3} \dot{\varphi}_{iz}^2 \right) \tag{7.2}$$

where: m mass

Q_{i1}, Q_{i2}, Q_{i3} mass moment of inertia for the three axes

Accordingly, the kinetic energy of system containing „n" masses:

$$E = \sum_{i=1}^{n} E_i = E(q_1, q_2, \ldots, q_n, \dot{q}_1, \dot{q}_2, \dot{q}_3) \tag{7.3}$$

The potential energy of the system

The potential energy of the oscillation system varies if its elements translate against the gravitational force, or potential energy is stored as deformation work. Since the movements are the functions of the geometrical coordinates, the instantaneous value of the potential energy:

$$U = \sum U_i = U\left(q_1, q_2, .., q_n\right) \tag{7.4}$$

Work performed by excitations

The elements of the system are subjected to external loads (forces, moments) hence works are performed which are the product of the force and the displacement along the force or the torque and the angular displacement. (The reactions do not perform work since their points of application are fixed.) The work performed by the external forces and torques (excitations) summed from the time: $t = 0$: „L".

Work performed by damping

Damping built in the mechanical system and friction between moving parts dissipate energy of the system.

The work performed by the damping summed from the time $t = 0$: „W".

The level of energy in the moment of „t", if the energies of the system at $t = 0$: E_0 and U_0:

$E + U = E_0 + U_0 - W + L$, which time derivative: (7.5)

$$\frac{dE}{dt} + \frac{dU}{dt} + \frac{dW}{dt} = \frac{dL}{dt}, \text{ where} \tag{7.6}$$

$$\frac{dU}{dt} = \sum_{i=1}^{n} \frac{\partial U}{\partial q_i} \dot{q}_i \tag{7.7}$$

$$\frac{dW}{dt} = \sum_{i=1}^{n} P_i \dot{q}_i,$$

where P_i: damping force (7.8)

$$P_i = \frac{\partial D}{\partial \dot{q}_i}$$, where D: dissipation function

$$\frac{dW}{dt} = \sum_{i=1}^{n} \frac{\partial D}{\partial \dot{q}_i} \dot{q}_i \tag{7.9}$$

$$\frac{dL}{dt} = \sum_{i=1}^{n} Q_i \dot{q}_i \,, \tag{7.10}$$

where Q_i: generalized component of force

$$\frac{dE}{dt} = \sum_{i=1}^{n} \left(\frac{d}{dt} \frac{\partial E}{\partial \dot{q}_i} \dot{q}_i \right) - \sum_{i=1}^{n} \left(\frac{\partial E}{\partial q_i} \dot{q}_i \right) \tag{7.11}$$

As it may be seen every member of the energy equilibrium equation is a function of velocity of the moving hence if $\dot{q}_i \neq 0$, then after substituting them the general form of Lagrangian second order equation of motion is gained:

$$\frac{d}{dt} \frac{\partial E}{\partial \dot{q}_i} - \frac{\partial E}{\partial q_i} + \frac{\partial U}{\partial q_i} + \frac{\partial D}{\partial \dot{q}_i} = Q_i \qquad i = 1, 2, \ldots, n \tag{7.12}$$

In excitation and damping free case the second order equation ($Q_i = 0$ and $D = 0$):

$$\frac{d}{dt} \frac{\partial E}{\partial \dot{q}_i} - \frac{\partial E}{\partial q_i} + \frac{\partial U}{\partial q_i} = 0 \tag{7.13}$$

7.1. Equation of motion of torsion oscillation

A common drive layout is set up from the following units (Fig. 7.1):

- prime mover
- transmission machineries
- couplings, clutches
- universal-joint shaft supported with bearings
- machine

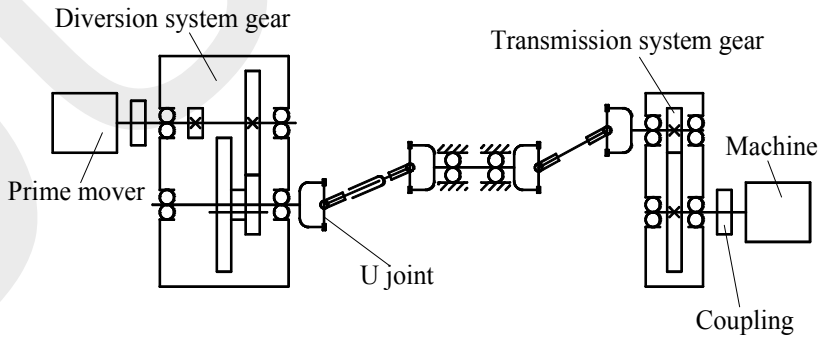

Figure 7.1: Common cardan drive layout

The common drive layout contains not only chain type sections like as universal-joint shaft (see Fig. 7.1) but transmission and diversion system gears as well. In the case of transmission system due to the kinematic connection of the parts (e.g. meshing

gears) there is only one generalized coordinate necessary to describe its motion. In the case of diversion system the power flow branches. It may be implemented in a way that there is no power transmission in every chain, however in spite of it, these chains have effects on each other because of the mass moment of inertia and the flexibility of the parts. The term "bearing" means not only the supporting of the shafts but the base of the prime mover, machines, transmissions which can be featured with bearing stiffness or spring stiffness. For determining the bearing stiffness of the supports, we have to analyse the connection of the parts (connection in series, connection in parallel or compound connection). For example the ICE of vehicles is fixed in the chassis through rubber engine support. However the chassis contacts the road through the suspension and the tire, hence because of the connection in series, the tire is decisive having less stiffness.

We checked this situation by carrying out dynamic tests on drivetrain driven by a tractor in two ways. At first the tractor was standing on its tires, after that it was supported stiff on its axles. The effect of the two supporting method for the experimental results were obvious.

The method for writing the torsion equation of motion of the common layout drivetrain may be introduced by analysing the parts from the mechanical point of view.

The spring model set up with springs having no mass and mass moment of inertia, and with discs having mass and mass moment of inertia. When modelling, all of the geometrical, mechanical and operation features of the parts have to be known. The torsion and bending spring constant of the shafts may be determined either by measuring or by calculation from its parameters. The parts assembled on the shaft (discs, gears, couplings, clutches, ect.) may be modelled with discs to which the mass moment of inertia of the shaft or a part of it must be counted on the bases of technical specifications. The operation features of joints (e.g. ball joint, cardan joint) are taken into consideration with transmission coefficient expressing the correlation of the angular displacements, angular velocities and angular accelerations of the shafts coupled with joints.

7.1.1. Equation of motion for elemental chain-type model

The general features of the equation of motion may be ascertained by deriving the equation of motion of a three degree of freedom torsion oscillation system.

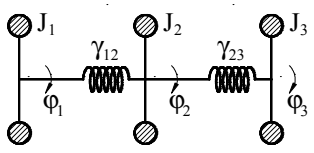

Figure 7.2: Three degree of freedom torsion oscillation system

The q_1, q_2, q_3 generalized coordinates are defined as the angular displacement of the discs.

The equation of motion may be derived from the Lagrangian second order equation:

$$\frac{d}{dt}\frac{\partial E}{\partial \dot{q}_i} - \frac{\partial E}{\partial q_i} + \frac{\partial U}{\partial q_i} = 0$$

The kinetic energy of the oscillating disc

$$E = \frac{1}{2}J_1\dot{q}_1^2 + \frac{1}{2}J_2\dot{q}_2^2 + \frac{1}{2}J_3\dot{q}_3^2 \tag{7.14}$$

The potential energy stored in the springs:

$$U = \frac{(q_1 - q_2)^2}{2\gamma_{12}} + \frac{(q_2 - q_3)^2}{2\gamma_{23}} \tag{7.15}$$

The equation system describing the torsion oscillations:

$$J_1\ddot{q}_1 + \frac{q_1 - q_2}{\gamma_{12}} = 0 \tag{7.16}$$

$$J_2\ddot{q}_2 + \frac{q_2 - q_1}{\gamma_{12}} + \frac{q_2 - q_3}{\gamma_{23}} = 0 \tag{7.17}$$

$$J_3\ddot{q}_3 + \frac{q_3 - q_2}{\gamma_{12}} = 0 \tag{7.18}$$

The matrix equation of the equation of motion:

$$\underline{\underline{m}}\,\underline{\ddot{q}} + \underline{\underline{c}}\,\underline{q} = \underline{0} \tag{7.19}$$

where: $\underline{\underline{m}}$ mass matrix

$\underline{\underline{c}}$ spring matrix

$$\underline{\underline{m}} = \begin{bmatrix} J_1 & 0 & 0 \\ 0 & J_2 & 0 \\ 0 & 0 & J_3 \end{bmatrix} \qquad \underline{\underline{c}} = \begin{bmatrix} \frac{1}{\gamma_{12}} & -\frac{1}{\gamma_{12}} & 0 \\ -\frac{1}{\gamma_{12}} & \frac{1}{\gamma_{12}} + \frac{1}{\gamma_{23}} & -\frac{1}{\gamma_{23}} \\ 0 & -\frac{1}{\gamma_{23}} & \frac{1}{\gamma_{23}} \end{bmatrix} \qquad \underline{q} = \begin{bmatrix} q_1 \\ q_2 \\ q_3 \end{bmatrix} \qquad \underline{\ddot{q}} = \begin{bmatrix} \ddot{q}_1 \\ \ddot{q}_2 \\ \ddot{q}_3 \end{bmatrix}$$

The feature of the elementary chain-type system may be realized by studying the matrixes:

- the mass matrix is diagonal (it contains elements only in the principal diagonal different from 0),
- the spring matrix is tri-diagonal (it contains elements only in the principal diagonal and in the diagonal below and above, different from 0) and the sum of row elements is 0.

Elementary chain-type system fixed to the wall

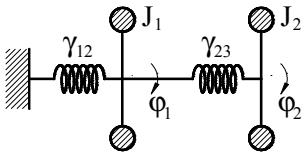

Figure 7.3: Torsion oscillation system fixed to the wall

The energy equations:

$$E = \frac{1}{2} J_1 \dot{q}_1^2 + \frac{1}{2} J_2 \dot{q}_2^2 \tag{7.20}$$

$$U = \frac{q_1^2}{2\gamma_{12}} + \frac{(q_1 - q_2)^2}{\gamma_{23}} = 0 \tag{7.21}$$

The equation system of the motion:

$$J_1 \ddot{q}_1 + \frac{q_1}{\gamma_{12}} + \frac{q_1 - q_2}{\gamma_{23}} = 0 \tag{7.22}$$

$$J_2 \ddot{q}_2 + \frac{q_2 - q_1}{\gamma_{23}} = 0 \tag{7.23}$$

The matrix equation of the equation of motion:

$$\underline{\underline{m}}\,\underline{\ddot{q}} + \underline{\underline{c}}\,\underline{q} = \underline{0}$$

$$\underline{\underline{m}} = \begin{bmatrix} J_1 & 0 \\ 0 & J_2 \end{bmatrix} \qquad \underline{\underline{c}} = \begin{bmatrix} \frac{1}{\gamma_{12}} + \frac{1}{\gamma_{23}} & -\frac{1}{\gamma_{23}} \\ -\frac{1}{\gamma_{23}} & \frac{1}{\gamma_{23}} \end{bmatrix}$$

In the spring matrix it can be realized that in the row indicating the place of fixing to the wall, the sum of its elements are not 0. Since the oscillation system is elementary chain-type, hence the mass matrix is diagonal and the spring matrix is tri-diagonal.

7.1.2. Transforming common drive layout system

We will see from the examples detailed later that:

- in the case of transmission system the mass matrix is diagonal and the spring matrix is tri-diagonal but at least in two rows the sum of the elements are not 0,
- in the case of diversion system neither the mass matrix is necessarily diagonal nor the spring matrix is tri-diagonal.

For transforming the common drive layout system into elementary chain-type one, the equation of motion of the common drive layout system has to be derived.
The natural frequencies of the oscillating system may be calculated from the frequency equation provided by analysing the solvability of the equation of motion.

Although the natural frequencies of the common drive layout system can be determined however it requires individual solutions which can be found in complicated cases with difficulty. It can be justified that the natural frequencies of a common drive layout system and its elementary chain-type system correspond with each other. However the natural frequencies of a chain-type system can be determined simply.

The aim of the transformation accordingly is to bring the equation of motion into uniform form, by this means the further calculations may be formalized and programmed on computer. The common drive layout system can be transformed into an elementary chain-type system in two steps:

- transforming the diversion system into a transmission system,
- transforming the transmission system into an elementary chain-type system.

7.1.2.1. Transforming transmission system into elementary one

The equation of motion of the transmission drive system:

$$\underline{\underline{M}}\,\underline{\ddot{p}} + \underline{\underline{C}}\,\underline{p} = \underline{0} \tag{7.24}$$

where: $\underline{\underline{M}}$ diagonal mass matrix

$\underline{\underline{C}}$ tri-diagonal spring matrix, where the sum of the matrix row elements at least in two rows are not 0

$\underline{p}$ generalized coordinate of the transmission drive system

This equation can be transformed with the $\underline{\underline{S}}$ transform matrix [19]:

$$\underline{s} = \underline{\underline{S}}^{*}\,\underline{\underline{M}}\,\underline{\underline{S}} \qquad \underline{c} = \underline{\underline{S}}^{*}\,\underline{\underline{C}}\,\underline{\underline{S}} \qquad \underline{q} = \underline{\underline{S}}\,\underline{p} \tag{7.25), (7.26), (7.27}$$

The transformed matrix equation: $\underline{\underline{m}}\,\underline{\ddot{q}} + \underline{\underline{c}}\,\underline{q} = \underline{0}$ is of already a chain type drive system. We present the steps of transformation on a 3 degree of freedom oscillation system (see chapter 7.1.1). The elements of the $\underline{\underline{S}}$ matrix can be determined from the assumption that the sum of the row elements of the $\underline{\underline{c}} = \underline{\underline{S}}^{*}\,\underline{\underline{C}}\,\underline{\underline{S}}$ matrix has to be 0.

$$\underline{\underline{c}} = \begin{bmatrix} S_1 & S_2 & S_3 \end{bmatrix} \begin{bmatrix} C_{11} & C_{12} & 0 \\ C_{21} & C_{22} & C_{23} \\ 0 & C_{32} & C_{33} \end{bmatrix} \begin{bmatrix} S_1 \\ S_2 \\ S_3 \end{bmatrix}$$

The S_1 element of the $\underline{\underline{S}}$ matrix may be chosen arbitrarily. Expediently $S_1 := 1$

Carrying out the matrix product, the sum of the elements in the first row of the $\underline{\underline{C}}$ matrix:

$S_1 C_{11} S_1 + S_1 C_{12} S_2 = 0$, from which $S_2 = \frac{C_{11}}{C_{12}}$

The sum of the elements in the second row:

$S_2 C_{21} S_1 + S_2 C_{22} S_2 + S_2 C_{23} S_3 = 0$, from which S_3 can be expressed.

The analogy of the calculation may be easy realized. With the expression of every further row merely one additional unknown of the $\underline{\underline{S}}$ matrix appears which can be expressed and calculated. This way the transformation matrix of arbitrary degree of freedom drive system may be determined.

7.1.2.2. Transformation of the diversion drive system

The equation of motion of the diversion drive system

$$\underline{\underline{N}}\,\underline{\ddot{r}} + \underline{\underline{Q}}\,\underline{r} = \underline{0} \qquad (7.28)$$

where: $\underline{\underline{N}}$ mass matrix

$\underline{\underline{Q}}$ not tri-diagonal spring matrix

$\underline{r}$ generalized coordinate of the diversion drive system

This equation can be transformed with the $\underline{\underline{T}}$ transform matrix into transmission drive system [19]:

$$\underline{\underline{M}} = \underline{\underline{T}}^{*}\,\underline{\underline{N}}\,\underline{\underline{T}} \qquad \underline{\underline{C}} = \underline{\underline{T}}^{*}\,\underline{\underline{Q}}\,\underline{\underline{T}} \qquad \underline{p} = \underline{\underline{T}}\,\underline{r} \qquad (7.29), (7.30), (7.31)$$

The elements of the $\underline{\underline{T}}$ matrix may be determined from the assumption that the spring matrix has to be tri-diagonal. The transformed matrix equation: $\underline{\underline{M}}\,\underline{\ddot{p}} + \underline{\underline{C}}\,\underline{p} = \underline{0}$ is of already transmission drive system which may be transformed further into elementary chain-type system with the $\underline{\underline{S}}$ transform matrix. The method with which the elements of the $\underline{\underline{T}}$ matrix may be calculated is very complicated and requires individual solutions this is why we do not discuss it. If the dynamic modelling does not aim the prime mover and the transmission machinery, they can be modelled with discs to carry out the simplified dynamic modelling of the drivetrain.

7.1.3. Examples for deriving the equation of motions

When deriving the equation of motion of a drivetrain, at first the degree of freedom system has to be ascertained.

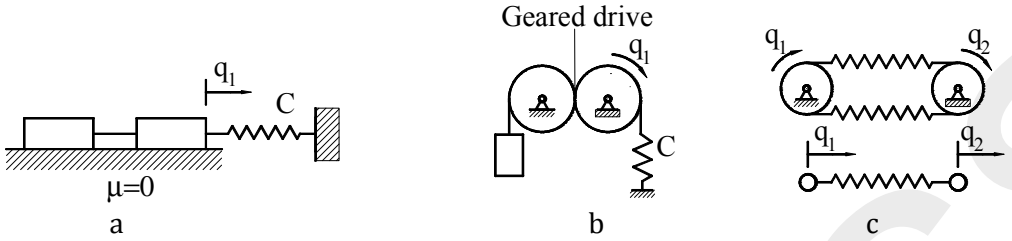

Figure 7.4: Different degree of freedom systems

In Fig. 7.4.a two blocks connected together rigid are fixed to the wall through a spring. Although the two blocks represent two different parts, because of the rigid connection they are only one part from mechanical point of view. Accordingly the oscillating system is of one degree of freedom system.
In Fig. 7.4.b two connecting discs (meshing gears, friction gears) can be seen having positive or rigid frictional connection. The angular position of the discs correlates with each other. Since there are two discs actually, this one degree of freedom system is of transmission drive system.
In Fig. 7.4.c two discs connect to each other through flexible belt (belt drive, chain drive).
To describe the angular position of the discs, two generalized coordinates are needed consequently the system is of two degree of freedom system.

7.1.3.1. Example for transmission drive system

On the basis of definitions studied in the previous chapter, in Fig. 7.5 we can see a three degree of freedom transmission oscillation drive system. The rods (shafts) are modelled with torsion springs having no mass and mass moment of inertia, therefore their mass moment of inertia are taken into consideration in the adjoining discs. Let's choose the angular displacement of number 1, 2 and 3 discs for generalized coordinates.

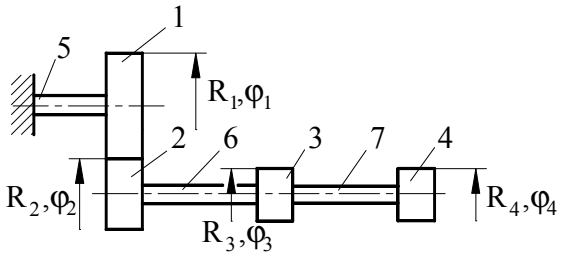

Figure 7.5: Transmission drive system

$p_1 = \varphi_1$, $p_2 = \varphi_3$, $p_3 = \varphi_4$

Due to the geared transmission:

$$R_1\varphi_1 = R_2\varphi_2$$

The torsion spring compliances of the rods:

$$c_5 = \frac{l_5}{I_{p_5}G},\ c_6 = \frac{l_6}{I_{p_6}G},\ c_7 = \frac{l_7}{I_{p_7}G}$$

The kinetic and potential energy of the oscillating system:

$$E = \frac{1}{2}J_1\dot{p}_1^2 + \frac{1}{2}J_2\left(\frac{R_1}{R_2}\dot{p}_1\right)^2 + \frac{1}{2}J_3\dot{p}_2^2 + \frac{1}{2}J_4\dot{p}_3^2$$

$$U = \frac{p_1^2}{2c_5} + \frac{\left(p_2 - \frac{R_1}{R_2}p_1\right)^2}{2c_6} + \frac{(p_3 - p_2)^2}{2c_7}$$

The equation of motion according to the Lagrangian second order equation $\left(\frac{d}{dt}\left(\frac{\partial E}{\partial \dot{p}}\right) + \frac{\partial U}{\partial p} = 0\right)$:

$$\left(J_1 + \left(\frac{R_1}{R_2}\right)^2 J_2\right)\ddot{p}_1 + \frac{p_1}{c_5} + \frac{\left(\frac{R_1}{R_2}\right)^2 p_1}{c_6} - \frac{\frac{R_1}{R_2}p_2}{c_6} = 0$$

$$J_3\ddot{p}_2 + \frac{p_2}{c_6} - \frac{\frac{R_1}{R_2}p_1}{c_6} + \frac{p_2}{c_7} - \frac{p_3}{c_7} = 0$$

$$J_4\ddot{p}_3 + \frac{p_3}{c_7} - \frac{p_2}{c_7} = 0$$

The matrix form of the equation of motion:

$\underline{\underline{M}}\,\underline{\ddot{p}} + \underline{\underline{C}}\,\underline{p} = \underline{0}$, where:

$$\underline{\underline{M}} = \begin{bmatrix} J_1 + \left(\frac{R_1}{R_2}\right)^2 J_2 & 0 & 0 \\ 0 & J_3 & 0 \\ 0 & 0 & J_4 \end{bmatrix} \qquad \underline{\underline{C}} = \begin{bmatrix} \frac{1}{c_5} + \left(\frac{R_1}{R_2}\right)^2\frac{1}{c_6} & -\frac{R_1}{R_2}\frac{1}{c_6} & 0 \\ -\frac{R_1}{R_2}\frac{1}{c_6} & \frac{1}{c_6} + \frac{1}{c_7} & -\frac{1}{c_7} \\ 0 & -\frac{1}{c_7} & \frac{1}{c_7} \end{bmatrix}$$

As it can be seen, the $\underline{\underline{M}}$ mass matrix of the derived equation of motion is of diagonal, the $\underline{\underline{C}}$ spring matrix is tri-diagonal just as in the case of elementary chain type system however the sum of the row elements are not 0 in two rows.

After that the equation of motion may be transformed into elementary chain type system by means of the $\underline{\underline{S}}$ transform matrix. Without derivation, the elements of the $\underline{\underline{S}}$ matrix:

$$S_1 := 1$$

$$S_2 = -\frac{C_{11}}{C_{12}} = \frac{\frac{1}{c_5} + \left(\frac{R_1}{R_2}\right)^2 \frac{1}{c_6}}{\frac{R_1}{R_2}\frac{1}{c_6}}$$

$$S_3 = \frac{-C_{21} - S_2 C_{22}}{C_{23}} = \frac{\frac{R_1}{R_2}\frac{1}{c_6} - \frac{\frac{1}{c_5} + \left(\frac{R_1}{R_2}\right)^2 \frac{1}{c_6}}{\frac{R_1}{R_2}\frac{1}{c_6}}\left(\frac{1}{c_6} + \frac{1}{c_7}\right)}{-\frac{1}{c_7}}$$

7.1.3.2. Example for the equation of motion of a belt drive

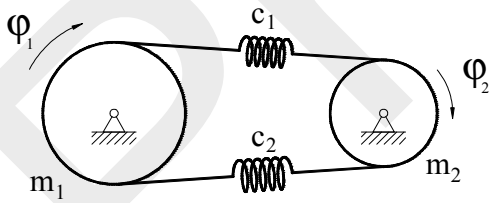

Figure 7.6: Belt drive

Fig. 7.6 represents a belt drive (chain drive) which is of two degree of freedom system. The tight and the slack side belts are modelled with different spring compliances.

The combined spring constant of the belt sides:

$$\left(\frac{1}{c_1} + \frac{1}{c_2}\right) = \frac{1}{c_{12}}$$

The kinematic and potential energy of the system:

$$E = \frac{1}{4} m_1 R_1^2 \dot{p}_1^2 + \frac{1}{4} m_2 R_2^2 \dot{p}_2^2$$

$$U = \frac{1}{2c_1}\left(R_1 p_1 - R_2 p_2\right)^2 + \frac{1}{2c_2}\left(R_1 p_1 - R_2 p_2\right)^2 = \frac{1}{2}\left(\frac{1}{c_1} + \frac{1}{c_2}\right)\left(R_1 p_1 - R_2 p_2\right)^2$$

The equation of motion according to the Lagrangian second order equation

$$\left(\frac{d}{dt}\left(\frac{\partial E}{\partial \dot{p}}\right) + \frac{\partial U}{\partial p} = 0\right):$$

$$\frac{1}{2}m_1R_1^2\ddot{p}_1+\frac{1}{c_{12}}\left(R_1p_1-R_2p_2\right)R_1=0$$

$$\frac{1}{2}m_2R_2^2\ddot{p}_2+\frac{1}{c_{12}}\left(R_2p_2-R_1p_1\right)R_2=0$$

The matrix form of the equation of motion:

$$\underline{\underline{M}}\,\underline{\ddot{p}}+\underline{\underline{C}}\,\underline{p}=\underline{0}$$

$$\underline{\underline{M}}=\begin{bmatrix}\frac{1}{2}m_1R_1 & 0\\ 0 & \frac{1}{2}m_2R_2\end{bmatrix} \qquad \underline{\underline{C}}=\begin{bmatrix}\frac{1}{c_{12}}R_1 & -\frac{1}{c_{12}}R_2\\ -\frac{1}{c_{12}}R_1 & \frac{1}{c_{12}}R_2\end{bmatrix}$$

As it can be seen, the $\underline{\underline{M}}$ mass matrix of the derived equation of motion is of diagonal, the $\underline{\underline{C}}$ spring matrix is of tri-diagonal. Since the sum of the row elements are not 0 in two rows, therefore the oscillation system is not elementary chain type one. The equation of motion may be transformed into elementary chain type system by means of the $\underline{\underline{S}}$ transform matrix.

Without derivation, the elements of the $\underline{\underline{S}}$ matrix:

$$S_1:=1$$

$$S_2=-\frac{C_{11}}{C_{12}}=\frac{\frac{1}{c_{12}}R_1}{\frac{1}{c_{12}}R_2}$$

7.1.3.3. Example for a diversion system

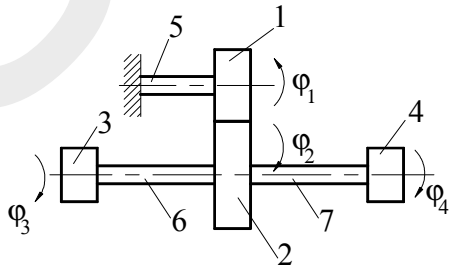

Figure 7.7: Diversion drive system

The diversion drive system represented in Fig. 7.7 because of its branch-off point is three degree of freedom system.

Due to the geared transmission:

$$R_1\varphi_1 = R_2\varphi_2$$

The torsion spring compliances of the rods:

$$c_5 = \frac{l_5}{I_{p_5} G} \qquad c_6 = \frac{l_6}{I_{p_6} G} \qquad c_7 = \frac{l_7}{I_{p_7} G}$$

The generalized coordinates:

$$\varphi_1 \equiv r_1 \;\; \varphi_3 \equiv r_2 \;\; \varphi_4 = r_3$$

The kinetic and potential energy of the oscillating system:

$$E = \frac{1}{2} J_1 \left(\frac{R_2}{R_1} \right)^2 \dot{r}_1^2 + \frac{1}{2} J_2 \dot{r}_1^2 + \frac{1}{2} J_3 \dot{r}_2^2 + \frac{1}{2} J_4 \dot{r}_3^2$$

$$U = \left(\frac{R_2}{R_1} \right)^2 \frac{1}{2c_5} r_1^2 + \frac{1}{2c_6} (r_1 - r_2)^2 + \frac{1}{2c_7} (r_1 - r_3)^2$$

The equation of motion according to the Lagrangian second order equation $\left(\frac{d}{dt} \left(\frac{\partial E}{\partial \dot{p}} \right) + \frac{\partial U}{\partial p} = 0 \right)$:

$$\left(J_1 \left(\frac{R_2}{R_1} \right)^2 + J_2 \right) \ddot{r}_1 + \left(\frac{R_2}{R_1} \right)^2 \frac{1}{c_5} r_1 + \frac{1}{c_6} r_1 - \frac{1}{c_6} r_2 + \frac{1}{c_7} r_1 - \frac{1}{c_7} r_3 = 0$$

$$J_3 \ddot{r}_2 + \frac{1}{c_6} r_2 - \frac{1}{c_6} r_1 = 0$$

$$J_4 \ddot{r}_3 + \frac{1}{c_7} r_3 - \frac{1}{c_7} r_1 = 0$$

The matrix form of the equation of motion:

$$\underline{\underline{N}}\,\ddot{\underline{r}} + \underline{\underline{Q}}\,\underline{r} = \underline{0}$$

$$\underline{\underline{M}} = \begin{bmatrix} J_1 \left(\frac{R_2}{R_1} \right)^2 + J_2 & 0 & 0 \\ 0 & J_3 & 0 \\ 0 & 0 & J_4 \end{bmatrix} \qquad \underline{\underline{C}} = \begin{bmatrix} \left(\frac{R_2}{R_1} \right)^2 \frac{1}{c_5} + \frac{1}{c_6} + \frac{1}{c_7} & -\frac{1}{c_6} & -\frac{1}{c_7} \\ -\frac{1}{c_6} & \frac{1}{c_6} & 0 \\ -\frac{1}{c_7} & 0 & \frac{1}{c_7} \end{bmatrix}$$

As it can be seen, the $\underline{\underline{M}}$ mass matrix of the derived equation of motion is of diagonal however the $\underline{\underline{C}}$ spring matrix is not of tri-diagonal. Applying this feature, the diversion drive system may be transformed into transmission system and after that the transmission system into elementary chain-type system. Because of its complexity we do not discuss the transformation procedure.

7.1.4. Natural frequencies of torsion oscillating system

The equation of motion of an oscillating system after transforming into elementary chain-type system:

$$\underline{\underline{m}}\,\underline{\underline{\ddot{q}}} + \underline{\underline{c}}\,\underline{\underline{q}} = \underline{\underline{0}}$$

It is expedient to search the general solution of the homogeneous equation in a form whose second time derivative deviates from the basic relation in a constant. This way the solution of the equation of motion becomes simple. The solution may be found in the following exponential function:

$$\underline{\underline{q}} = \underline{\underline{y}} e^{i\alpha t} \tag{7.32}$$

Where i: imaginary unit, and $i^2 = -1$

$$\underline{\underline{\ddot{q}}} = -\alpha^2 \underline{\underline{q}} = -\alpha^2 \underline{\underline{y}} e^{i\alpha t} \tag{7.33}$$

After substituting $\underline{\underline{q}}$ and $\underline{\underline{\ddot{q}}}$ into the equation of motion, a linear equation system is obtained for y:

$$\left(-\alpha^2 \underline{\underline{m}} + \underline{\underline{c}}\right) \underline{\underline{y}} = 0 \tag{7.34}$$

The Eq. 7.34 has solution only in that case if the following equation fulfils:

$$\det\left(-\alpha^2 \underline{\underline{m}} + \underline{\underline{c}}\right) = 0 \tag{7.35}$$

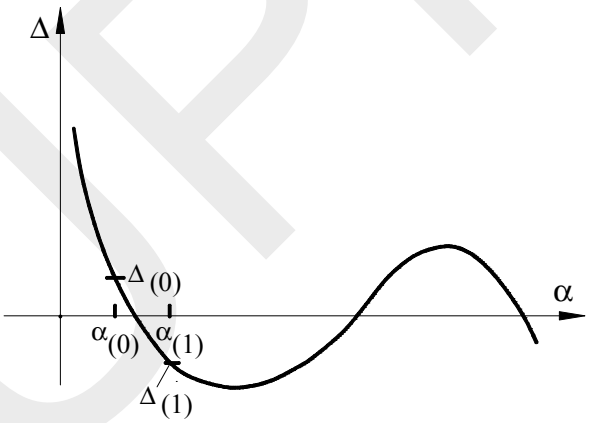

Figure 7.8: Natural frequency determining with iterative method

By developing the determinant, the frequency equation is obtained. In the case of many-degree-of-freedom system (five or more) there are no solution formulas to find the solutions this is why we do not calculate the α natural frequencies directly but indirectly by an iterative method. In this method the value of α increased by very little increments from the value of 0 is substituted into the determinant whose result is calculated with a computer program. The sign reversal of the result means that the determinant has zero between the two substituted values to which applying frequency is a natural frequency [19], see Fig. 7.8.

Let's determine the determinant of a three degree of freedom torsion system providing the frequency equation (see Fig. 7.2). The mass and spring matrixes:

$$\underline{\underline{m}} = \begin{bmatrix} J_1 & 0 & 0 \\ 0 & J_2 & 0 \\ 0 & 0 & J \end{bmatrix} \qquad \underline{\underline{c}} = \begin{bmatrix} \frac{1}{\gamma_{12}} & -\frac{1}{\gamma_{12}} & 0 \\ -\frac{1}{\gamma_{12}} & \frac{1}{\gamma_{12}}+\frac{1}{\gamma_{23}} & -\frac{1}{\gamma_{23}} \\ 0 & -\frac{1}{\gamma_{23}} & \frac{1}{\gamma_{23}} \end{bmatrix}$$

Constituting the $\det\left(-\alpha^2 \underline{\underline{m}} + \underline{\underline{c}}\right) = 0$:

$$\begin{vmatrix} -\alpha^2 J_1 + \frac{1}{\gamma_{12}} & -\frac{1}{\gamma_{12}} & 0 \\ -\frac{1}{\gamma_{12}} & -\alpha^2 J_2 + \frac{1}{\gamma_{12}} + \frac{1}{\gamma_{23}} & -\frac{1}{\gamma_{23}} \\ 0 & -\frac{1}{\gamma_{23}} & -\alpha^2 J_3 + \frac{1}{\gamma_{23}} \end{vmatrix} = 0$$

The natural frequencies may be determined by developing the determinant or by applying the iterative method.

Let's determine the formula of the natural frequency in the case of the one degree of freedom oscillating system fixed to the wall, see Fig. 7.3. The above determinant becomes simplified for the following equation, from which the well-known formula can be expressed:

$$-\alpha^2 J_1 + \frac{1}{\gamma_{12}} = 0, \qquad \alpha = \sqrt{\frac{1}{J_1 \gamma_{12}}}$$

7.1.5. The motion equation of a cardan drive

In the case of angle deflection cardan joints built into a driveline transmit the drive with altering angular velocity. The shafts modelled with torsion springs are subjected to altering deformation even if the operation is smooth by this means the energy stored in the spring is altering too in the function of angular displacement.

The state of motion of the shaft driven by a cardan joint in the function of angular displacement and velocity of the driver shaft:

$$\varphi_{12} = \varphi_{11} + \delta_1 \sin 2\varphi_{11} \tag{7.36}$$

$$\omega_{12} = \omega_{11}\left(1 + 2\delta_1 \cos 2\varphi_{11}\right) \tag{7.37}$$

$$\varepsilon_{12} = -4\omega_{11}^2 \delta_1 \sin 2\varphi_{11} \tag{7.38}$$

The transmission coefficient of the i^{th} joint:

$$\frac{\partial \varphi_{i2}}{\partial \varphi_{i1}} = 1 + 2\delta_i \cos 2\varphi_{i1} \tag{7.39}$$

where: $\delta_i \cong \frac{\beta_i^2}{4}$ (7.40)

φ_i angular displacement of the i[th] joint

β_i angular deflection between the joints coupled with the i[th] joint

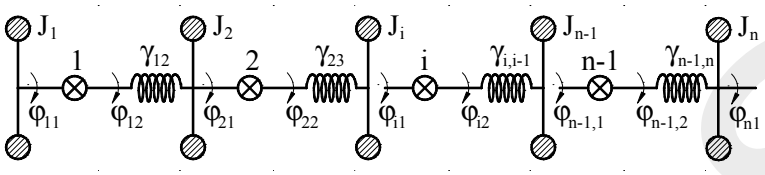

Figure 7.9: Torsion spring model of the cardan drive

The motion equation of the model transformed into elementary chain-type:

$$\begin{aligned}
&J_1\ddot{\varphi}_{11} - \frac{1}{c_{12}}(\varphi_{21} - \varphi_{12})\frac{\partial \varphi_{12}}{\partial \varphi_{11}} = 0 \\
&J_2\ddot{\varphi}_{12} + \frac{1}{c_{12}}(\varphi_{21} - \varphi_{12}) - \frac{1}{c_{23}}(\varphi_{31} - \varphi_{22})\frac{\partial \varphi_{22}}{\partial \varphi_{21}} = 0 \\
&\cdot \\
&\cdot \\
&J_n\ddot{\varphi}_{n1} + \frac{1}{c_{n-1,n}}(\varphi_{n,1} - \varphi_{n-1,2}) = 0
\end{aligned} \tag{7.41}$$

The members $(\varphi_{i+1,1} - \varphi_{i2})$ of the motion equation expressing the deformation of the springs may be written by the difference of the angular displacements of the shafts coupled by the cardan joint.

$$\varphi_{i+1,1} - \varphi_{i2} = \varphi_{i+1,1} - \varphi_{i1} + \varphi_{i1} - \varphi_{i2}$$

Introducing the $\varphi_{i+1,1} - \varphi_{i1} = X_i$ $(i = 1, 2, \ldots, n-1)$ function, the deformation of the springs:

$$\varphi_{i+1,1} - \varphi_{i2} = X_i - \delta_i \sin 2\varphi_{i1}$$

After substituting the transmission coefficient of the cardan joints and the spring deformation into the motion equation and reduction, the motion equation is:

$$\underline{\underline{\ddot{X}}} + \underline{\underline{A}}\,\underline{X} + \underline{\underline{B}}\,\underline{\underline{X\cos 2\varphi}} + \underline{\underline{C}}\,\underline{\underline{\sin 2\varphi}} + \underline{\underline{D}}\,\underline{\underline{\sin 2\varphi \cos 2\varphi}} = 0 \tag{7.42}$$

The coefficients A, B, C, D in matrix form may be found in [20].

The solution of the motion equation is searched in the form of $\underline{X} = \underline{\underline{y}}e^{i\alpha t}$.

The following boundary conditions are applied:

$$\varphi_{22} = \varphi_{11} + 90°$$

$$\varphi_{32} = \varphi_{21} + 90° = \varphi_{11} + 180°$$

$$\varphi_{n2} = \varphi_{11} + (n-1)90°$$

After substituting the $\underline{\underline{X}}$ and $\ddot{\underline{\underline{X}}}$ functions into the motion equation, the natural frequencies may be determined from the zero of the determinant set up from the coefficients of the homogeneous equation. The frequency equation contains periodic altering coefficients producing not only the parametric excitation of the drivetrain but the alteration of the natural frequencies in the function of angular displacement.

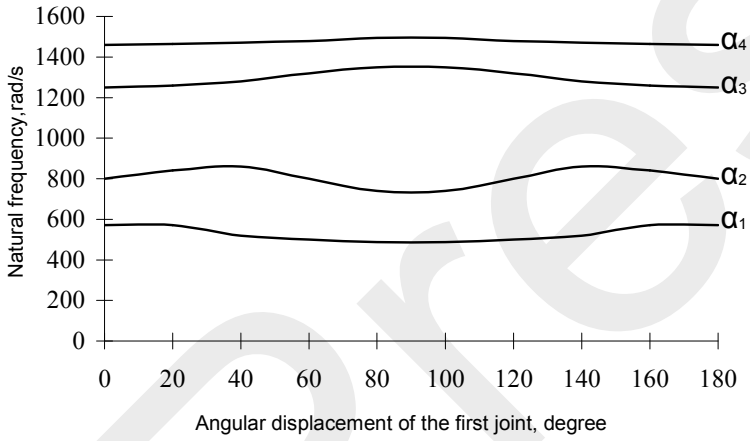

Figure 7.10: graphic chart of the torsion natural frequencies
Source: [20]

It is justifiable, that apart from the calculated natural frequency ranges there may be resonance frequencies which can be determined by the stability analysis of the differential equation. There are several graphic and calculative methods elaborated (e.g. Hill and Mathieu) whose discussion however is far from the aim of this notes.
With the developed computer simulation program the natural frequencies of the drivetrain transformed into elementary chain-type system can be calculated and graphic data processed in the function of the angular displacement. If the angular deflection of the cardan joints built in the drivetrain $\beta_i = 0°$, then $\alpha_1, \alpha_2, \ldots, \alpha_n$ natural frequencies are not functions any more but constants.

7.2. Dynamic model of bending oscillation

For describing the bending oscillation the continuum model of rods may be applied if the angular velocity is relatively small and the mass moment of inertia of the discs assembled on the shaft are small or else the gyroscopic effect would modify the nature of oscillation.

When modelling the following simplifications and assumption are made:

- the moment of inertia of the rotating shaft in any angular displacement has to be the same, this is why we do not have to take parametric bending excitation into consideration. To this precondition the circular and the hollow shaft cross section correspond.
- there is no distinguished direction of the bending oscillation therefore any oscillation direction may be checked. Since the aim of the examination is the determination of the oscillation frequency and amplitude, therefore on grounds of expedience we chose $q_{(z,t)}$ for generalized coordinate which is the vertical displacement of the mass point of the cross section.
- assuming furthermore, that during oscillation the cross sections stay plain and turn only around the axis parallel to the x axis.
- only the y component of the dynamic effects of the unbalanced rotating elements is considered. Accordingly we consider only the y direction component of the reactions and hence the bearing stiffness in y direction.

The equation of motion of rod of uniform cross-section may be described with system with constant coefficients partial difference equation. For generalized coordinate $q_{(z,t)}$, we choose the vertical displacement of the mass point of the cross section and assume that during oscillation the cross sections stay plain and turn only around the axis parallel to the x axis [19].

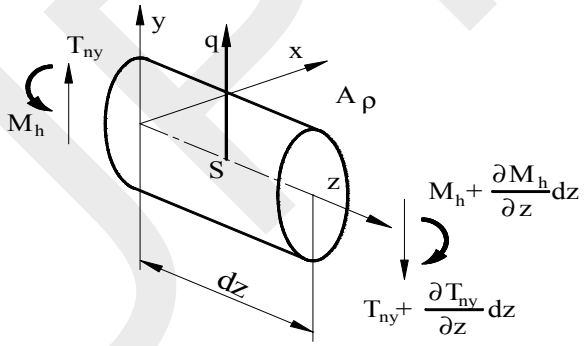

Figure 7.11: The dz length rod element

The momentum equation for the rod element on the basis of Fig. 7.11:

$$dm\ddot{q} = -\frac{\partial T_{ny}}{\partial z} dz \tag{7.43}$$

where: $dm = \rho A dz$ (7.44)

In the case of small vibration:

$$M_h = -IE\frac{\partial^2 q}{\partial z^2}, \quad t = 0 \qquad T_{ny} = -\frac{\partial M_h}{\partial z} \tag{7.45), (7.46}$$

The equation of motion of rod of uniform cross-section is gained after substituting the Eq. 7.45 and Eq. 7.46 into the Eq. 7.43:

$$A\rho\frac{\partial^2 q}{\partial t^2}+IE\frac{\partial^4 q}{\partial z^4}=0 \tag{7.47}$$

The solution of the equation of motion is searched in the following form:

$$q=v_z\cos(\alpha t+\varepsilon) \tag{7.48}$$

$$-\alpha^2 A\rho\cos(\alpha t+\varepsilon)+IEv^{IV}\cos(\alpha t+\varepsilon)=0 \tag{7.49}$$

Introducing the $k^4=\alpha^2\frac{A\rho}{IE}$ coefficient, (7.50)

the differential equation of small vibration:

$$v_{(z)}^{IV}-k^4 v_{(z)}=0 \tag{7.51}$$

It is expedient to choose the Krülov functions for basic functions of differential equation.

The general solution may be searched in the following form, where

$S_{(kz)}$, $T_{(kz)}$, $U_{(kz)}$, V_{kz} are Krülov functions and D_1, D_2, D_3, D_4 are coefficients:

$$v_{(z)}=D_1S_{(kz)}+D_2T_{(kz)}+D_3U_{(kz)}+D_4V_{(kz)} \tag{7.52}$$

where:

$$S_{(kz)}=\frac{1}{2}(chkz+\cos kz) \qquad T_{(kz)}=\frac{1}{2}(shkz+\sin kz) \tag{7.53), (7.54}$$

$$U_{(kz)}=\frac{1}{2}(chkz-\cos kz) \qquad V_{(kz)}=\frac{1}{2}(shkz-\sin kz) \tag{7.55), (7.56}$$

The features of Krülov functions are, that their derivatives differ from another Krülov function only with a constant multiplier and at q_1,q_2,q_3 the value of $\frac{d}{dt}\frac{\partial E}{\partial\dot{q}_i}-\frac{\partial E}{\partial q_i}+\frac{\partial U}{\partial q_i}=0$ Krülov function is 1 and the others are 0.

$f_{(kz)}$	$f_{(0)}$	$k^{-1}f'$	$k^{-2}f''$	$k^{-3}f'''$
S	1	V	U	T
T	0	S	V	U
U	0	T	S	V
V	0	U	T	S

D_1, D_2, D_3, D_4 coefficient may be determined from boundary conditions.

$$v_{(0)}=v_0=D_1 \tag{7.57}$$

$$v'_{(0)}=\phi_0=kD_2\Rightarrow D_2=\frac{\phi_0}{k} \tag{7.58}$$

$$v''_{(0)} = -\frac{M_0}{IE} = k^2 D_3 \Rightarrow D_3 = -\frac{M_0}{k^2 IE} \tag{7.59}$$

$$v'''_{(0)} = \frac{\overline{T}_0}{IE} = k^3 D_4 \Rightarrow D_4 = \frac{\overline{T}_0}{k^3 IE} \tag{7.60}$$

where: $v_{(z)}$ the cross-section displacement

$\phi_{(z)} = v'_{(z)}$ the cross-section angular deflection around the x axis

$M_{(z)} = -IEv''_{(z)}$ bending moment acting on the cross-section

$\overline{T}_{(z)} = IEv'''_{(z)}$ shear force amplitude acting on the cross-section

The mechanical parameters of the cross-section of rod are given by the four mechanical parameters which are arranged in state vector:

$$\underline{\underline{\eta_i}} = \begin{bmatrix} v_i \\ \phi_i \\ M_i \\ \overline{T}_i \\ 1 \end{bmatrix} \tag{7.61}$$

The state matrix is extended with a row with a value of 1. It has computing technique reason, hence this way an addition to the matrix can be achieved in the form of multiplication which is easier to be programmed.

The mechanical parameters of the cross-section of rod can be determined in the function of the $v_{(z)}$ displacement.

$$v_{(z)} = v_0 S_{(kz)} + \frac{\phi_0}{k} T_{(kz)} - \frac{M_0}{k^2 IE} U_{(kz)} + \frac{\overline{T}_0}{k^3 IE} V_{(kz)} \tag{7.62}$$

$$\phi_{(z)} = v'_{(z)} = v_0 k V_{(kz)} + \phi_0 S_{(kz)} - \frac{M_0}{kIE} T_{(kz)} + \frac{\overline{T}_0}{k^2 IE} U_{(kz)} \tag{7.63}$$

$$M_{(z)} = -IEv''_{(z)} = -v_0 IEk^2 U_{(kz)} - \phi_0 kIEV_{(kz)} + M_0 S_{(kz)} - \frac{\overline{T}_0}{k} T_{(kz)} \tag{7.64}$$

$$\overline{T}_{(z)} = IEv'''_{(z)} = v_0 IEk^3 T_{(kz)} + \phi_0 IEk^2 U_{(kz)} - M_0 kV_{(kz)} + \overline{T}_0 S_{(kz)} \tag{7.65}$$

The mechanical relation of two adjoining arbitrary cross-sections in matrix form:

$$\underline{\underline{\eta_1}} = \underline{\underline{F}}\,\underline{\underline{\eta_0}} \tag{7.66}$$

where: $\underline{\underline{F}}$ transpose matrix, containing the coefficients of the equations (Eq. 7.62 – Eq. 7.65)

$$\underline{\underline{F}} = \begin{bmatrix} S_{(kz)} & \frac{1}{k}T_{(kz)} & -\frac{1}{k^2 IE}U_{(kz)} & \frac{1}{k^3 IE}V_{(kz)} & 0 \\ kV_{(kz)} & S_{(kz)} & -\frac{1}{kIE}T_{(kz)} & \frac{1}{k^2 IE}U_{(kz)} & 0 \\ -k^2 IEU_{(kz)} & -kIEV_{(kz)} & S_{(kz)} & -\frac{1}{k}T_{(kz)} & 0 \\ k^3 IET_{(kz)} & k^2 IEU_{(kz)} & -kV_{(kz)} & S_{(kz)} & 0 \\ 0 & 0 & 0 & 0 & 1 \end{bmatrix} \tag{7.67}$$

If the diameter of the cross-section is changing, or supported flexible, or subjected to loads or bending moment, than the mechanical relations at the cross-section boundary have to be connected. The mechanical parameters of the cross-section may be determined from the connecting conditions (two geometry conditions, momentum equation, and law of moment of momentum applied for the cross-section boundary).

Between the state vectors representing the two sides of the section boundaries, the $\underline{\underline{P}}$ connecting matrix expresses the mechanical relations. Fig. 7.12 shows the model of an articulated shaft supported in several places. We defined section boundary everywhere, that parts are assembled on the shaft (coupling); the shaft is supported flexible (bearings, suspensions); joints are built in; the cross-section of the shaft is changing; excitation forces and moments act. In the following these effects are analysed and the connecting matrixes based on the mechanical relations are determined.

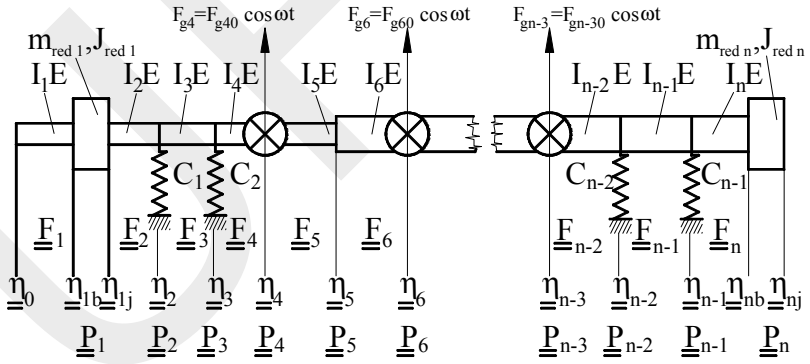

Figure 7.12: Defining section boundaries of bending model

7.2.1. Connecting matrix for rotating disc and bearing

We assume that the rod vibrates with α frequency.

Geometry condition on the basis of Fig. 7.13: the rod won't break at the section boundary.

$$v_j = v_b \text{ and } \phi_j = \phi_b \tag{7.68), (7.69}$$

The law of moment of momentum for the z axis:

$$J\frac{\partial^3 q}{\partial z \partial t^2} = M_{hb} - M_{hj} - M_\gamma \tag{7.70}$$

$$\text{where: } M_\gamma = \frac{\phi_b}{\gamma}\cos(\alpha t + \varepsilon) \tag{7.71}$$

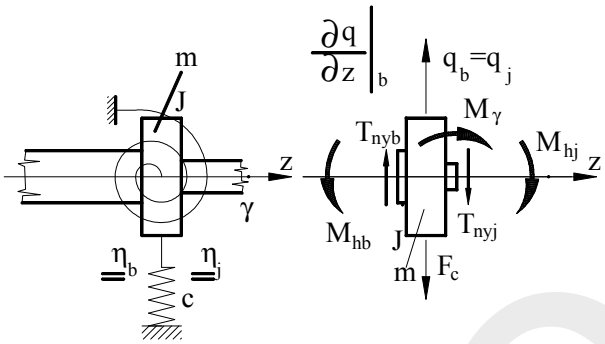

Figure 7.13: Flexible supporting of the shaft

Searching the solution in the form: $q = v\cos(\alpha t + \varepsilon)$ and considering that $v' = \phi$:

$$\frac{\partial^3 q}{\partial z \partial t^2} = -\alpha^2 \phi_b \cos(\alpha t + \varepsilon) \tag{7.72}$$

The correlation between the bending moments acting on the two sides of section boundary:

$$M_{hj} = M_{hb} + \left(J\alpha^2 - \frac{1}{\gamma}\right)\phi_b \tag{7.73}$$

Momentum equation for the rod section:

$$m\ddot{q}_b = T_{nyb} - T_{nyj} - F_c \tag{7.74}$$

$$\text{where: } \ddot{q}_b = -\alpha^2 v_b \cos(\alpha t + \varepsilon) \tag{7.75}$$

$$F_c = R_c \cos(\alpha t + \varepsilon) = \frac{v_b}{c}\cos(\alpha t + \varepsilon) \tag{7.76}$$

The correlation between the shear forces acting on the two sides of section boundary:

$$\overline{T}_{nyj} = \overline{T}_{nyb} + \left(m\alpha^2 - \frac{1}{c}\right)v_b \tag{7.77}$$

The $\underline{\underline{P}}$ connecting matrix containing the mechanical correlations:

$$\underline{\underline{P}}_i = \begin{bmatrix} 1 & 0 & 0 & 0 & 0 \\ 0 & 1 & 0 & 0 & 0 \\ 0 & J\alpha^2 - \dfrac{1}{\gamma} & 1 & 0 & 0 \\ m\alpha^2 - \dfrac{1}{c} & 0 & 0 & 1 & 0 \\ 0 & 0 & 0 & 0 & 1 \end{bmatrix} \tag{7.78}$$

where: m, J : the mass and mass moment of the disc assembled on the shaft

c, γ : radial and torsion spring compliance of the supporting

We note, that the spring stiffness modelling the bearings are load-dependent, therefore their spring constant have to be modified in several steps in conformity with the actual load.

7.2.2. Connecting matrix for excitation force and moment

Geometry condition: the rod wont break at the section boundary.

$$v_j = v_b \text{ and } \phi_j = \phi_b \tag{7.79), (7.80}$$

The law of moment of momentum for the z axis:

$$M_{hj} = M_{hb} + M_g \text{ and } M_g = N_i \cos(\alpha t + \varepsilon) \tag{7.81), (7.82}$$

Momentum equation for the rod section:

$$T_{nyj} = T_{nyb} + T_g \text{ and } T_g = R_i \cos(\alpha t + \varepsilon) \tag{7.83), (7.84}$$

The correlation between the shear forces and moments acting on the two sides of section boundary:

$$\overline{T}_{nyj} = \overline{T}_{nyb} + R_i \tag{7.85}$$

$$\overline{M}_{nyj} = \overline{M}_{nyb} + N_i \tag{7.86}$$

The state vector at the section boundary:

$$\underline{\underline{\eta_{ij}}} = \underline{\underline{E}}\,\underline{\underline{\eta_{ib}}} + \begin{bmatrix} 0 \\ 0 \\ 1 \\ 0 \\ 0 \end{bmatrix} N_i + \begin{bmatrix} 0 \\ 0 \\ 0 \\ 1 \\ 0 \end{bmatrix} R_i = \underline{\underline{P}}\,\underline{\underline{\eta_i}} \tag{7.87}$$

The addition in Eq. 7.87 may be achieved by matrix product, see later.

The $\underline{\underline{P}}$ connecting matrix for excitation force and bending moment:

$$\underline{\underline{P}} = \begin{bmatrix} 1 & 0 & 0 & 0 & 0 \\ 0 & 1 & 0 & 0 & 0 \\ 0 & 0 & 1 & 0 & N_i \\ 0 & 0 & 0 & 1 & R_i \\ 0 & 0 & 0 & 0 & 1 \end{bmatrix} \tag{7.88}$$

7.2.3. Connecting matrix for ball joint

Geometry condition:

$$v_j = v_b \text{ and } \phi_j = \phi_b + \Delta\beta_i \tag{7.89), (7.90}$$

Operation feature of the ball joint:

$$M_j = M_b = 0 \tag{7.91}$$

Momentum equation for the section boundary:

$$T_j = T_b \tag{7.92}$$

Ball joints (cardan joints, cv joint, ect.) are not able to transmit bending moment. The shaft subjected to external load deforms, deflects. $\Delta\beta_i$ expresses the difference of angular deflection at the installation of the joint relative to the angular displacement without joint [20].

The connecting matrix for ball joint considering its mass and mass moment of inertia and any excitation forces (in the case of cardan joint):

$$\underline{\underline{P}}_i = \begin{bmatrix} 1 & 0 & 0 & 0 & 0 \\ 0 & 1 & 0 & 0 & \Delta\beta_i \\ 0 & J\alpha^2 & 1 & 0 & 0 \\ m\alpha^2 & 0 & 0 & 1 & R_i \\ 0 & 0 & 0 & 0 & 1 \end{bmatrix} \tag{7.93}$$

The $\Delta\beta_i$ is an unknown in the matrix, therefore it has to be calculated.

The general form of the connecting matrix:

$$\underline{\underline{P}}_i = \begin{bmatrix} 1 & 0 & 0 & 0 & 0 \\ 0 & 1 & 0 & 0 & \Delta\beta_i \\ 0 & J_i\alpha^2 - \dfrac{1}{\gamma} & 1 & 0 & N_i \\ m_i\alpha^2 - \dfrac{1}{c} & 0 & 0 & 1 & R_i \\ 0 & 0 & 0 & 0 & 1 \end{bmatrix} \tag{7.94}$$

The connecting matrix in the case of the change of cross section diameter is merely a unit matrix. For modelling the bending oscillation, in every section and section boundary, all of the $\underline{\underline{F}}$ and $\underline{\underline{P}}$ matrixes have to be determined containing the α natural frequency. Between the mechanical parameters of the first and the last cross section the following matrix equation gives correlation.

$$\underline{\underline{\eta_n}} = \underline{\underline{F_n}}\,\underline{\underline{P_{n-1}}} \ldots \underline{\underline{P_1}}\,\underline{\underline{F_1}}\,\underline{\underline{\eta_0}} \tag{7.95}$$

In an arbitrary cross section of a drivetrain containing cardan joints the mechanical parameters (displacement, angular deflection, bending moment and shear force) and the natural frequencies of the drivetrain may be determined. The calculation is very complicated therefore we introduce the calculation method starting from the simplest case.

7.2.4. Applying the bending dynamic model

7.2.4.1. Rod element without excitation

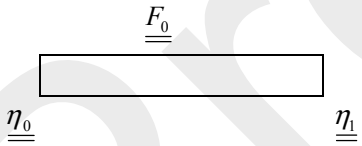

Figure 7.14: Rod element

A rod element has no practical utility since it is not supported by bearings and not subjected to load (see Fig. 7.14). Accordingly both rod ends are free. The boundary conditions in the case of free rod ends: $M = 0$ and $T = 0$ (the bending moment and the shear force are 0 in the load diagram). Satisfying the boundary conditions, the state vector of the first and the last cross-section are:

$$\underline{\underline{\eta_0}} = \begin{bmatrix} v_0 \\ \phi_0 \\ 0 \\ 0 \\ 1 \end{bmatrix} \qquad \underline{\underline{\eta_1}} = \begin{bmatrix} v_1 \\ \phi_1 \\ 0 \\ 0 \\ 1 \end{bmatrix} \tag{7.96), (7.97}$$

The matrix equation expressing the mechanical relation between the two state vectors:

$\underline{\underline{\eta_1}} = \underline{\underline{F_1}}\,\underline{\underline{\eta_0}}$, thus

$$\begin{bmatrix} v_1 \\ \phi_1 \\ 0 \\ 0 \\ 1 \end{bmatrix} = \begin{bmatrix} S_{(kz)} & \frac{1}{k}T_{(kz)} & -\frac{1}{k^2 IE}U_{(kz)} & \frac{1}{k^3 IE}V_{(kz)} & 0 \\ kV_{(kz)} & S_{(kz)} & -\frac{1}{kIE}T_{(kz)} & \frac{1}{k^2 IE}U_{(kz)} & 0 \\ -k^2 IEU_{(kz)} & -kIEV_{(kz)} & S_{(kz)} & -\frac{1}{k}T_{(kz)} & 0 \\ k^3 IET_{(kz)} & k^2 IEU_{(kz)} & -kV_{(kz)} & S_{(kz)} & 0 \\ 0 & 0 & 0 & 0 & 1 \end{bmatrix} \begin{bmatrix} v_0 \\ \phi_0 \\ 0 \\ 0 \\ 1 \end{bmatrix} \tag{7.98}$$

The unknown in the $\underline{\underline{\eta}}_0$ state vector: v_0 , ϕ_0

In the $\underline{\underline{\eta}}_1$ state vector due to the boundary conditions: $M_1 = 0$, $T_1 = 0$

The boundary conditions consequently provide two equations for determining the two unknowns, this way the equation system can be solved. With the development of the 3. and 4. row of the matrix product the following equations are gained:

$$-k^2 IEU_{(kz)} v_0 - kIEV_{(kz)} \phi_0 = 0 \tag{7.99}$$

$$k^3 IET_{(kz)} v_0 + k^2 IEU_{(kz)} \phi_0 = 0 \tag{7.100}$$

The homogeneous differential system containing two unknowns has solution apart from the trivial solution, if the determinant constituted from the coefficient of v_0 and ϕ_0 is 0. Since the elements of the $\underline{\underline{F}}$ matrix are the function of the frequency, the α frequencies, belonging to the zero of the determinant, are the bending natural frequencies. In the excitation free case the equation system is homogeneous this is why the v_0 , ϕ_0 , and v_1 , ϕ_1 unknowns can be determined only with parameters of each other. The natural frequencies may be determined with the iterative method discussed before.

7.2.4.2. A rod element exited

Due to the excitation the equation system is inhomogeneous. The number of unknowns and equations corresponds with one of the case without excitation. The natural frequencies may be calculated as well with the determinant set up from the coefficients of the homogeneous equation system. The actual value of v_0 , ϕ_0 , and v_1 , ϕ_1 may be calculated.

7.2.4.3. Drivetrain with two cardan joints

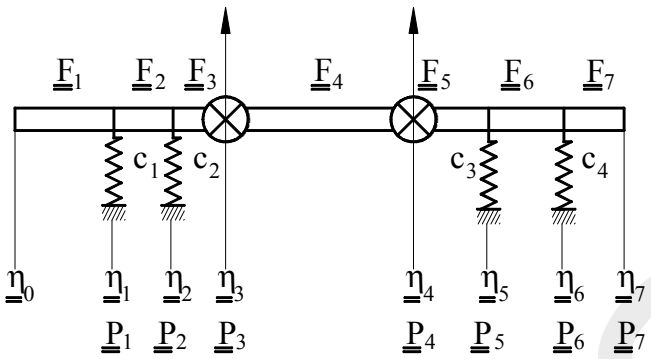

Figure 7.15: Drivetrain with two cardan joints

Fig. 7.15 shows a two joints drivetrain supported in several places. The bearings are modelled with springs and excitation forces are assumed at the cardan joints. It can be seen that everywhere where the drivetrain differs from an uniform rod section we defined a section boundary. To comply with the boundary conditions we construct the model with free rod ends. If there were a supporting or excitation force or moment, then in order to fulfil the boundary conditions, the drivetrain has to be completed with a short even only some micrometers long section. This way the ends of the drivetrain are free in terms of mechanical aspects. The correlation between the first and the last section boundary:

$$\underline{\underline{\eta_7}} = \underline{\underline{F_7}}\,\underline{\underline{P_6}}\,\underline{\underline{F_6}}\,\underline{\underline{P_5}}\,\underline{\underline{F_5}}\,\underline{\underline{P_4}}\,\underline{\underline{F_4}}\,\underline{\underline{P_3}}\,\underline{\underline{F_3}}\,\underline{\underline{P_2}}\,\underline{\underline{F_2}}\,\underline{\underline{P_1}}\,\underline{\underline{F_1}}\,\underline{\underline{\eta_0}} \tag{7.101}$$

The basic unknowns and equations of the common drivetrain correspond with the one of the rod element case supplemented with the equations describing the function of the cardan joint. Every cardan joint gives $\Delta\beta_i$ an additional unknown and an additional equation due to the boundary condition since a cardan joint can not transmit bending moment. We can construct these equations by developing the third row of the state vector at the section boundary of the joints ($M_i = 0$).

$$\underline{\underline{\eta_3}} = \underline{\underline{F_3}}\,\underline{\underline{P_2}}\,\underline{\underline{F_2}}\,\underline{\underline{P_1}}\,\underline{\underline{F_1}}\,\underline{\underline{\eta_0}} \tag{7.102}$$

$$\underline{\underline{\eta_4}} = \underline{\underline{F_4}}\,\underline{\underline{P_3}}\,\underline{\underline{F_3}}\,\underline{\underline{P_2}}\,\underline{\underline{F_2}}\,\underline{\underline{P_1}}\,\underline{\underline{F_1}}\,\underline{\underline{\eta_0}} \tag{7.103}$$

The number of unknowns and equations correspond with each other hence the equation system can be solved.

The excitation forces and moments resulting from the operation features of the cardan joint; out-of-balance effect of rotating parts; and external loads have to be taken into consideration at their operation places. Due to the excitation the equation system is inhomogeneous. The frequency equation is derived by developing the determinant set up from the coefficients of inhomogeneous part.

The spring constant of the spring modelling the rolling bearings, as we could see, is the function of the load. The bearing loads may be determined in the knowledge of excitation forces and moments, and the operation frequency. After substituting the ω operation frequency into the transfer and connection matrixes, the values of $v_0, \phi_0, \Delta\beta_3, \Delta\beta_4$ can be calculated. We indicated K_1, K_2, K_3, K_4 inhomogeneous members with letters.

In the case of installing two cardan joints, fulfilling the boundary conditions the following equation system may be derived, whose coefficients are indicated with a,...,m letters for lucidity:

$$\begin{aligned} &av_0 + b\phi_0 + c\Delta\beta_{30} + d\Delta\beta_{40} = K_1 \\ &ev_0 + f\phi_0 + g\Delta\beta_{30} + h\Delta\beta_{40} = K_2 \\ &iv_0 + j\phi_0 + k\Delta\beta_{30} = K_3 \\ &lv_0 + m\phi_0 = K_4 \end{aligned} \tag{7.104}$$

The unknowns of the equation system may be calculated with the Kramer method: An unknown may be calculated by division of two determinant. The determinant in the denominator is set up from the coefficient of the homogeneous equation while the determinant in the numerator is modified by substituting the inhomogenous members into the place of the coefficient of the unknown. E.g. the ϕ_0 can be calculated with the Eq. 7. 105. After calculating the unknowns, the reaction forces at the bearings may be calculated by developing the fourth row of the state vector at the relevant supporting. In the knowledge of bearing forces the radial spring constant of the bearings can be calculated by the bearing stiffness calculating computer program. After that the fictive value of the bearing stiffness in the connecting matrix will be changed with the calculated one. Because of the modified bearing stiffness, all of the mechanical parameters of the drivetrain change, this is why the unknowns of the equation system and the bearing forces have to be recalculated. After that we calculate the bearing stiffness again belonging to the again calculated bearing forces.

$$\phi_0 = \frac{\begin{vmatrix} a & K_1 & c & d \\ e & K_2 & g & h \\ i & K_3 & k & 0 \\ l & K_4 & 0 & 0 \end{vmatrix}}{\begin{vmatrix} a & b & c & d \\ e & f & g & h \\ i & j & k & 0 \\ l & m & 0 & 0 \end{vmatrix}} \tag{7.105}$$

This iterative method is carried out till the value of spring constant of the bearings alters significantly during two succeeding calculation. According to experiences, four-five iterative calculations are needed. After fixing the spring constant of the

bearings the α natural frequencies of the drivetrain may be calculated with the previously discussed method. If we analyse the resonance state of the drivetrain (one of the natural frequencies is input in the computer program as operation frequency), the calculated values of the mechanical parameters tend to infinite, which can not occur in the practice because of the premature break of the shaft. When calculating the unknowns namely the value of the determinant in the denominator set up from the coefficients of the homogeneous part of the equation system tends to 0 which is. The division with nearly 0 gives result tends to infinite.

7.2.4.4. Common drivetrain

The number of unknowns and equations of a common drivetrain are accordingly $2+k$, where k is the number of joints. The equation system based on the boundary conditions from which the unknowns and the bending natural frequencies can be determined without deduction [20]:

$$I_A v_0 + J_A \varphi_0 + \sum_{i=cs_1}^{cs_n} J_i \Delta\beta_i = -\left(\sum_{j=e_1}^{e_v} L_j F_{gj} + \sum_{k=ny_1}^{ny_w} K_k M_{gk} \right)$$

$$M_a v_0 + N_A \varphi_0 + \sum_{i=cs_1}^{cs_n} N_i \Delta\beta_i = -\left(\sum_{j=e_1}^{e_v} P_j F_{gj} + \sum_{k=ny_1}^{ny_w} O_k M_{gk} \right)$$

$$I_{cs_n} v_0 + J_{cs_n} \varphi_0 + \Delta\beta_{cs_n} + \sum_{i=cs_1}^{cs_{n-1}} J_i \Delta\beta_i = -\left(M_{gcs_n} + F_{gcs_n} + \sum_{j=e_1}^{cs_{n-1}} L_j F_{gj} + \sum_{k=ny_1}^{cs_{n-1}} K_k M_{gk} \right)$$

$$I_{cs_{n-1}} v_0 + J_{cs_{n-1}} \varphi_0 + \Delta\beta_{cs_{n-1}} + \sum_{i=cs_1}^{cs_{n-2}} J_i \Delta\beta_i = -\left(M_{gcs_{n-1}} + F_{gcs_{n-1}} + \sum_{j=e_1}^{cs_{n-2}} L_j F_{gj} + \sum_{k=ny_1}^{cs_{n-2}} K_k M_{gk} \right)$$

.

.

$$I_{cs_1} v_0 + J_{cs_1} \varphi_0 + \Delta\beta_{cs_1} = -\left(M_{gcs_1} + F_{gcs_1} + \sum_{j=e_1}^{cs_1} L_j F_{gj} + \sum_{k=ny_1}^{cs_1} K_k M_{gk} \right) \qquad (7.106)$$

where: $cs_1 - cs_n$ indenture number of the joint

$e_1 - e_v$ indenture number of boundary section of excitation forces

$ny_1 - ny_w$ indenture number of boundary section of excitation moments

The „A" index in the first two rows means the elements of the matrix constituted from the matrix product between the first and the last boundary sections.
The indexes of the coefficients (with the exception of the first two equations) mean the elements of the matrix constituted from the matrix production from the highest numbered connecting matrix to the first boundary section.

We indicated the coefficients constituted by the product of transfer and connecting matrixes with letters again for lucidity.

8. Simulation program

We reviewed the equations of motion describing the oscillation of the drivetrain and the dynamic models based on them step by step. The mechanical parameters of the drivetrain elements are the parameters of the frequency equation which exercise influence on the natural frequencies with different rate depending upon their function in the frequency equation. Although the mechanical and geometrical parameters and operation features of the drivetrain elements may be determined with simple calculations or simplified methods, however the dynamic calculations can be carried out only with computer program. There are a lot of CAD program available for dynamic calculation providing convenient application. After data input the program determines the results without getting any inside view of its calculation methods. For executing the drivetrain optimization, the dynamic modelling is only a tool for determining the operation features and natural frequencies. The optimization means that after calculating the operation parameters of the drivetrain, we analyse how to alter the operation features by modifying the parameters of the drive elements. The optimization of the driveterain operation may be achieved by modifying the input parameters successively, considering its disadvantageous effects on other drive features.
We developed a computer program for carrying out dynamic calculations with which the applied calculation method may be traced. In the following we briefly introduce the developed computer program and review the program charts. Next we show an actual drivetrain equipped with measuring gauges. Eventually some measuring results represented in measurement records are analysed.

8.1. The operation of simulation program

The simulation program based on the dynamic models was developed together with Mr. Darai programmer. The parameters of the drivetrain are the input data of the simulation program.
The program is written under Turbo Pascal version 7.0. The source file consists of approximately 2300 program rows, the translated size is 110 kB, and due to the program's restricted capacity it also contains an external UNIT named INPUTV4A, which consists of approximately 400 rows and translated size is 10 kB. The program is menu controlled, and returns to the main menu from the sub-routines serving the four sub-programs.

The sub-programs:

- bearing stiffness program

- torsion oscillation program
- bending oscillation program

The bearing stiffness program is developed for calculating the spring constant in radial and axial direction of single-row deep grooved ball bearing and self aligning ball bearing. The program offers two computing operations, the Sjövall method and the approximate one based on experimental results. The program operates both ways, independently and as a sub-program of the bending oscillation program.

The torsion oscillation program is based on the torsion spring model. The input data of the program are the torsion spring compliance, the mass moment of inertia of the discs and the deflection angle of joints. The torsion natural frequencies are represented on a graph in the function of the angular displacement of the shaft.

The bending oscillation program is based on the continuum model. The input data of the program are the coefficients of the transpose and connecting matrixes which are parameters of the drivetrain elements. The built up of the connecting matrixes are starting from the unit matrix and its coefficients are given when inputting data accordingly whether a supporting, different cross section diameter, joint is there, or excitation force or moment acts at the cross section boundary. The supporting, assembled additional parts, joints, excitations are defined this way at the section boundary.

The numbering of the cross section boundaries is proceeded ten by ten. It makes possible to insert additional nine section boundaries between two adjacent ones. The input data of the computer program is the coefficient of the frequency equation.
Of course, the dynamic models have to be fitted to the assembled drivetrain which may be implemented by the appropriate modifying of the eligible parameters.
When inputting data, only the spring stiffness of the supporting are not known, hence the bearing forces necessary for the spring stiffness calculation will be determined afterwards. This is why the first computation is made with fictive values which are modified several times by iterative calculations. After computing the unknowns of the equation system, belonging to an actual operation frequency may be modified, the program facilitates to inquiry the state vector at every cross section boundary involving the displacement, angular displacement, bending moment and shear force. At every cross section boundary where supportings are defined, the program calculates the bearing forces automatically without inquiring the state vector of them. Then the program offers the iteration calculation of the spring stiffness of the bearings. If this function is applied, then the bearing stiffness program is loaded into the bending oscillation program as a sub-program with the previously calculated bearing forces. After inputting the geometry and other parameters of the rolling-contact bearing, the bearing stiffness program calculates the actual spring constants which are afterwards substituted into the connecting matrix of the appropriate cross section boundary. After carrying out this calculation for every

bearing, the bending oscillation program computes in addition to the bending natural frequencies, the unknowns of the equation system and the bearing forces. By this means one iteration calculation is completed and it starts again till reaching the previously adjusted number of iteration. This calculation procedure may be tracked on the screen.

After fixing the spring constants of the bearings, the program calculates the natural frequencies with the iterative method. Here the program offers three increments increasing the α. According to the applied increment the natural frequencies are calculated. Since the proximity of the natural and operation frequencies to each other influences the running of the drivetrain, the detuning of them from each other has to be achieved.

The program allows of modifying the operation frequency and the input data, this way mechanical parameters of the drivetrain can be checked in or close to resonance state as well. For detuning the natural frequencies there are so many options as input data of the program.

Table 8.1: Chart of the bearing stiffness program

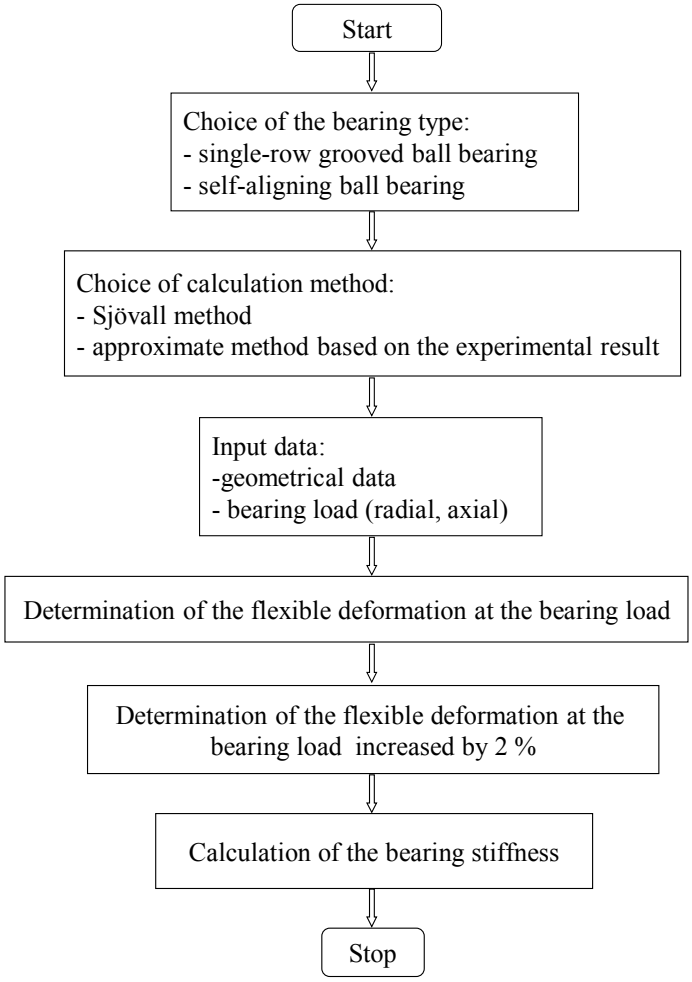

Table 8.2: Chart of the torsion oscillation program

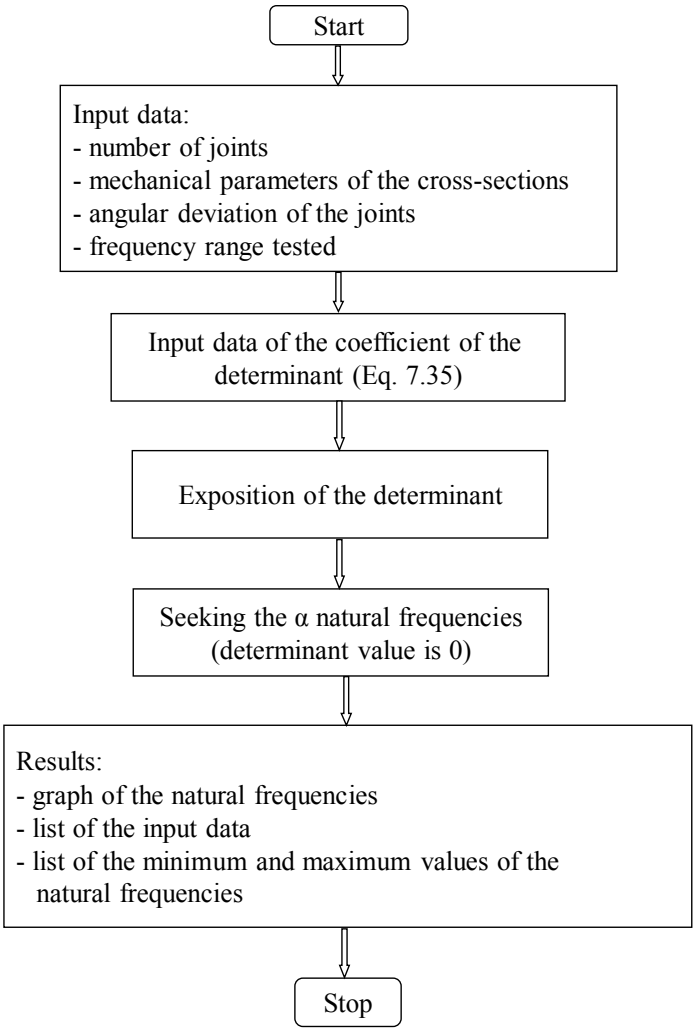

Table 8.3: Chart of the bending oscillation program

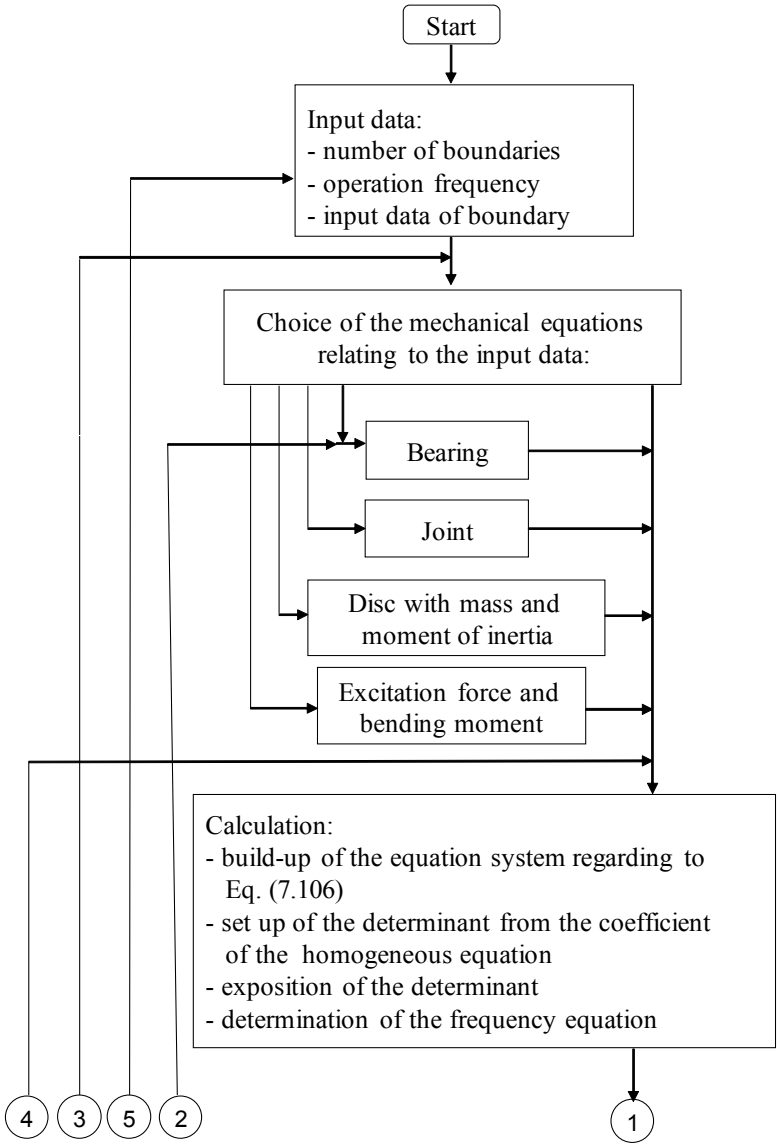

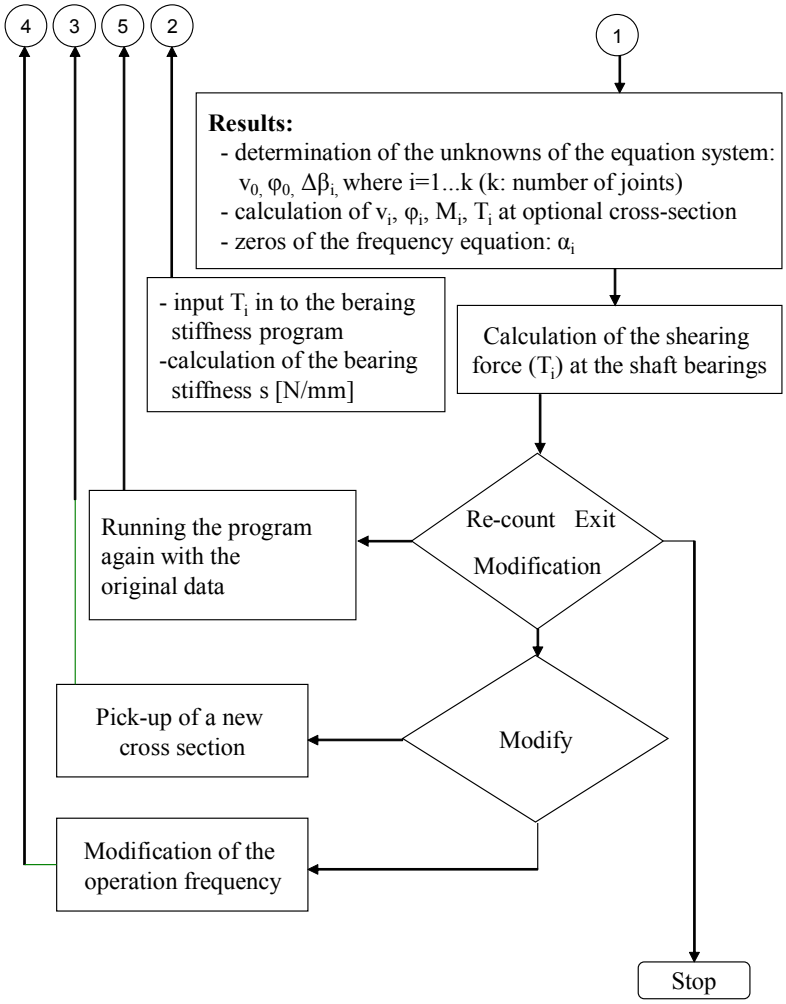
4
3
5
2
1
Results:
- determination of the unknowns of the equation system:
$v_{0,}$ $\varphi_{0,}$ $\Delta\beta_{i,}$ where i=1...k (k: number of joints)
- calculation of v_i, φ_i, M_i, T_i at optional cross-section
- zeros of the frequency equation: α_i
- input T_i in to the beraing stiffness program
-calculation of the bearing stiffness s [N/mm]
Calculation of the shearing force (T_i) at the shaft bearings
Re-count Exit
Modification
Running the program again with the original data
Modify
Pick-up of a new cross section
Modification of the operation frequency
Stop

9. Bench test

The primary object of the simulation program when designing is to determine the loads acting on the drivetrain and the natural frequencies in order to provide either a smooth running or a resonance state depending on the function of the drivetrain.
Another application field is the redesign of a drivetrain to detune the natural frequencies. To assembly a drivetrain with different parameters in different drive layout is very costly and time-consuming. With the modelling the number of eligible constructions may be reduced to some of them expedient to build in order to prove its suitability by measuring.
In any case, the matching of the model to the drivetrain has to be performed. For matching an operating drivetrain instrumented is needed with appropriate measuring equipment.
In the following we introduce this procedure through an actual drivetrain application.

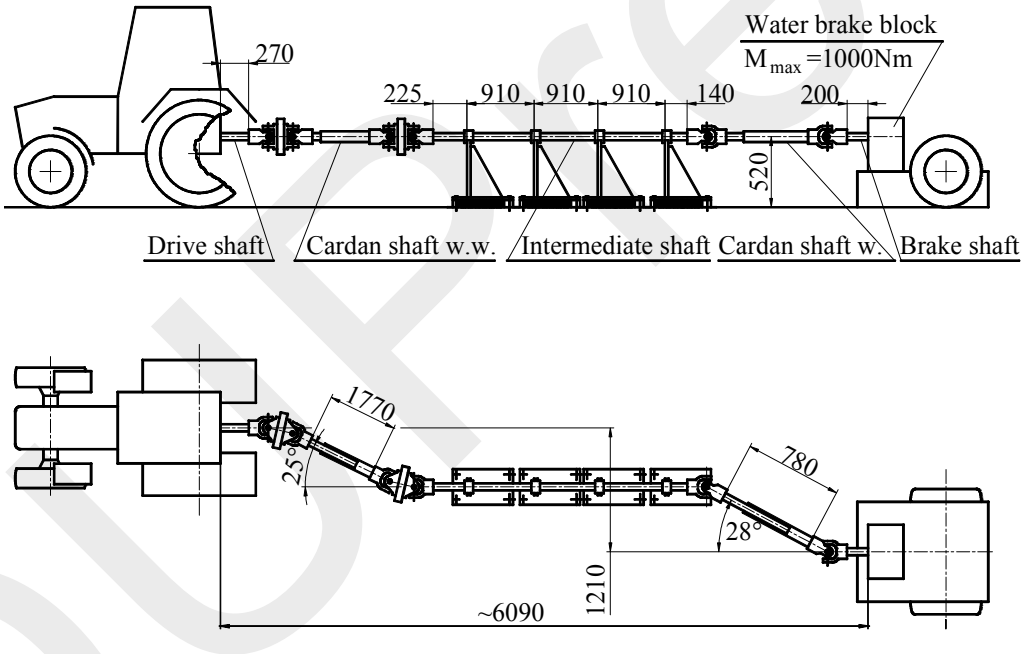

Figure 9.1: Test-bench

The test-bench was built in the experimental plant of the Walterscheid Ltd. in Lohmar, Germany. We modelled drivetrains applied mostly in the agriculture field where the agricultural machine is towed by tractor and driven by cardan drive. Accordingly the cardan drive is long and contains several cardan joints. The drivetrain can be seen in Fig. 9.1 is driven by a FIAT tractor and loaded by a water brake. Based on the hydrodynamic friction principle the water brake transforms the mechanical energy of the prime mover into heat energy and this way brakes the drivetrain. Because of the large heat development the water brake was connected to

the drainage network and the sewer network, removing the heat energy by the flowing through water. The nominal speed of the drivetrain provided by the tractor PTO is 540 1/min and its load was adjusted by the water brake. The measurements were reproducible hence considering the dispersion of the measuring result we got like measuring results with repeated measurements. The drivetrain was equipped for the following measurements: rotational speed and torque of the shaft, the reaction force in vertical direction at a bearing bracket.
The number of bearing brackets and stiffness of them might be modified by changing the number of the rubber blocks (see Fig. 9.2). Additional to this, the drivetrain could be assembled in different layout and length.

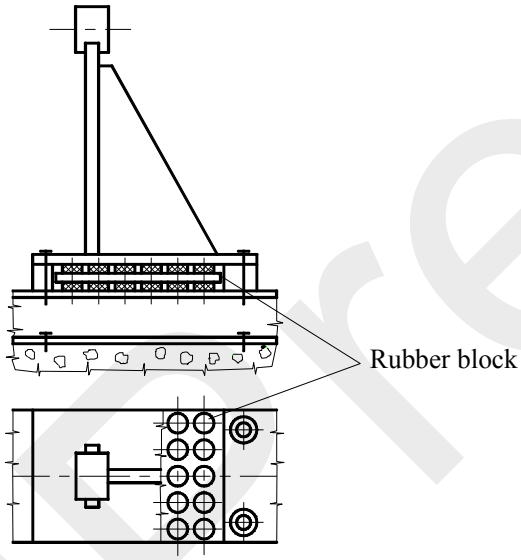

Figure 9.2: Bearing bracket with adjustable mounting stiffness

9.1. Testing parameters and factors

For testing we have to define a testing parameter (numerical signal) to be measured. Afterwards, all of the factors have to be determined which have an effect on the tested process.
Requirements stated against factors [21]:

- controllability: it can be adjusted with a prescribed accuracy,
- objective measurability,
- direct effect on the process,
- independence: factors have no effect on each other.

A combination of the factors with fixed values provides a possible experimental set-up. Experimental results may be used for setting up the mathematical model of the process.
This model is the functional relationship between the testing parameters and factors. In the case of testing the bending oscillation, y may be used as testing parameter that

is the ratio of the maximum and minimum value of the reaction force in vertical direction which is a non-dimensional unit coefficient. Its maximum value appears close to the resonance state.

The value of the testing parameter (y) is affected additional to the drive layout by the following factors:

- moment of inertia of the cross section of the shaft:= X_1
- dimension of the cross section of the shaft:= X_2
- length of shaft:= X_3
- mass moment of inertia of the driven parts:= X_4
- mass of parts rotating with the shaft:= X_5
- radial spring constant of the bearings:= X_6

Thus: $Y = Y_{(X_1, X_2, \ldots, X_6)}$

For testing the torsion oscillation, the testing parameter may be the ratio of the maximum and minimum value of the torque acting on the shaft which is a non-dimensional unit coefficient. The factors may be the followings:

- torsion spring constants of the shafts:= X_1
- mass moment of inertia of driven parts:= X_2
- angle of deflection of shafts:= X_3

Thus: $Y = Y_{(X_1, X_2, X_3)}$

The coefficients of dynamic models conform with the given parameters of the drivetrain.

This is why the test-bench is designed with respect to adjustment facility of the parameters conforming with the given factors.

The aim of the measurements is to find unequivocal correlation between the modification of the dynamic model factors and the measurement results.

Therefore it is very important that the factors do not depend on each other, or if they do, we should be aware of it and the correlation between them has to be described mathematical correctly. For example if the distance between two bearing brackets is increased, it results in increasing the shaft length and decreasing torsional spring constant as well, if the cross section of the shaft is not changed.

On the test bench the following adjustments can be carried out:

1. Changing the bearing stiffness by means of the flexible mounting of bearing brackets. The stiffness can be adjusted by changing the number of rubber blocks.
2. Changing the length of the cardan shafts by pulling out or pushing in the telescopically constructed shaft coupling. This way the distance between the bearing brackets can be adjusted.

3. Varying the number of bearings by the installation of additional bearing brackets.
4. Adjusting the joint angles. The joint angles have to be adjusted at assembly. During the measurement further modification is not possible.
5. Adjusting the flywheel position on the intermediate shaft that can be carried out by the use of a tapered clamping sleeve.

9.2. Experimental method

During the experiments bearing force, torque of the drive shaft and the speed were measured in the function of the time and recorded results were printed in diagrams.
The smallest natural frequency of the drivetrain was measured by slowly increasing the drivetrain speed. The cardan shaft was instrumented with a torque transducer and one of the bearing brackets was instrumented with force transducer. In the case of bending, or torsion resonance the measured values were considerably higher than the nominal ones.
Since a certain period is necessary for developing the resonance, it was very important to accelerate the RPM of the drivetrain uniformly with the same acceleration in each measurement.
If the acceleration of the RPM was too high the resonance could not develop. However, when increasing the RPM too slowly the developing vibration amplitude did not make it possible to increase the RPM further. When measuring the bending vibrations the drivetrain was assembled with constant velocity joints instead of cardan joints to eliminate the excitations of the cardan joint operation. For carrying out the test we applied the measuring system of the Hottinger Baldwin Messtechnik Ltd. comprising the Catman measuring software [22]. The acceleration of the shaft's RPM had a significant effect on the measuring result since it provides the time necessary for developing the vibration amplitude. The more or less uniform increasing of the RPM was effected by steady pushing of the accelerator pedal of the tractor.
Analysing the measurement records made under same conditions, it was obvious that we could not implement the uniform increasing of the RPM, which results in approximately 5% of dispersion. The measuring records shown in the following chapter should be considered only as informative diagrams since we neglect the detailed review of the drivetrain on which bases the dynamic model was constructed and the input data of the simulation program was determined.

9.2.1. Torsion vibrations

Parameters affecting the torsion vibration frequencies and amplitudes:
- mass moment of inertia of the rotating parts
- length of the cardan shaft influencing the torsion spring constant of the shaft
- joint angles

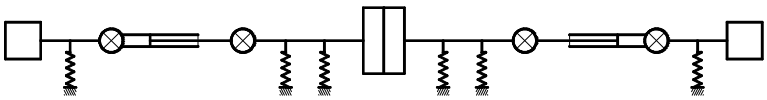

Figure 9.3: Drivetrain layout of torsion vibration test

Tests were conducted on the drivetrain shown in Fig. 9.3. The effect of the mass moment of inertia of a part on the torsion natural frequencies is represented in Fig. 9.4.

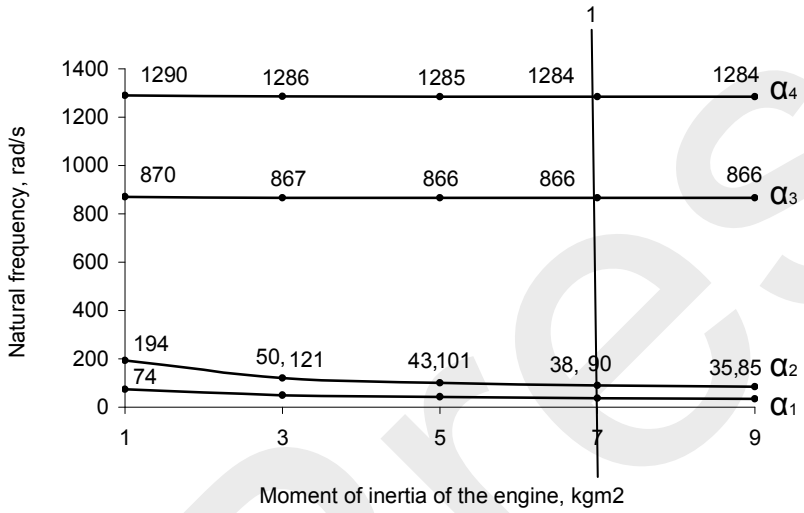

Figure 9.4: The effect of the mass moment of inertia
Source: [20]

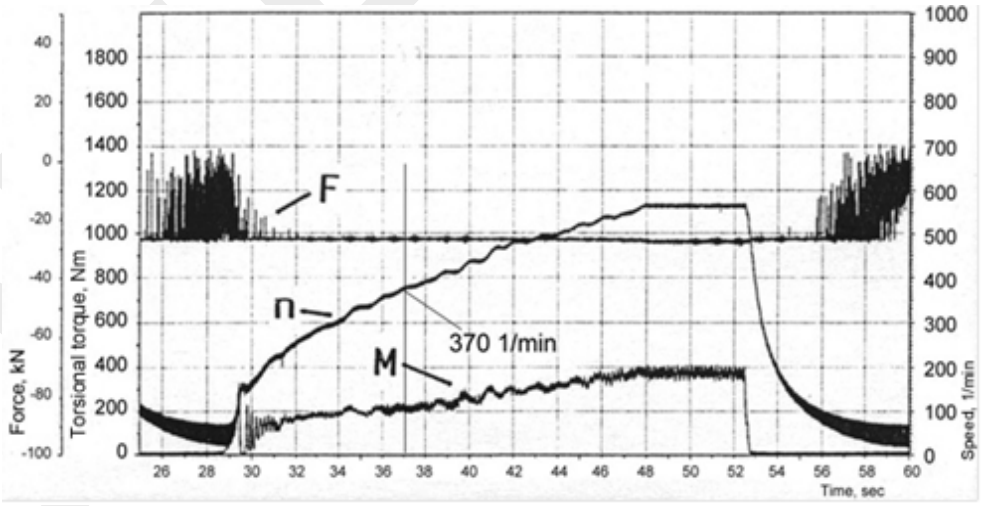

Figure 9.5: The effect of the joint angle alterations I.
(joint angle: 0°) Source: [20]

The smallest natural frequency is 38 rad/s (363 1/min) pertaining a fixed value of mass moment of inertia of the part. The measurement records pertaining to different joint angles are shown in from Fig. 9.5 to 9.7. It can be seen that the smaller the joint

angle the smaller the excitation is resulting from the supplementary load and the vibration amplitude develop.

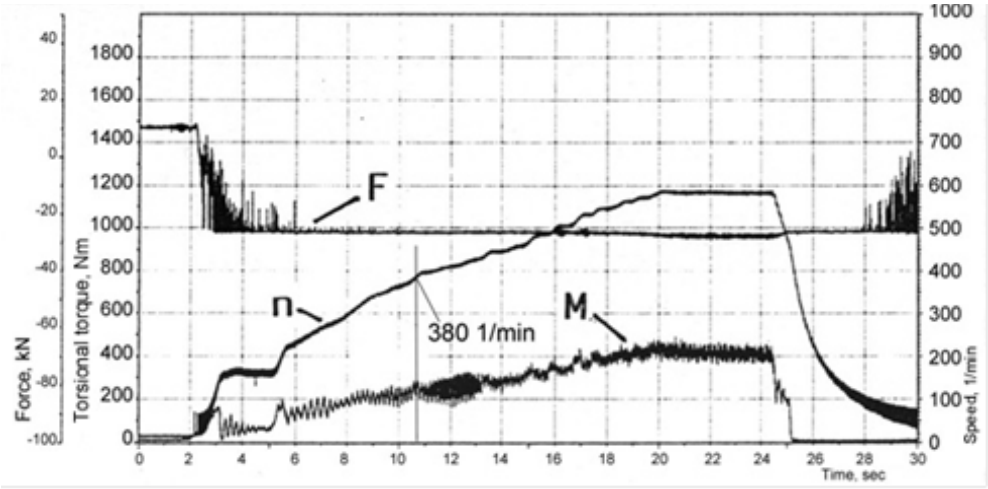

Figure 9.6: The effect of the joint angle alterations II. (joint angle: 15°) Source: [20]

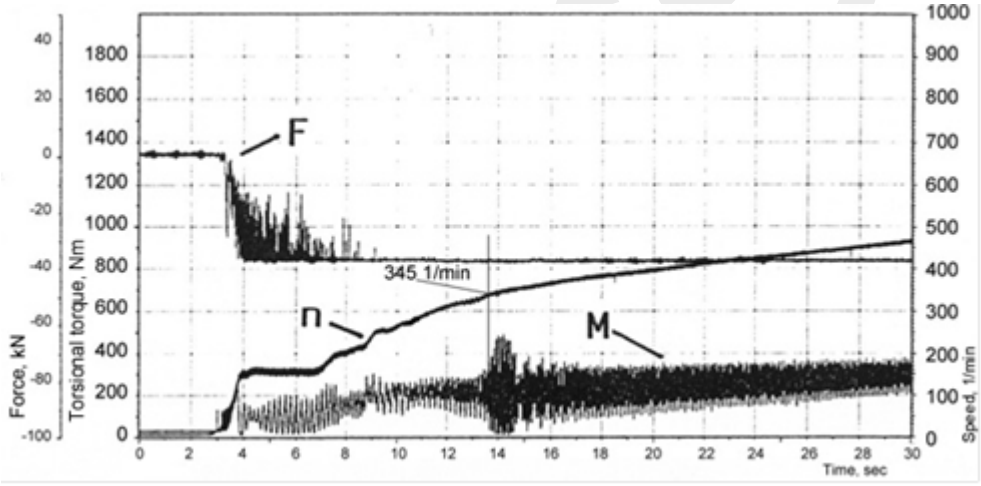

Figure 9.7: The effect of the joint angle alterations III. (joint angle: 30°) Source: [20]

By increasing the joint angles the torsion frequencies alter in the function of angular displacement. Fig. 9.8 shows the boundary values of natural frequencies at different joint angles.

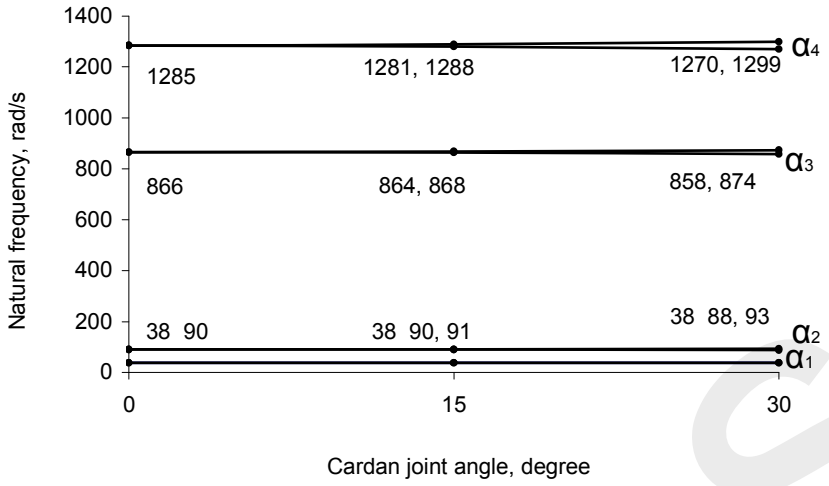

Figure 9.8: Torsion natural frequencies at different joint angles
Source: [20]

Fig. 9.9 shows the effect of the torsion spring constant of the shaft on the torsion natural frequencies. The torsion spring constant can be modified either by the cross section dimension or by the length.

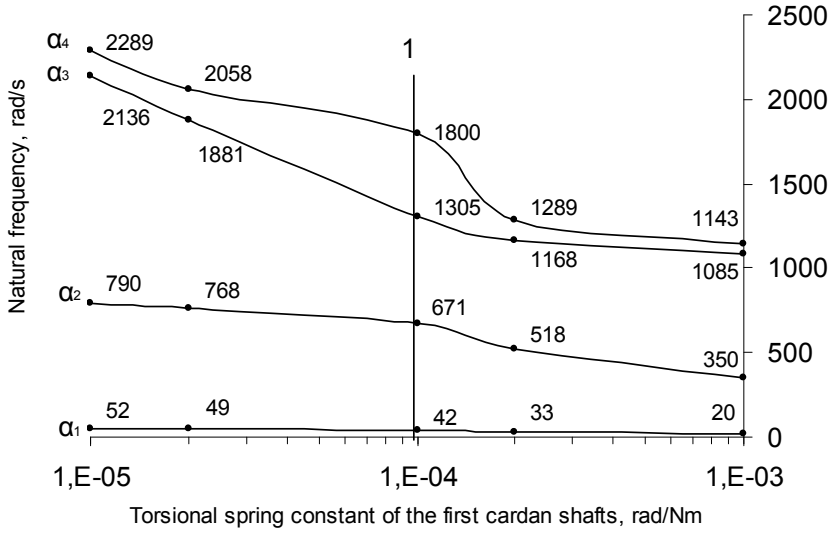

Figure 9.9: The effect of the torsion spring constant
Source: [20]

9.2.2. Bending vibration

Figure 9.10 shows one of the drivetrain layouts on which test were conducted.

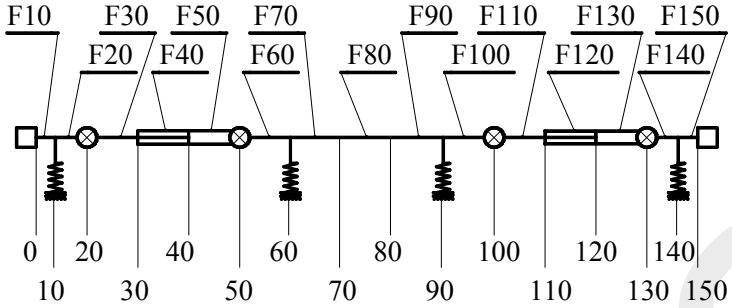

Figure 9.10: Drivetrain layout for testing bending vibrations

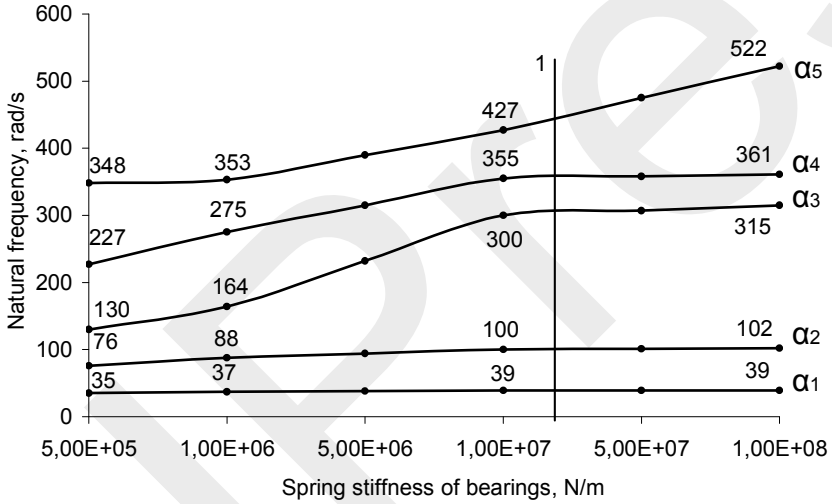

Figure 9.11: The effect of the bearing stiffness
($s \sim 2 \cdot 10^7$ N/m) Source: [20]

Fig. 9.11 shows the effect of bearing stiffness on the bending natural frequencies. The bearing stiffness can be modified by changing the number of the rubber blocks. The less natural frequency was 39 rad/s that is 372 1/min. Fig. 9.12 represents the measurement record in the acceleration and the engine brake stage.

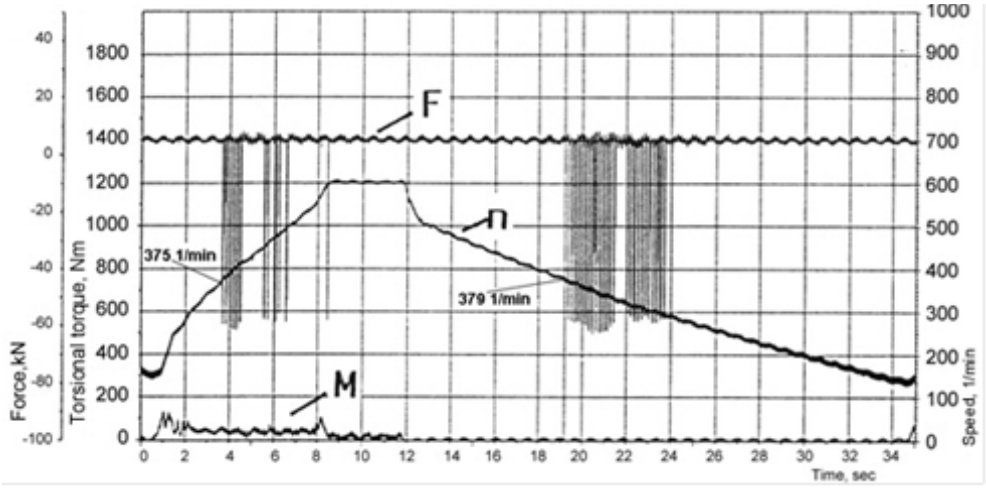

Figure 9.12: The effect of different accelerations
($s \sim 2 \cdot 10^7$ N/m) Source: [20]

The calculation results of drivetrains specified with L_1, L_2, L_3 shaft length, where $L_1 > L_2 > L_3$ are represented in Fig. 9.13. The measuring result of the drivetrain specified with L_2 shaft length is represented in Fig. 9.14.

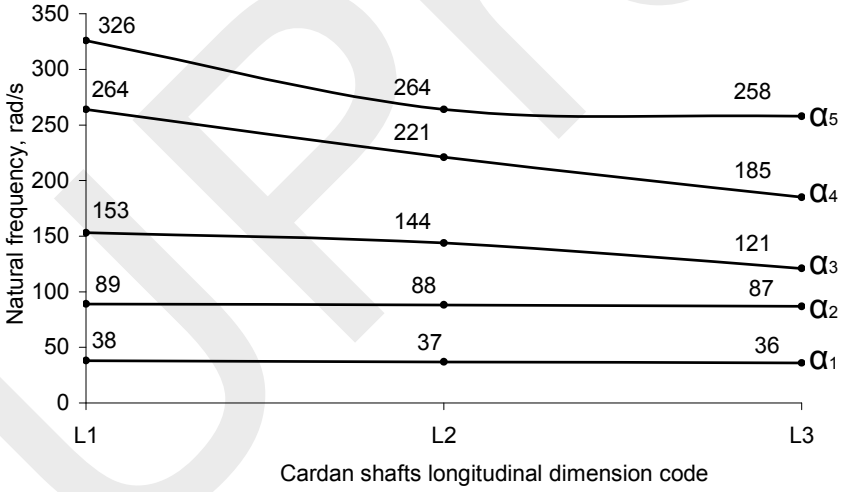

Figure 9.13: The effect of the cardan shaft length I.
($s \sim 2 \cdot 10^7$ N/m,) Source: [20]

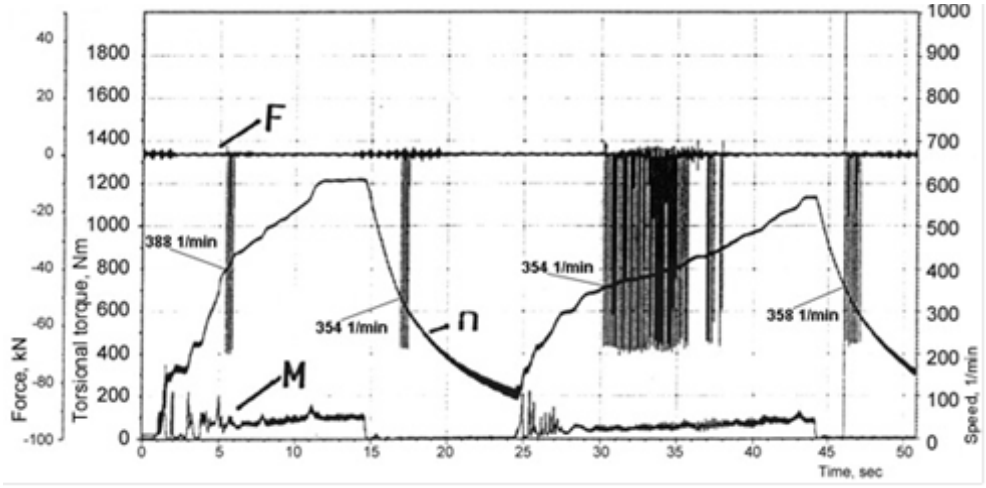

Figure 9.14: The effect of the cardan shaft length II.
($s \sim 2 \cdot 10^7$ N/m, shaft length: L_2) Source: [20]

It can be seen, that although the calculated value was 372 1/min the measured one was between 354-388 1/min. The reason for the dispersion is partly the measurement inaccuracy caused by the altering acceleration of rotational speed, partly the effect of altering bearing stiffness on the bending natural frequencies. Fig. 9.15 represents the spring constant of the 2209.2RS.TV type self aligning ball bearing in the function of bearing load.

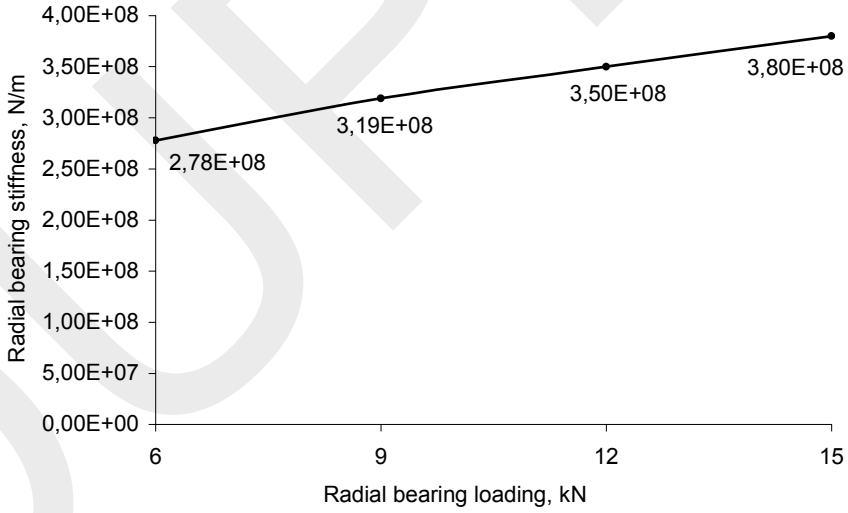

Figure 9.15: The effect of the bearing load on the bearing stiffness
Source: [20]

9.2.3. Conclusions drawn from measurement results

9.2.3.1. Torsion vibrations

- In the case of deflection angle of cardan joint, the torsion natural frequencies alter periodic in the function of the angular displacement of the joint. The mean value of the curves are not affected by the joint angle, it corresponds to the natural frequency of the drivetrain having no deflection angle. The joint angles affect the particular natural frequencies. Its effect is determined by the frequency equation.
- By increasing the mass moment of inertia of the shaft and the part rotating with the shaft, and by decreasing the torsion spring constant of the parts, the torsion natural frequencies decrease.

9.2.3.2. Bending vibrations

- By increasing the mass, the mass moment of inertia of the rotating parts and the distance between the bearing brackets, the natural frequencies decrease.
- By increasing the bearing stiffness and additional supporting with bearing brackets results in increasing the natural frequencies. With the additional supporting namely the distances between the brackets and accordingly the length of the shafts are decreased.
- The bending natural frequencies follow the operation frequency to a certain degree if the spring constant of the supporting is of altering bearing stiffness. Although the excitation forces and moments do not affect the natural frequencies directly however they have a direct effect on the spring constant of the bearings. With increased bearing load namely the spring constant of the bearings increases causing the increasing of the natural frequencies of the drivetrain. This is why, if we accelerate the drivetrain through the critical RPM slowly, the resonance range will widen due to the increasing natural frequency.

REFERENCES

[1] Tiba Zs.: Dynamic driveline modelling. Kiadó: Debrecen University Press 2010., 109 pages, ISBN 978-963-318-044-0

[2] Ansel Ugural, NEW JERSEY INSTITUTE TECH: Mechanical Design: An Integrated Approach, 1st Edition Hardcover with access card, ©2004, ISBN-13 9780072921854

[3] SKF General Catalogue
http://www.skf.com/group/knowledgecentre/subscriptions/displayfactbox.html?itemid=tcm:12-121486
Downloaded: 08. 01.2014.

[4] OPTIBELT V-belt drives Power Transmission Technical manual
www.optibelt.com
Downloaded: 07. 10. 2014.

[5] BRANDO Power transmission belt selector
www.bando.co.jp
Downloaded: 07. 10. 2014.

[6] REXNORD Chain Drive Design
http://www.rexnordkette.de/fileadmin/downloads/qualitaetsketten_2009_DE.pdf
Downloaded: 07. 05. 2014.

[7] Fenner Roller Chain Technical manual
http://www.fptgroup.com/
Downloaded: 06. 05. 2014.

[8] REXNORD Link-Belt Drive and Roller Chain Catalog
http://pdf.directindustry.com/pdf/rexnord-industries-llc/link-belt-driveandroller-chain-catalog/7386-89868.html
Downloaded: 06. 05. 2014.

[9] Schmelz, v. Seherr-Thoss, Aucktor: Gelenke und Gelenkwellen
Springer-Verlag Berlin Heidelberg 1988, ISBN 3-540-18322-1

[10] GKN Walterscheid GmbH: Spare Parts Catalogs
http://www.gkn-walterscheid.de/en/downloads/spare-parts-catalogs/

[11] Duditza, F.: Kardangetriebe und ihre Anwendungen VDI-Verlag GmbH, Düsseldorf 1973.

[12] COOPER Power Tools: Universal Joints
http://www.apexpowertools.com/news-events/MP5187NeedleScaler.cfm
Downloaded: 06. 05. 2014.

[13] VOITH: High-Performance Universal Joint Shafts
http://www.voith.com/en/products-services/power-transmission/universal-joint-shafts-10128.html
Downloaded: 06. 05. 2014.

[14] Shigley J., Charles Mischke, Richard Budynas: Mechanical Engineering Design, 7th Edition Hardcover with access card, 1056 pages©2004, ISBN-13 9780072921939

[15] Molnár, L.; Varga, L.: Gördülőcsapágyazások tervezése Műszaki Könyvkiadó, Budapest 1997. ISBN 963-10-2073-8

[16] Terplán Zénó, Lendvai Pál: Általános Géptan. Tankönyvkiadó Budapest, 1989

[17] BMW 3 Series Sedan Catalogue
http://www.bmw.com/com/en/newvehicles/3series/sedan/2011/_shared/pdf/BMW_3series_sedan_catalogue.pdf?download=true&exporturi=/hu_rb/_shortcuts/prospektus/3aslimousine.jsp
Downloaded: 06. 02. 2016.
[18] Bosznay, Á.: Műszaki rezgéstan. Műszaki Könyvkiadó, Budapest. 1962
[19] Ludvig, Gy.: Gépek dinamikája. Műszaki Könyvkiadó, Budapest. 1983. ISBN: 9631048020
[20] Tiba, Zs.: Kardánhajtások lengéstani viszonyai. PhD Thesiss 1998
[21] Adler - Markova Ganovszkij: Kísérletek tervezése optimális feltételek meghatározására. Budapest, Műszaki könyvkiadó 1977.
[22] Tiba Zs., Husi G.: Mechanical Design of a Mechatronics Systems: Laboratory Handbook, Debrecen: [University of Debrecen Faculty of Engineering], 2012, ISBN: 978 963 473 525 0, 152 pages
[23] http://mag.ebmpapst.com/en/industries/automotive/audi-a4-the-adaptive-steering_1321/
[24] http://www.ai-online.com/Adv/Previous/show_issue.php?id=277#sthash.iu0kpP3D.dpbs
[25] Toyota Owner's manual
[26] Techstream on-line help
Toyota Motor Corporation, V10.00.028, 2015.
[27] Imre Toth's Thesis 2015
University of Debrecen, Faculty of Engineering, Department of Mechanical Engineering